MOLECULAR MOBILITY IN PHARMACEUTICAL GLASSES: IMPLICATIONS ON PHYSICAL STABILITY

A Dissertation
SUBMITTED TO THE FACULTY OF
UNIVERSITY OF MINNESOTA

BY

MEHAK MEHTA

IN PARTIAL FULFILLMENT OF THE REQUIREMENTS
FOR THE DEGREE OF
DOCTOR OF PHILOSOPHY

RAJ SURYANARAYANAN
(ADVISOR)

MAY, 2016

Acknowledgements

I would like to express my deepest appreciation and gratitude to my advisor, Prof. Raj Suryanarayanan, for his mentorship, faith, encouragement and unwavering support throughout the doctoral program. I am grateful to have learnt the ropes of science, the principles of solid-state chemistry, and more importantly the art of asking the right questions. I am thankful to him for providing incredible opportunities for professional growth. I will always cherish the lessons learnt under his tutelage in both my professional and personal life.

I am indebted to Prof. Gregory McKenna for his generosity, expert guidance and extremely valuable inputs for helping develop a nuanced understanding of pharmaceutical glasses. I am thankful to have had an opportunity to work with him. He has always been very enthusiastic to discuss existing projects and new ideas. His passion for science, dedication and clarity of thought have set an example, I someday hope to emulate.

I want to thank my committee members, Prof. Ronald Siegel, Prof. Calvin Sun and Prof. Gregory McKenna for serving on my thesis committee and critically reviewing my thesis. Dr. Siegel taught me the basics of writing scripts in MATLAB and has always made himself available for discussions related to my thesis work. I am also thankful to Prof. Chris Macosko for serving on my oral examination committee.

Sincere thanks to the faculty, staff and graduate students at the Department of Pharmaceutics, University of Minnesota without whom my graduate experience would be

an incomplete one. I would like to thank the past lab members: Dr. Prakash Sundaramurthi, Dr. Bakul Bhatnagar, Dr. Aditya Kaushal, Dr. Nitin Tayade, Dr. Kapildev Arora, Dr. Sunny Bhardwaj, Dr. Khushboo Kothari, Dr. Vishard Ragoonanan, Dr. Sarat Mohapatra, Michael Burcusa, Dr. Naveen Thakral as well as current lab members - Dr. Seema Thakral, Karlis Berzins, Pinal Mistry, Michelle Fung, Sampada Koranne and Kweku Konadu for their friendship and scientific exchange of ideas. A special thanks to Ms. Candice McDermott, Mrs. Erica Stapic, Ms. Sarah J Sexton, Ms. Courtney Meeker, Ms. Jody Tracy who form the backbone of our department and are indispensable.

I would like to thank my friends: Chaitali, Nidhi, Shruthi, Isha, Mamta, Vikrant, Rashmi, Ashank and Sudeepto who made my stay in Minneapolis a memorable experience. I want to express my heartfelt gratitude towards my family for their unconditional love and support - grandmother, mom, dad, brother, sister in law and my precious niece, Yohanna. Thank you for encouraging me to reach new heights of success. Last but not the least, I would like to thank Kshitij for his support and encouragement in the last leg of the journey.

Dedicated to my family

Abstract

Amorphous pharmaceuticals have gained widespread importance due to their advantageous increase in solubility and dissolution rate. However, a major challenge with this approach is the high risk of physicochemical instability in comparison to its crystalline counterparts. The goal of my research was to investigate the correlations between molecular mobility and physical stability in model amorphous systems (both drug substance and solid dispersions), specifically in the glassy state. This will potentially enable development of effective strategies to stabilize amorphous pharmaceuticals. Use of time-temperature, time-aging and time-concentration superposition principle enabled comprehensive characterization of structural relaxation behavior in the glassy state. This was followed by the investigation of correlation between crystallization behavior and different mobility modes in glassy celecoxib and indomethacin. Structural relaxation time correlated well with characteristic crystallization time in the supercooled state. On the other hand, a stronger correlation was observed between the Johari-Goldstein relaxation time and physical instability in the glassy state but not with structural relaxation time. Effect of polymer additive and polymer concentration on the structural relaxation behavior in nifedipine dispersions was investigated. We found that stronger drug-polymer interactions enhanced physical stability by reducing the molecular mobility. With an increase in polymer concentration, the relaxation times were longer indicating a decrease in molecular mobility. The effect of sorbed water on molecular mobility and physical stability in a model amorphous drug and dispersion was also evaluated. Sorbed water, in a concentration dependent manner, increased mobility and accelerated crystallization - attributable to the plasticization effect of water. The extent of coupling between molecular mobility and crystallization time (defined as time for 2.5% crystallization) was found to be unaffected in the range of water content studied (< 2% w/w). Based on this finding, we have proposed the use of “water sorption” as an accelerated stability approach to predict crystallization in slow crystallizing systems.

Table of Contents

List of Figures

List of Tables

1 Introduction

1.1 Introduction

A large fraction of the new drugs under development are characterized by poor aqueous solubility[1]. As a result, their absorption following oral administration can be a challenge. Drug amorphization is an effective and popular strategy to enhance solubility[2]. However, a major challenge with this approach is the risk of crystallization due to physical instability. This can negate the bioavailability advantage brought about by the solubility enhancement. An added complication with amorphous materials is that the thermal history imparted by the preparation method and storage conditions can impact the pharmaceutical properties of interest such as vapor sorption and crystallization propensity. The overall goal of the current research is to investigate the role of molecular mobility on the physical stability of amorphous pharmaceuticals in single (drug alone) and multi-component systems (solid dispersion).

1.2 Motivation

The amorphous form of a compound is inherently unstable due to its higher free energy than its crystalline counterpart. This instability could be chemical i.e. chemical degradation as well as physical i.e. crystallization to the stable low energy form. Excellent analytical tools are available to characterize chemical instability especially in the solution state. Studying degradation kinetics at elevated temperatures and extrapolating to room temperature is an approach classically used to predict chemical degradation. However, such an approach cannot be used for physical stability (crystallization) prediction. The two steps involved in crystallization i.e. nucleation and crystal growth exhibit different temperature dependence. Additionally, water sorbed

either during processing or storage can have a dramatic influence on the physical stability of these materials. Therefore, predicting physical stability under relevant storage conditions is not straightforward. This poses a major obstacle in the widespread use of amorphous pharmaceuticals.

Molecular mobility has been extensively investigated in light of its possible role in governing physical stability[3,4,5,6,7]. Molecular mobility comprises both global and local motions. Global motion is cooperative in nature and is responsible for bringing about the glass transition. It is also referred as α- or structural relaxation. On the other hand, local motions (or secondary relaxations) are non-cooperative in nature and arise from either a part or an entire molecule[8,9]. In several compounds, structural relaxation time has been linked to physical instability in the supercooled state ($T > T_g$)[10,11,12]. Interestingly, β-relaxation (also referred to as Johari-Goldstein relaxation[13]) has been implicated in physical instability of glasses ($T < T_g$)[14,15,16,17]. We believe that any approach used to build predictive models should consider the influence of both global and local motions.

Dielectric spectroscopy (DES) allows direct measurement of molecular motions associated with dipole reorientation in the frequency range of 10^{-6} to 10^{12} Hz[18]. Time domain dielectric techniques such as isothermal depolarization and thermally stimulated current[19,20] have been employed to characterize molecular motions in glassy pharmaceuticals. Using DES, different relaxations can be studied simultaneously and correlation between a specific mobility and stability can be established.

In the present work, we have extensively used DES to comprehensively characterize the molecular motions in model amorphous systems. In Chapter 2, nifedipine, an antihypertensive, was used as a model compound. The time-aging time or time-

temperature superposition principle was used as an approach to calculate the time or temperature dependence of global motions respectively in glassy nifedipine. This enabled the comprehensive characterization of structural relaxation. In Chapter 3, we investigated the correlations between crystallization time (time for 2.5% crystallization) and different relaxations (both local and global) in glassy celecoxib and indomethacin. This not only enabled the identification of a specific mobility mode responsible for the observed instability but allowed the development of models to predict crystallization at temperatures below T_g.

In an effort to stabilize amorphous compounds, they are fabricated as solid dispersions which are molecular drug – polymer mixtures. Different mechanisms such as hydrogen-bonding, physical barrier or anti-plasticization effect have been proposed to explain the stabilization mechanism of polymer[21,22,23]. However, a comprehensive understanding is still lacking. Very few studies have investigated the stabilization mechanism in the glassy state. In Chapter 4, in an effort to explain the observed effect of polymer on physical stability, we have studied the influence of polymer additives and their concentration on relaxation behavior in glassy dispersions.

Amorphous systems are typically characterized by a pronounced tendency to sorb water. Water, by increasing the free volume[24], causes plasticization leading to an increase in mobility. This can potentially increase the risk of physicochemical instability in amorphous materials[25,26,27]. One approach to minimize water uptake by amorphous materials is to tightly control the water vapor pressure in the atmosphere. However, during the manufacture and storage of amorphous pharmaceuticals, there are practical limits to the extent to which the ambient water vapor pressure can be reduced. It is

therefore valuable to investigate the role of water on the physical stability of amorphous pharmaceuticals. In Chapter 5, we systematically vary the water content in a model amorphous system to determine the effects on (i) molecular mobility, and (ii) crystallization behavior. Based on these results, in Chapter 6, we are proposing the use of water sorption as an accelerated stability approach to predict crystallization in amorphous solid dispersions.

1.3 Isothermal crystallization kinetics

Devitrification involves two steps: formation of stable nuclei followed by growth of these nuclei into crystals. Nucleation can be of two types – homogenous and heterogeneous. Homogenous nucleation occurs spontaneously whereas nucleation taking place under the influence of an external stimulus such as impurities or seeds is termed heterogeneous nucleation[28]. The rate of homogenous nucleation, J, i.e. the number of nuclei formed per unit time per unit volume is described by the classical nucleation theory[28,29]:

$$J = Aexp(-\frac{\Delta G}{k_B T}) \qquad (1.1)$$

where A is a pre-exponential factor, , k_B is the Boltzmann constant, T is the temperature and ΔG is the change in Gibbs free energy associated with the formation of nuclei of a critical size. It is given by [28]:

$$\Delta G = \Delta G_s + \frac{4}{3}\pi r^3 \Delta G_v \qquad (1.2)$$

where ΔG_s is free energy difference the surface of the particle and the bulk of the particle and ΔG_v is the excess free energy between a very large particle ($r = \infty$) and the solute in solution. The driving force for nucleation increases as the degree of undercooling increases. However, the viscosity of the system increases as the temperature is lowered

resulting in reduced molecular mobility and increased kinetic barrier for nucleation. Turnbull and Fisher quantified this behavior and derived a modified form of equation 1.1 [28, 30]:

$$I = A' \exp\left[-\frac{16\pi\gamma^3 v^2}{3k^3 T^3 (lnS)^2} - \frac{\Delta G'}{kT}\right] \qquad (1.3)$$

where γ is the interfacial tension between the developing crystalline surface and the supersaturated solution, ν is the molecular volume, S is the degree of supersaturation and ΔG' is the kinetic barrier to nucleation. The kinetic barrier is related to the viscosity and is the activation energy for molecular motion across the embryo-matrix interface[29]. Nucleation is thermodynamically favored at higher degrees of supercooling and crystal growth is favored at lower degrees of supercooling (that is, higher temperatures). The growth rate of individual crystals, U, is given by the following relationship [29, 31]:

$$U = \frac{CTw}{\eta}\left[1 - \exp\left(-\frac{\Delta G_v}{kT}\right)\right] \qquad (1.4)$$

where C and w are constants and w depends on the mechanism of growth and η is viscosity of the system and reflects the molecular mobility . As can be seen from equations 1.3 and 1.4, the two processes, nucleation and crystal growth show different temperature dependences. There is only a very narrow temperature window where the two processes i.e. nucleation and crystal growth overlap. However, it has been found experimentally that crystallization can occur at temperatures where nucleation is predominant. This makes the independent characterization of the two processes extremely difficult. Hence, the models used to study the kinetics of crystal growth take into account nucleation and crystal growth. The Kolmogorov-Johnson-Mehl-Avrami (KJMA) theory is widely used to describe the overall process of crystallization [29, 32]:

$$\alpha(t) = 1 - \exp\left[-(k(t - t_o))^n\right] \qquad (1.5)$$

where α is the fraction crystallized at time t, k is a constant described by nucleation and growth rate constants, t_o is the induction time and n represents the morphology of growth depending on the nucleation mechanism. The following assumptions have been made in deriving the above expression: (i) rates of nucleation and growth are time independent, (ii) nucleation is homogenous, and (iii) linear steady state growth[29]. This model has been used to describe isothermal crystallization in the area of pharmaceutical research[33].

1.4 Molecular mobility and crystallization

As mentioned before, in equation 3, the overall rate of nucleation can be described by a free energy change upon nucleation based on thermodynamic considerations and a 'kinetic barrier' representing the energy required for molecular transport. Furthermore, we can incorporate the effect of molecular mobility on crystallization through this expression given by Ngai et al [34]:

$$k = D(T).f(T) \qquad (1.6)$$

In this equation, k is the overall rate of crystallization, D (T) is the molecular diffusion coefficient which is a function of temperature (can be correlated to the viscosity of the system) and f (T) represents the free energy term for nucleation (thermodynamic driving force for crystallization). If this relation holds and diffusion is the dominant factor in determining the crystallization rate, then crystallization rate at different temperatures can be described by the following equation [34a]:

$$\frac{k_1}{k_2} \approx \frac{D_1}{D_2} \approx \left(\frac{T_1}{T_2}\right)\left(\frac{\tau_2}{\tau_1}\right)^{\xi} \qquad (1.7)$$

where D_1 and D_2 are translational diffusion coefficients at temperatures T_1 and T_2 respectively and ξ is a factor introduced to compensate for any decoupling between the diffusion coefficient and viscosity of the matrix.

Molecular mobility is being extensively studied in the field of amorphous pharmaceuticals and has been thought to a be a major factor governing the physicochemical instability of amorphous pharmaceuticals [33c, 35]. Several studies have shown a correlation between molecular mobility and physical instability of amorphous materials [33b, c, 34a, 36] and higher mobility is often held responsible for the increased instability in the amorphous state. Therefore, current research efforts are aimed at reducing molecular mobility to enhance physical stability. However, it is only recently, that researchers have attempted to predict crystallization on the basis of molecular mobility measurements [33a, 36a, 37].

Traditionally, the glass transition temperature (T_g) has been considered as a marker of global mobility and based on that assumption, several studies have attempted to correlate it with physical stability. Many systematic studies have shown the effect of plasticizers compound which lower T_g) and anti-plasticizers (increase T_g) on the crystallization behavior of amorphous pharmaceuticals [38]. However, there are several studies in the literature where the systems show drastically different crystallization behavior despite having nearly the same glass transition temperature [33c, 39].

The molecular mobility responsible for the glass transition is cooperative in nature and is termed as global mobility [40]. Structural relaxation or α- relaxations are often used interchangeably to describe global mobility. The temperature dependence of structural relaxation above T_g is well described by the Vogel-Tamman-Fulcher (VTF) model [41]:

$$\tau(T) = \tau_o \exp\left(\frac{DT_o}{T-T_o}\right) \qquad (1.8)$$

where τ is the average α-relaxation time, T is the temperature; τ_o, D and T_o are constants where τ_o corresponds to the relaxation time of the unrestricted material, D is the strength

parameter and is a measure of the fragility of the material and T_o is considered to be the temperature of zero mobility (theoretical Kauzmann temperature) .

Due to the extremely high viscosity, structural relaxation in the glassy state is very slow in timescales of interest. According to the Adam – Gibbs theory, molecular relaxation requires cooperative rearrangement of a group of molecules[42]. There is a marked increase in viscosity as the temperature decreases and the movement of one molecule will disturb an increasingly large number of its neighboring molecules. The energy barrier for molecular rearrangement is proportional to the size of rearranging unit. The relaxation time, τ, can be expressed as

$$\tau(T) = \tau_o \exp\left(\frac{\Delta\mu S_c^*}{T S_C k_B}\right) \qquad (1.9)$$

In the above equation, Δμ is the potential energy barrier per molecule and S_c is the configurational entropy of the smallest rearranging unit. The configurational entropy, S_c, in supercooled liquids can be expressed using a hyperbolic relationship with temperature ($C_{p,conf}$ = K/T, where K is a proportionality constant). In the glassy state, the Kauzmann temperature (approximated as T_0) marks the lower limit of the excess entropy in the amorphous state. The concept of fictive temperature (T_f) was introduced by Tool and Narayanaswamy[43]. It is defined as the temperature at which a non-equilibrium property *p* (enthalpy or entropy) of a glass, *in excess with respect to the stable crystalline state*, would have the same value as in the equilibrium supercooled liquid. The configurational entropy can then be calculated as follows

$$S_c = S_o(T_o) + \int_{T_f}^{T_o} \frac{\Delta C_p}{T} = \int_{T_f}^{T_o} \frac{K}{T^2} dT = K\left(\frac{1}{T_o} - \frac{1}{T_f}\right) \qquad (1.10)$$

where $\Delta C_p = C_{p,l} - C_{p,g}$ at T_o

In eq 1.10, $S_c(T_o)$ is assumed to be 0 at T_o. By substituting eq 1.10 in the Adam-Gibbs model, eq 1.9 becomes

$$\tau(T) = \tau_o \exp\left(\frac{DT_o}{T(1-\frac{T_o}{T_f})}\right) \qquad (1.11)$$

Eq 1.11 is also known as the Adam-Gibbs-Vogel equation and is used to calculate the temperature dependence of structural relaxation time in the glassy state. This model does not completely describe the non-linear and non-exponential nature (i.e. the β- parameter) of structural relaxation. Moreover, the effects of thermal history and preparation method on structural relaxation are not taken into account. However, the approach is experimentally convenient and has found extensive application[27,44,45].

The most successful phenomenological framework used to describe the structural relaxation behavior in glasses is the Tool-Narayanaswamy-Moynihan model[43,46,47]. It can explain the non-isothermal and non-exponential temperature of structural relaxation for complex temperature histories. The description of this model is given elsewhere[48]. Several techniques including differential scanning calorimetry (DSC) [49], dielectric spectroscopy [33b, c, 36a, 39a, 49a], shear viscosity measurement [50] and nuclear magnetic resonance [51] have been used to study structural relaxation in amorphous pharmaceuticals.

Glassy systems exhibit local motions involving either the entire molecule or intramolecular reorientations and are termed as β- or secondary relaxations or "local mobility" [52]. In contrast to the α-relaxations, they are non-cooperative in nature and are typically much faster with relaxation time < 10^{-1} seconds. They show an Arrhenius temperature dependence and are characterized by a much smaller activation energy as compared to α-relaxations[53]. Unlike α-relaxation, a molecule can possess many local motions, the most important being the Johari-Goldstein (JG) relaxations [52a]. These

relaxations involve the motion of the entire molecule and are supposed to be the precursor to the cooperative α-relaxations[54]. Dynamic dielectric spectroscopy has been commonly used to investigate β-relaxations in amorphous pharmaceuticals [33b, c, 39a].

1.4.1 Supercooled state

Earlier work from Ngai et al demonstrated partial coupling between crystallization rate and structural relaxation time for trinapthylbenzene and 1,2-diphenylbenzene [34b]. Previous work from our laboratory has established an excellent correlation between the α- relaxation time and crystallization onset time above T_g in amorphous pharmaceuticals [33b, c, 39a]. Systematic studies have been carried out to investigate the influence of additives such as plasticizers (sorbitol) and antiplasticizers (polyvinylpyrrolidone; PVP) on global mobility and crystallization of amorphous sucrose [39a]. PVP showed an antiplasticization effect whereas sorbitol plasticized the global motions in amorphous sucrose. The influence on global mobility correlated well with the crystallization onset time. In another similar study of amorphous solid dispersions of itraconazole and hydroxypropylmethylcellulose acetate succinate (HPMCAS), HPMCAS significantly increased the α- relaxation time which translated to an increase in crystallization onset time[55]. Bhardwaj et al demonstrated the influence of preparation method (freeze-drying; spray drying and dehydration) on molecular mobility and crystallization behavior of amorphous trehalose[33c]. A strong coupling between the crystallization onset time and global mobility enabled development of predictive models. An excellent agreement was observed between the experimental and predicted onset time for crystallization around T_g. The α- relaxation appears to be strongly coupled to the physical instability observed

above T_g in case of trehalose and itraconazole. However, it remains to be established if such a correlation exists in a wide variety of amorphous pharmaceuticals.

1.4.2 Glassy state

Two kinds of dynamics are observed in the glassy state: local mobility as evidenced by secondary relaxations and global mobility or slow dynamics due to the segmental motions which, although characterized by long relaxation times, are not completely frozen [41b, 56]. DSC and time domain dielectric spectroscopy have been employed to study the structural relaxation below T_g in amorphous pharmaceuticals [36a, 37a, b, 41b, 56]. DSC, frequency domain dielectric spectroscopy and spin-lattice relaxation time measurement have been utilized to investigate the local mobility in the glassy regime of pharmaceuticals [33b, 39a, 57]. There are several studies showing evidence of nucleation or crystallization at temperatures far below T_g [36a, 37, 57a, 58]. However, there is a lack of understanding of factors governing crystallization in glassy pharmaceuticals.

There are a few studies in the literature evaluating the potential role of local mobility in determining the physical stability of amorphous pharmaceuticals. Vyazovkin et al observed endothermic peaks almost 50 °C below T_g and attributed them to β-relaxation [58-59]. In a follow up study, the peaks were correlated with nucleation in the glassy state [57a]. It was suggested that β-relaxation may control the crystallization process in this temperature range where α-relaxation is thought to be negligible. In another study, molecular mobility in amorphous salicin and indomethacin below T_g was probed using nuclear magnetic resonance [57b]. The molecular mobility was faster in salicin as compared to indomethacin and this correlated with the crystallization behavior. However, enthalpic relaxation studies were not able to provide insight into the observed crystallization

behavior. Bhugra and Pikal speculate that if local mobility renders the molecules in a certain conformation feasible for nucleation, then β-relaxation would be correlated to the crystallization behavior [29]. Few studies have shown a direct correlation of chemical stability with local mobility reinforcing its potential significance [60]. However there are no studies in the literature demonstrating a direct correlation between β-relaxation and crystallization behavior.

Aso et al calculated the mean relaxation time for amorphous nifedipine and phenobarbital using the Adam-Gibbs-Vogel (AGV) equation and it correlated well with the crystallization rate though a partial decoupling was observed in the case of amorphous nifedipine[34a]. In another study, the authors attempted to predict crystallization onset below T_g from correlations observed above T_g in amorphous sucrose [36a, 37a]. The predictions were based on the assumption that similar motions are being measured by dielectric spectroscopy above T_g and calorimetry below T_g. However, reliable prediction of crystallization onset time was not possible. They observed coupling between crystallization onset and mobility above T_g. In an effort to predict crystallization, similar coupling was assumed below T_g which may not be the case. In a follow up study, the authors utilized the same approach to predict crystallization at pharmaceutically relevant temperatures below T_g for a group of compounds [37b]. However, a good agreement was observed in only two of the four investigated compounds indicating that the assumptions may not be valid in all cases. In view of the current understanding, it seems important to investigate the dynamics (local and structural relaxations) in the glassy state of amorphous pharmaceuticals and establish a correlation with crystallization over a pharmaceutically relevant temperature range below T_g.

1.5 Influence of water on physical stability

It is difficult to prepare pharmaceutical dosage forms where water is completely excluded. This will be especially challenging in amorphous materials which have an extremely strong tendency to sorb moisture. Water, by increasing the free volume, plasticizes amorphous materials. This results in reduction of glass transition temperature and increased mobility [61]. Amorphous pharmaceuticals can sorb water during processing and/or storage thus making it important to understand the role of water in influencing the physical instability in these systems. However, very few studies in the pharmaceutical literature have investigated the influence of water on accelerating crystallization [38a, 38c, 62]. As mentioned earlier, T_g has been considered to be a determinant of physical stability and attempts have been made to develop models to predict T_g as a function of water content [62c]. However, this information would not allow the pharmaceutical formulator to accurately predict physical stability of amorphous pharmaceuticals. The increase in relative humidity accelerated crystallization in amorphous sucrose and glucose [63]. It was attributed to the decrease in viscosity leading to increased probability of nucleation followed by crystallization. A decrease in peak crystallization temperature was observed with increasing water content during non-isothermal crystallization studies of amorphous lactose [64]. Water has a strong plasticizing effect as observed in amorphous indomethacin, wherein sorption of 1% w/w water resulted in a 10 °C reduction in T_g [38a]. In the same study, the authors noted the overall rate of crystallization decreased as the RH increased from 21% to 43% which seems counterintuitive. However, this was attributed to surface initiated crystallization below 21% RH requiring less mobility as compared to the bulk crystallization prevalent above 21% RH which would require comparatively higher

mobility. The influence of water on mobility has been investigated using dielectric spectroscopy, nuclear magnetic resonance (NMR) and differential scanning calorimetry [62a, 65]. With increase in RH of colyophilized sucrose-PVP mixtures, no change in motions of MHz-order was observed either in the side chain of PVP or sugar ring in sucrose [65b]. However, a small increase in mid-KHz-order motions was observed for sucrose in colyophilized mixtures. An increase, although small, in T_1 relaxation time was observed in fused nifedipine-excipient mixtures with increase in water content [62a]. However, the type of mobility measured by NMR is unclear i.e. whether it is α- or β-relaxation. Andronis et al showed a significant increase in mobility of amorphous indomethacin at 56% and 83% RH measured using DES and presence of water did not seem to influence the fragility [65a]. An increase in water content had an opposite effect on the different local motions (γ- and β- relaxation) in amorphous lactose [66]. They observed a drastic decrease in the relaxation time of β motions, which they refer to as the Johari Goldstein motions, and saw an increase in relaxation time of γ- motions attributed to the bridging effect of water between the adjacent hydroxymethyl groups. Similar results were obtained in amorphous cyclodextrins wherein the addition of water influenced the activation energy barrier for γ- and β- relaxation in completely opposite ways [67]. Similarly, in amorphous glucose, an increase in water content shifted the α-relaxations to a lower temperature and β-relaxations to a higher temperature [65c]. These results make it important to investigate the influence of water on mobility in cases where it plays a role in physical stability of amorphous pharmaceuticals.

1.6 Thesis overview and hypotheses

Chapter 2

The extremely long time scale of global motions and the non-ergodic nature of glasses, pose a challenge in experimentally characterizing the structural relaxation. The non-exponential, non-linear and history dependence of structural relaxation needs to be suitably addressed by the model to accurately estimate the relaxation time. However the Adam-Gibbs model, commonly employed in the pharmaceutical community does not adequately capture all the key features of structural relaxation mentioned above. Our primary objective was to comprehensively characterize the structural relaxation behavior in glassy nifedipine using dielectric spectroscopy.

The importance of "physical aging" stems from the fact that it could lead to a glassy matrix closer to the equilibrium state. If the mobility (measured as relaxation time) governs stability, aging by reducing the mobility can serve as an effective stabilization strategy. In fact, annealing (deliberate physical aging) has been shown to improve the chemical stability of peptides. In this study, we comprehensively studied the effect of physical aging on the structural relaxation behavior at several temperatures. To the best of our knowledge, this is the first direct experimental measurement of structural relaxation time in pharmaceutical glasses.

Chapter 3

Physical instability or crystallization during manufacture or storage can adversely affect the amorphous drug product performance. Therefore, factors governing stability should be thoroughly and comprehensively investigated in order to develop predictive models

for crystallization. Several reports have shown a correlation between global motions and physical stability in the supercooled state. However, amorphous pharmaceuticals are typically stored as glasses. Thus, evaluation of such correlations in this state is of immense practical value. We had two specific objectives: (i) comprehensively characterize the molecular mobility, i.e. both global and local motions, in supercooled and glassy states of two model compounds (celecoxib and indomethacin) and (ii) investigate the potential correlation between crystallization and the specific mobility mode in the glassy state. This would enable the development of stabilization approaches by modulating the specific mobility correlating with the observed physical instability.

The working hypothesis was:

Physical instability (measured as time for 2.5% crystallization) is correlated to global molecular mobility in glassy celecoxib and indomethacin.

A combination of time and frequency domain dielectric spectroscopy was used to map the different types of molecular motions present in the glassy state. Isothermal crystallization was monitored by powder X-ray diffractometry using either a laboratory source (supercooled state) or synchrotron source (glassy state). Structural (α-) relaxation time correlated well with characteristic crystallization time in the supercooled state. On the other hand, a stronger correlation was observed between the Johari-Goldstein (β-) relaxation time and physical instability in the glassy state. These results suggest that Johari-Goldstein relaxation is a potential predictor of physical instability in the glassy state of these systems.

Chapter 4

Solid dispersions, molecular drug − polymer mixtures, are known to physically stabilize amorphous drugs. However, the mechanism of stabilization by the polymer in the glassy state is not comprehensively understood. Our objective was to study the effect of (i) polymer additive and (ii) polymer concentration on the drug stability in NIF-polymer dispersions. This will not only enhance our understanding of the basic mechanism of polymer stabilization, but also rationalize the polymer selection in the formulation of solid dispersions.

The working hypotheses were:

i. *Time-temperature superposition (TTS) principle would be valid in solid dispersions enabling the calculation of temperature dependence of structural relaxation time in glassy dispersions.*
ii. *The addition of polymer, affects the physical stability by influencing the molecular mobility of the resulting dispersion.*
iii. *PVP, in a concentration dependent manner, will increase the relaxation time and thereby enhance the physical stability of nifedipine in glassy dispersions.*

Dielectric spectroscopy was used to characterize the structural relaxation in pharmaceutical dispersions containing NIF and either PVP or HPMCAS. For pure NIF as well as the dispersions, the validity of the TTS principle was established. We found that strong drug - polymer hydrogen bonding interactions improved the physical stability (i.e. delayed crystallization) by reducing the molecular mobility. The strength of hydrogen bonding, structural relaxation time and crystallization followed the order: NIF-PVP > NIF-HPMCAS > NIF. With an increase in PVP concentration, the relaxation times were longer indicating a decrease in molecular mobility. This is the first application of the

superposition principle to characterize structural relaxation in glassy pharmaceutical dispersions.

Chapter 5

Amorphous systems are typically characterized by a pronounced tendency to sorb water. This can potentially increase the risk of physicochemical instability. During the manufacture and storage of amorphous pharmaceuticals, there are practical limits to the extent to which the ambient water vapor pressure can be reduced. Thus, it is important to understand the role of sorbed water content on molecular mobility and consequently the crystallization behavior of amorphous pharmaceuticals. The objective of this study was to systematically vary the water content and determine the effects on (i) molecular mobility, and (ii) crystallization behavior. These investigations were conducted using nifedipine - polyvinylpyrrolidone vinyl acetate 64 (NIF - PVPVA) as a model solid dispersion.

The working hypothesis was:

Water, in a concentration dependent manner, increases the molecular mobility and accelerates crystallization of the drug in NIF - PVPVA dispersions - effects attributable to plasticization.

The temperature scaling (T_g/T) allowed us to simultaneously evaluate the effects of water content and temperature on the relaxation time. In the supercooled dispersions, once scaled, the relaxation times of the systems with different water content overlapped. Thus, the observed increase in mobility could be explained by the "plasticization" effect of water. This effect also explained the decrease in crystallization onset temperature brought about by water. That is, plasticization is the underlying mechanism governing the observed increase in mobility and physical instability in the supercooled state.

Chapter 6

One of the major challenges in the development of amorphous formulations is the reliable prediction of long term physical stability. Studying degradation kinetics at elevated temperatures and extrapolating to room temperature, an approach classically used for predicting chemical degradation, cannot be used for physical stability (crystallization) prediction. In this chapter, we are proposing the use of "water sorption" as an accelerated stability approach to predict crystallization in solid dispersions. The study was conducted using felodipine - polyvinylpyrrolidone (FEL-PVP) as a model solid dispersion.

The working hypothesis was:

At low water contents, the coupling coefficient between molecular mobility and crystallization time will remain unaffected in FEL - PVP dispersions

With an increase in water content, the α-relaxation time (measured by dielectric spectroscopy) decreased reflecting an increase in molecular mobility. The temperature dependence of relaxation time indicated that the fragility of the dispersion was independent of the water concentration. The time for felodipine crystallization also decreased with an increase in water content. The plot of crystallization versus inverse temperature showed an Arrhenius temperature dependence. In the range of water contents studied, the slope value was independent of the water content. This indicates that the decrease in relaxation as well as crystallization time can be explained by the plasticization effect. The effect was manifested in the value of the coupling coefficient, a measure of the coupling between molecular mobility and crystallization time, which was unaffected by the water content in the dispersion.. Based on these findings, we are

proposing the use of “water sorption” as an “accelerated stability tool” to predict crystallization in dry dispersions.

2 Dielectric spectroscopy - a tool to characterize structural relaxation behavior in pharmaceutical glasses

2.1 Introduction

A variety of materials including ceramics, polymers, foods and pharmaceuticals exist in or are deliberately prepared in the amorphous state. While the amorphous state can confer many desirable properties, the potential physical and chemical instability due to the higher free energy compared to its crystalline counterpart, remains a major challenge. This issue is of particular concern with small molecule pharmaceuticals and has been the subject of numerous investigations. Molecular mobility, which encompasses both global and local motions, has been proposed as a major factor governing crystallization as well as accelerating the chemical reactivity in the amorphous state[1,2,3,4,5,6,7]. Global motions are cooperative in nature and are also referred to as primary, structural, or α-relaxation. Fast non-cooperative motions, emanating from a part of a molecule or involving a complete molecule, are termed local motions or as secondary relaxations. This investigation deals exclusively with structural relaxation with a focus on the glassy state.

In the glassy state, the structure evolves continuously towards equilibrium, and the relaxation time provides a measure of the mobility of the system. The term *physical aging* is used to describe this phenomenon. The consequence of structural relaxation on material properties in polymers, ceramics and gels has long been established[8,9,10,11,12,13,14]. The theoretical and phenomenological aspects of structural relaxation have been the subject of several excellent reviews[15,16,17,18]. This subject has recently gained a lot of attention in the pharmaceutical literature. Several groups have documented a correlation between relaxation time and crystallization behavior in the supercooled state. The desired stability of amorphous pharmaceuticals necessitates their storage below the glass transition temperature. Thus, evaluation of such correlations in the glassy state is of

immense practical value. However, the extremely long time scale of these motions and the non-ergodic nature of glasses, pose a challenge in experimentally characterizing the structural relaxation. It is also necessary to recognize that the structural relaxation is non-linear, non-exponential and history dependent. The consequences of these properties are not necessarily captured by the calorimetric approaches, widely used in pharmaceuticals. Recently, Mao et al[19], using heat capacity measurements, developed a simulation model to estimate relaxation times. However, this does not provide a direct measure of the relaxation time. In order to explore potential correlation between structural relaxation and other properties of practical interest (such as crystallization and water sorption), direct experimental measurement of structural relaxation time is warranted.

In this paper, we report the non-equilibrium structural relaxation behavior of glassy nifedipine using time domain dielectric spectroscopy, a method pioneered by Mopsik et al[20,21]. We have also studied the effect of physical aging on the relaxation time in the glassy state. The importance of "physical aging" stems from the fact that it could lead to a glassy matrix closer to the equilibrium state. If the mobility (measured as relaxation time) governs stability, aging by reducing the mobility can serve as an effective stabilization strategy. In fact, annealing (deliberate physical aging) has been shown to improve the chemical stability of peptides and antibiotics[7, 22,23].

2.2 Experimental section

Preparation and baseline characterization of Amorphous Nifedipine. Nifedipine ($C_{17}H_{18}N_2O_6$) was purchased from Laborate Pharmaceutical Ltd, India and used as received. Nifedipine films (50 μm thick) were prepared by melting the crystalline powder between two electrodes (sample assembly of the dielectric spectrometer) followed by

quenching on an aluminum block precooled to -20 °C. From this point onwards, the sample was handled under "dry" conditions (in a glove box maintained at < 5% RH; RT).

Dielectric spectroscopy. The experiments were performed using a time-domain dielectric spectrometer. A schematic of the experimental setup is shown in Figure 2.1. The sample cell assembly consists of two outer electrodes isolated with to provide electrical and thermal insulation. The inner electrodes (sample film sandwiched between two steel plates) are placed between the outer electrodes to form a parallel-plate capacitor. A power supply (TREK model 610C) is used to apply 200 V for 100 seconds to polarize the sample. The voltage drop across the integrating capacitor (2.2 nF), reflective of the polarization in the sample capacitor, was measured using an electrometer (Keithley 6514). The entire setup is controlled using a LABVIEW® program through a data acquisition board.

Measurements above the glass transition temperature. The film sample was heated from room temperature to the temperature of interest. The voltage pulse was applied as soon as the temperature stabilized (± 0.2 ^{o}C). This was repeated for a series of temperatures above T_g as shown in Figure 2.2a.

Measurements below the glass transition temperature. First, the measurements were carried out in samples out of equilibrium so as to obtain the relaxation time of a "*minimally aged glass*". The sample was first heated to (T_g + 10 ^{o}C) to remove the effect of thermal history and then cooled to the desired measurement temperature. In order to ensure that the dielectric probe is not influenced by the ongoing structural recovery, the measurement time (in this case 100 seconds) was less than 10% of the aging time[24]. Therefore, after thermally equilibration, the sample was aged for 1020 seconds and then

pulsed. This cycle was repeated for a series of temperatures as shown in Figure 2.2b. In a second set of experiments, the dielectric response was monitored as the sample was aged isothermally (Struik's protocol[24]). A fresh sample was used for each measurement temperature.

Data analysis

Relaxation time measurements. Time domain dielectric spectroscopy has been used to study the dynamics in glass forming materials, and specifically polymers[25,26]. In this technique, a constant dielectric stress (application of an electric field) is applied and the resultant dielectric strain (dielectric compliance) is measured as a function of time. The dielectric compliance is given by the relationship[27]:

$$\varepsilon(t) = \frac{D(t)}{E\varepsilon_o} \leftrightarrow \frac{Dielectric\ strain}{Dielectric\ stress} \quad (2.1)$$

where ε(t) is the dielectric compliance, D(t) is the dielectric displacement, E is the applied electric field and ε_o is the dielectric permittivity of vacuum. The modified KWW function[27] (eq 2.2) was used to fit the dielectric compliance measurements and a set of representative fitted parameters are provided in Table 2.1.

$$\varepsilon(t) = \varepsilon_1 + \varepsilon_2\left(1 - e^{-\left(\frac{t}{\tau}\right)^{\beta}}\right) + \frac{t}{\tau_c} \quad (2.2)$$

In equation 2.2, ε_1 is the zero time compliance, $\varepsilon_1 + \varepsilon_2$ is the long time plateau compliance, β is the shape parameter, τ is the relaxation time and τ_c is the conductivity time.

Time-temperature and time-aging time superposition. The superposition principle is based on the assumption that shape of the dynamic response curve (permittivity versus log time in this case) is independent of temperature or aging time. Thus, the curves can be

shifted horizontally to a reference curve thereby constructing a master curve in reduced time (t_{red}).

$$t_{red} = \frac{t}{a(i)} \qquad (2.3)$$

where a(*i*) is the horizontal shift factor and is determined by

$$a(i) = \frac{\tau(i)}{\tau(i)_r} \qquad (2.4)$$

In equation 2.3 *i* can represent either temperature (T) or aging time and $\tau(i)_r$ is the reference relaxation time. Instead of using the KWW equation to fit each curve, and then estimating $\tau(i)$ and a(*i*), the master curve was constructed by manual shifting. First a reference curve was selected and then the rest of the profiles, obtained at different temperatures, were superimposed on the reference curve by shifting along the time axis. The $\tau(i)$ was then determined as

$$\tau(i) = a(i) * \tau(i)_r \quad (2.5)$$

The curves superimposed very well except at short and long times (Figure 2.3). At short times, this observation is attributed to the appearance of a weak β-relaxation. The lack of superposition at longer time scales is due to interference from dc conductivity. Only the data ascribed to the structural relaxation, separated from the β-relaxation, was considered in this calculation.

2.3 Results and discussion

Non-isothermal relaxation behavior

The increase in viscosity, as the temperature decreases, causes the dipoles to take longer to orient in the direction of the electric field. Hence, the dielectric compliance curves shift

to longer times attributed to an increase in relaxation time (Figure 2.3). The steep rise after the secondary plateau is characteristic of dc conductivity[25,28].

In Figure 2.4, the conductivity term and the relaxation terms are plotted as a function of temperature. The data was fitted using the Vogel[29] - Fulcher[30] - Tamman[31] (VFT) equation (eq 2.6)

$$\tau = \tau_o \exp\left(\frac{DT_o}{T-T_o}\right) \qquad (2.6)$$

where τ is the relaxation time, T is the temperature and τ_o, D and T_o are constants, τ_o is the relaxation time of the unrestricted material (10^{-14} s, the quasi-lattice vibration period[15]), D is the strength parameter and T_o is the temperature of zero mobility (theoretical Kauzmann temperature). The fitted parameters, provided in Table 2.2, are in agreement with previous literature reports[32]. The D-value or the strength parameter, which is a measure of the kinetic fragility was ~ 7.2. This is in good agreement with the reported value of 7.3 and is indicative of a fragile glass former[32]. The calorimetric T_g typically exceeds the kinetic T_g by 2 to 3 degrees and this difference varies with the fragility of the system[33]. Nifedipine exhibited a similar behavior. The kinetic T_g ($T_{g,kinetic}$) calculated using the VFT parameters, assuming a relaxation time of 100 s, was ~ 40.9 ^oC, whereas the calorimetric T_g ($T_{g,cal}$) was 44.5 ^oC. Unless otherwise mentioned, we will use the $T_{g,cal}$ value.

In the supercooled state, the temperature dependence of the relaxation time (τ) as well as conductivity (τ_c) is well described by the VFT model. However, since their fit parameters are different, a spread in the dielectric response is observed at longer times (Figure 2.3b). To eliminate the contribution of dc conductivity, the recoverable dielectric compliance ε_R (t) was estimated using equation 2.7[27]

$$\varepsilon_R(t) = \varepsilon(t) - \frac{t}{\tau_c} \qquad (2.7)$$

For each temperature, ε_R (t) was determined and plotted in Figure 2.5a. We observe an increase in ε_1 and a slight decrease in ε_2 as the temperature increased. This is in agreement with previous literature reports and is attributed to the "softening like" behavior of the secondary plateau[25, 27]. In equation 2.2, ε_1 is related to the glassy (short time) response and ε_2 is related to the transition to the long time plateau. In addition to the horizontal shift, the curves were shifted vertically to obtain a reasonable time-temperature superposition (Figure 2.5b).

In the glassy state, structural rearrangement is manifested by a reduction in molecular mobility and reflected by an increase in relaxation time. The relaxation time increases by ~ 3 orders of magnitude when the temperature decreases from T_g to (T_g – 14) (Figure 2.6a). As we enter the glassy state, the structural relaxation appears to be "in equilibrium" up to (T_g – 6) and then diverges from the equilibrium supercooled line. Another way of interpreting the data is by analyzing in terms of T_f (Figure 2.6b). The slope of the line in the supercooled liquid region is 1.0 reflecting T_f = T at equilibrium. On the other hand, as we enter the glassy state, the slope is approximately zero indicating that T_f does not change significantly with temperature and the glass is considered "stable".

Isothermal relaxation behavior

DSC is the technique of choice to study the physical aging behavior of amorphous pharmaceuticals[23,34,35,36,37]. However, the enthalpic recovery measurements necessitate real time storage of the glass at the specific temperatures of interest. Thus the experiments can become time consuming. In the dielectric physical aging carried out using the Struik's protocol[24,38], snapshots (dielectric response) are taken at regularly

timed intervals to track the path towards equilibrium. The material is considered to have *"aged into equilibrium"* when the dielectric response ceases to evolve. Physical aging studies were carried out at several temperatures below T_g. At (T_g – 2), the dielectric curve obtained after aging for 0.5 and 1 h completely overlapped implying completely relaxation into equilibrium in $\leq$ 1 hour (Figure 2.7a). Similar results were obtained at (T_g – 4) and (T_g – 6) (Figure 2.7b and c). With a decrease in temperature, it takes longer to achieve equilibrium as can be seen at (T_g – 12) (Figure 2.8a). As the aging time is increased, the curve is shifted to the right on the time axis i.e. the response is shifted to longer times. With aging, the free volume decreases and it takes longer for the dipoles to orient in the direction of the electric field. We used the principle of time - aging time superposition[39] to horizontally shift the curves onto a reference aging time curve (t_e = 0.5h) and obtain a master curve (Figure 2.8b). The successful construction of the master curve indicates that the shape parameter, β, remains unchanged during aging as has been shown in the polymer literature[40,41, 42]. The master curve provides the time dependence of aging time shift factor[39],(a_{te}), similar to the temperature shift factor (a_T). From this information, we calculated the relaxation time as a function of aging time (Figure 2.9a). Since the motions are faster near the glass transition, the sample ages into equilibrium within 0.5 h whereas, at lower temperatures, aging becomes slow and is not complete even after 16 h. At (T_g – 10) and (T_g – 12), a sharp increase in relaxation time is observed in the first 4 h and then the change is less pronounced. Such an effect of physical aging on relaxation time has been reported for numerous compounds[26,43,44,45]. At temperatures lower than (T_g - 8), the aging studies had to be discontinued because of crystallization (data not shown).

A stretched exponential function (eq 2.8) was used to fit the isothermal aging data obtained at select temperatures.

$$T_f - T_a = Ae^{-\frac{t^\beta}{\tau}} \quad (2.8)$$

where T_f is the fictive temperature, T_a is the annealing temperature, A is the pre-exponential factor, β is the stretched exponential and t is the aging time. T_f is defined as the temperature at which a non-equilibrium property *p* (enthalpy or entropy) of a glass, *in excess with respect to the stable crystalline state*, would have the same value as in the equilibrium supercooled liquid. In this case, T_f was estimated by the following relationship: $\tau(T)|_{glass} = \tau(T_f)|_{\text{ supercooled liquid}}$. We resorted to this approach since there was insufficient data to obtain a reasonable slope value in the glassy state. Equation 2.8 was fit to the data using MATLAB to minimize the least-squared criteria. First the model was used to fit the data set at 37 ^oC by allowing all the parameters to vary. We obtained a β value of 0.52 at 37 ^oC. Typically values between 0.2 and 0.8 have been observed for small molecule glass formers. Variation of all parameters provided physically insignificant values for the 33 and 35 ^oC data. Hence, the β parameter was fixed at 0.52 for both 33 and 35 ^oC. In addition, for 35 ^oC, the τ value was constrained to obtain a reasonable trend in τ values as a function of temperature. The fitted profiles are shown as black solid lines in Figure 2.9b. The few data points limit us from obtaining a reasonable fit. However, this study lays the groundwork for future in-depth investigations to model the structural relaxation behavior and predict the behavior under any given thermal history. The fit parameters obtained using the approach described above are provided in Table 2.3. The relaxation time, obtained from the fitting procedure, increases as the temperature decreases due to an increase in viscosity. The fitted τ values for 35 and 37

^{o}C, unlike 33 ^{o}C, are in good agreement with the equilibrium supercooled liquid. This may be because at these temperatures, the glass has aged closer to equilibrium as compared to 33 ^{o}C. For all aging temperatures, δ decreases as time evolves and approaches zero asymptotically (Figure 2.9b). As the aging temperature decreases, δ increases and the curves will eventually approach zero at longer times.

Figure 2.10 provides a comprehensive picture of the time and temperature dependence of structural relaxation (two essential characteristics) across the glass transition for nifedipine aged for different times (≤16 h). Aging led to an increase in the activation energy of structural relaxation and the glass progressively moved towards the VFT line, i.e. the "*equilibrium behavior*".

2.4 Significance and practical implications.

Many amorphous materials, specifically drug substances, are stored in the glassy state. The molecular mobility is of great relevance in light of its potential influence on numerous properties of practical interest including stability and water sorption behavior[46,47,32]. If these properties are directly correlated to molecular mobility, as has been demonstrated in a limited number of systems, rapid attainment of "equilibrium" may be desirable. This is the first investigation in a drug substance, detailing the direct measurement of the relaxation behavior (evolution of relaxation time).

Both the method of preparation of a glassy drug substance and the presence of additives (commonly referred to as excipients) in a drug product provide an avenue to modulate mobility. Bhardwaj et al[43] have shown the effect of preparation method on the mobility of glassy trehalose and further linked it to stability. Trehalose exhibits an unusual behavior

in that the structural relaxation below T_g is fast enough to be monitored by frequency domain dielectric measurements. However, such fast dynamics is not expected in a majority of organic compounds including pharmaceuticals. In these cases, time domain dielectric spectroscopy will be the technique of choice. Therefore, the next logical step will be to evaluate the effect of preparation method and excipients on the relaxation behavior (evolution of relaxation time) of pharmaceutical glasses.

2.5 Conclusions

Time domain dielectric spectroscopy was used to experimentally characterize the structural relaxation behavior in glassy nifedipine. Time - aging time and time - temperature superposition principle enabled us to calculate the time and temperature dependence of relaxation time. The departure from equilibrium during isothermal aging was well described by the stretched exponential fit. To the best of our knowledge, this is the first comprehensive investigation of structural relaxation behavior in a pharmaceutical glass. In light of the potential correlation between mobility and physical stability, the relaxation behavior is of significant practical importance.

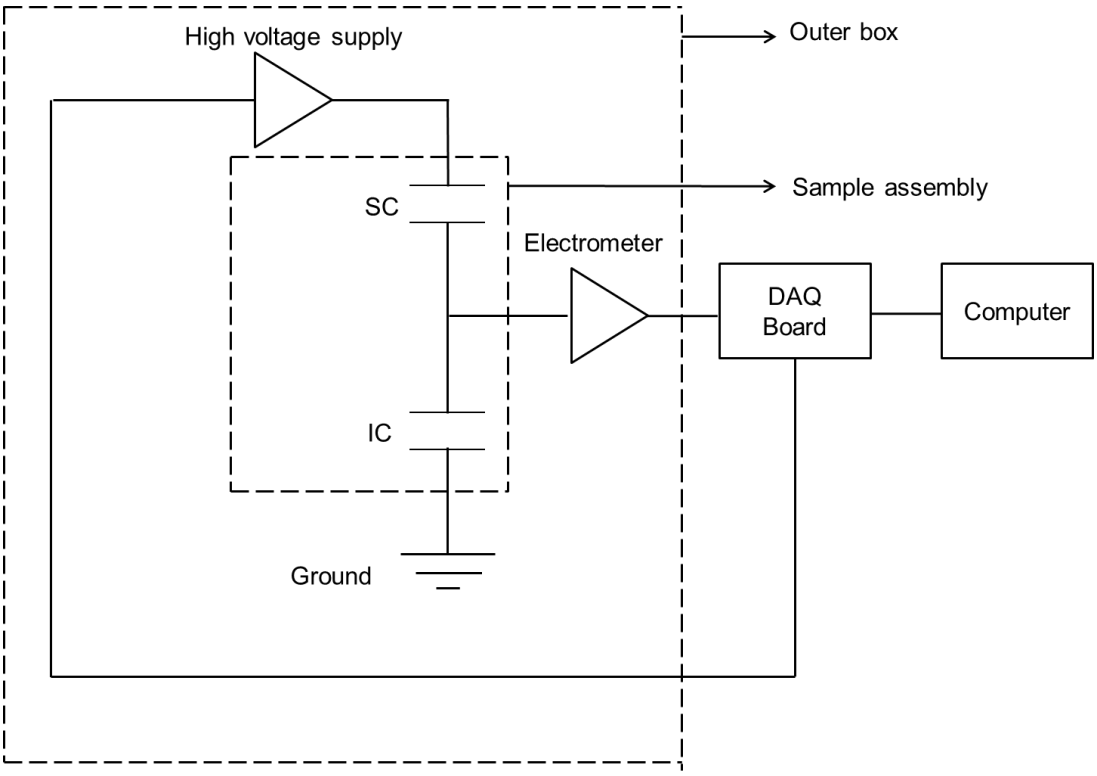

Figure 2-1 Schematic of the time domain dielectric spectrometer built in-house in the laboratory

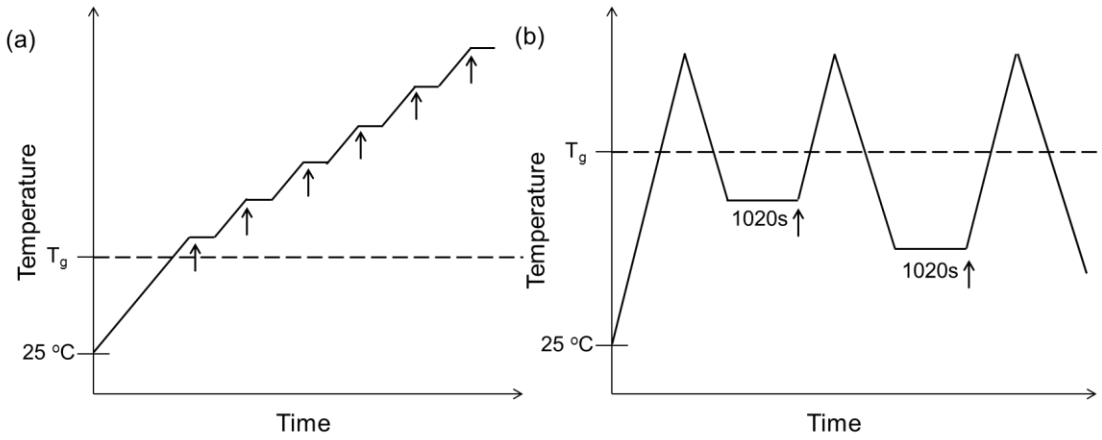

Figure 2-2 Schematic of the experimental protocol for time domain dielectric measurements performed (a) above and (b) below the glass transition temperature (*for a minimally aged glass*). The arrow indicates the application of dielectric probe (200 V, 100 s). Complete experimental details are provided in the text.

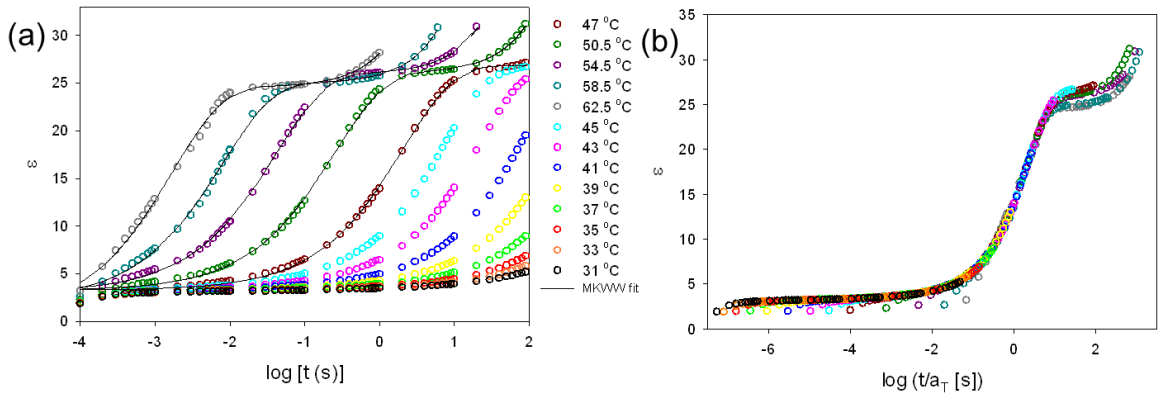

Figure 2-3 (a) The temperature dependence of the dielectric compliance response of nifedipine at temperatures above T_g (in equilibrium) and below T_g (non-equilibrium). The lines are the modified KWW function fitted curves. (b) The master curve was obtained using the principles of time-temperature superposition, with 47 ^oC as the reference temperature.

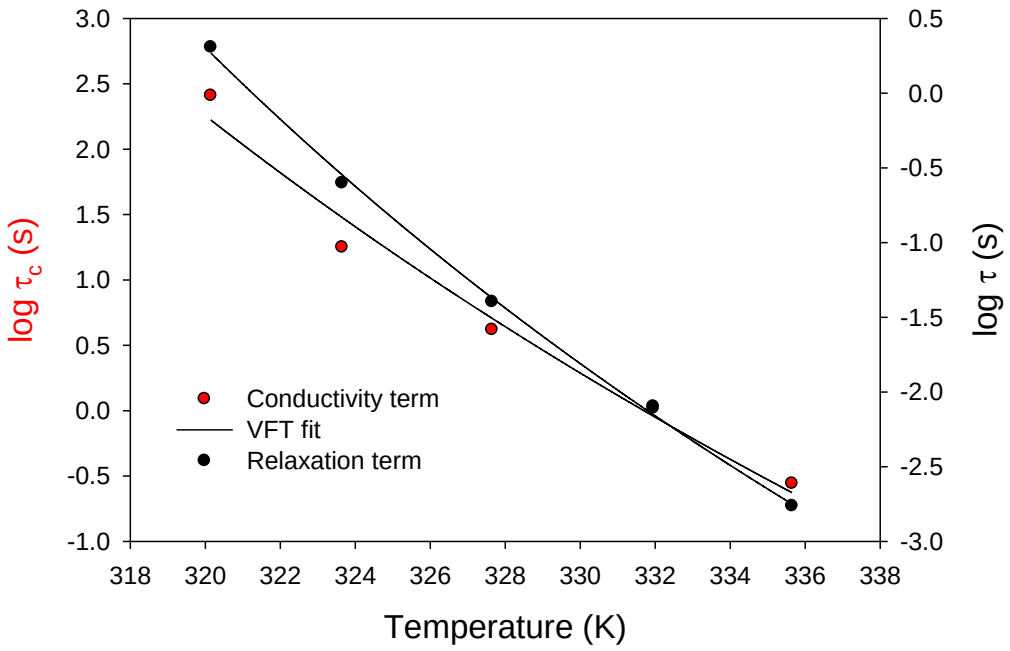

Figure 2-4 The dc conductivity term (τ_c) and dielectric relaxation time (τ) plotted as a function of temperature above T_g. The lines represent the VFT fits.

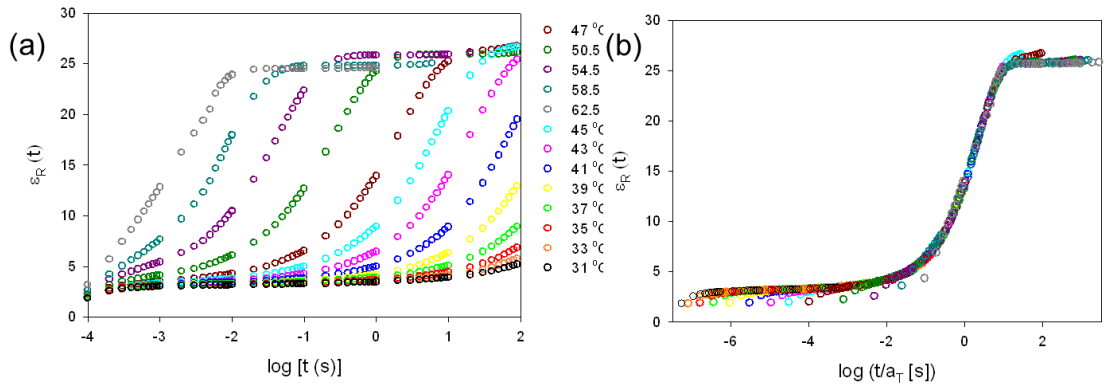

Figure 2-5 (a) The temperature dependence of the recoverable dielectric compliance response from 31 to 62.5 ^{o}C. (b) The master curve drawn with 47 ^{o}C as the reference temperature.

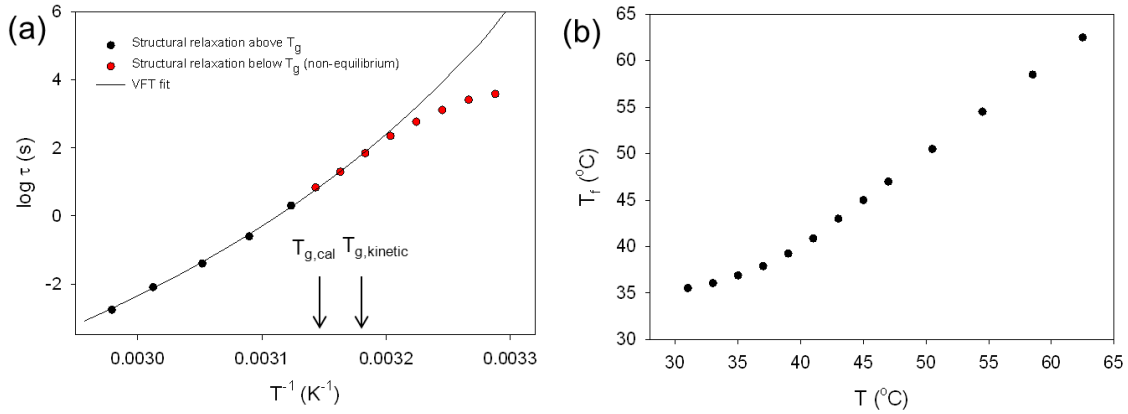

Figure 2-6 Plot of (a) temperature dependence of relaxation time and (b) T_f vs T in amorphous nifedipine

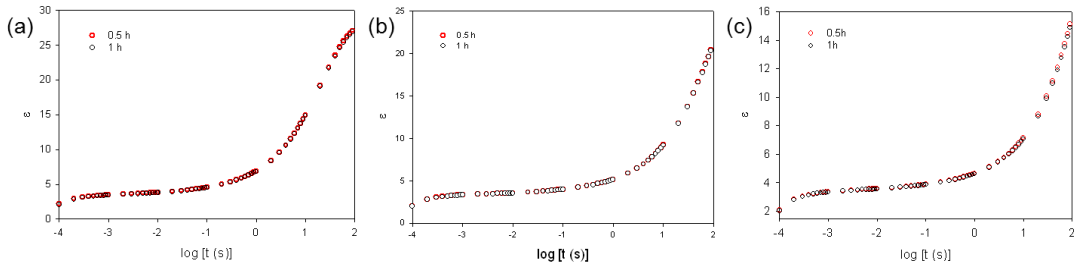

Figure 2-7 Time dependence of dielectric compliance at (a) 43 ^{o}C (T_g – 2), (b) 41 ^{o}C (T_g - 4), and (c) 39 ^{o}C (T_g – 6)

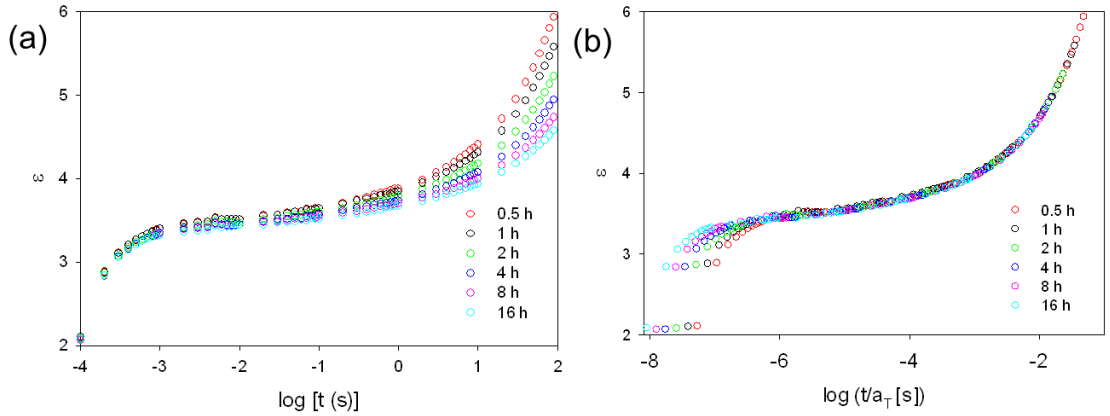

Figure 2-8 (a) Time dependence of dielectric compliance at 33 ^{o}C (T_g - 12) and (b) the master curve obtained using the principles of time - aging time superposition with 0.5 h curve as the reference.

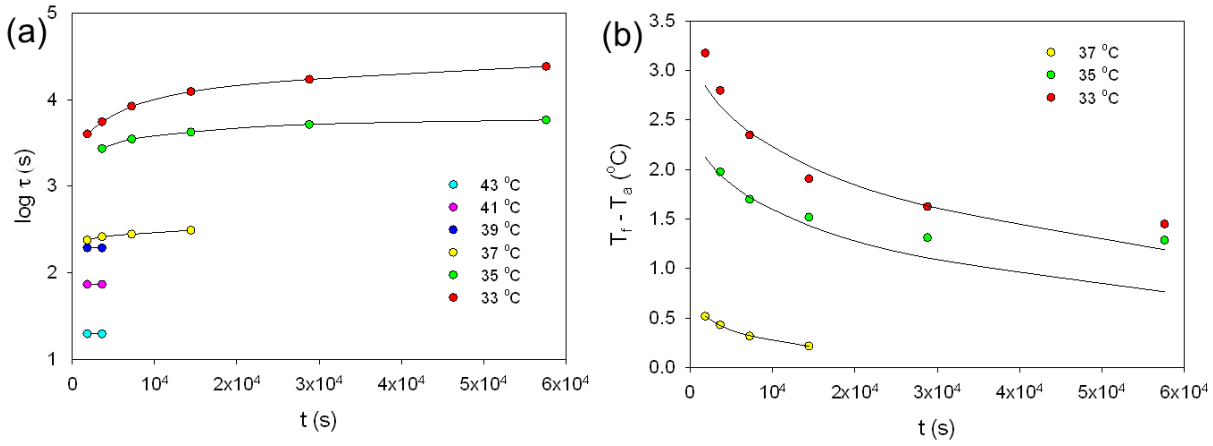

Figure 2-9 Plots of (a) average structural relaxation time and (b) departure from equilibrium, versus aging time. In the left panel, the solid lines are drawn to aid in visualizing whereas in the right panel the solid lines are the fitted profiles obtained using eq 2.8. For 35 °C, only the first four data points were used for fitting.

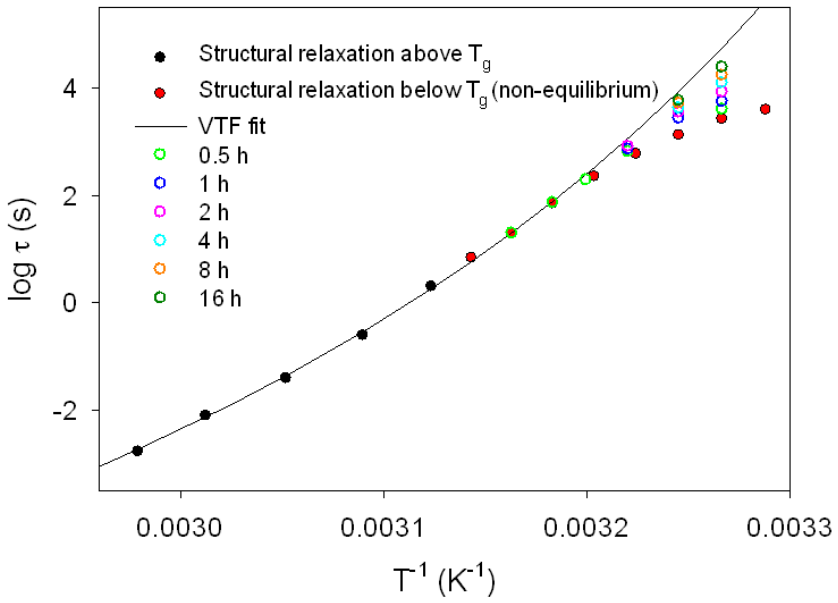

Figure 2-10 Comprehensive plot of the relaxation dynamics showing both the time and temperature dependence of structural relaxation

Table 2.1 Fit parameters for equation 2.2 at 52.5 ^{o}C (errors represent the standard errors of estimate for the fit parameters)

ε_1	ε_2	τ (s)	β	τ_c (s)
3.3 ± 0.1	22.7 ± 0.1	0.25	0.7	17.8 ± 0.6

Table 2.2 VFT parameter values obtained from model fitting of the relaxation time data (standard errors of fit are in parentheses).

	DT_o	T_o (K)
Nifedipine	1898 (42)	262 (1)

Table 2.3 Stretched exponential (eq 2.8) fit parameters obtained from model fitting of (T_f - T_a) versus logarithm of aging time

Temperature (°C)	A	β	τ (s)	
			Fitted	Calculated*
37	0.82	0.52	8225	10192
35	2.60	0.52	39000	67746
33	3.38	0.52	52976	539849

* Calculated τ value from the VFT fit

3 Correlation between molecular mobility and physical stability in supercooled & glassy pharmaceuticals*

http://pubs.acs.org/doi/abs/10.1021/acs.molpharmaceut.5b00853

3.1 Introduction

A large fraction of the new drugs under development are characterized by poor aqueous solubility[1]. As a result, their absorption following oral administration can be a challenge. Drug amorphization is an effective and popular strategy to enhance solubility[2]. However, a major challenge with this approach is the risk of crystallization due to physical instability. This can negate the bioavailability advantage brought about by the solubility enhancement. Hence, current research efforts are directed towards understanding the factors influencing crystallization. Molecular mobility has been extensively investigated in light of its possible role in governing physical stability[3,4,5,6,7]. Molecular mobility comprises both global and local motions. Global motion is cooperative in nature, and responsible for bringing about the glass transition. It is also referred as α- or structural relaxation. On the other hand, local motions (or secondary relaxations) are non-cooperative in nature and arise from either a part or an entire molecule[8,9]. In several compounds, structural relaxation time has been linked to physical stability in the supercooled state ($T > T_g$)[10,11,12]. Interestingly, β-relaxation (also referred to as Johari-Goldstein relaxation[13]) has been implicated in physical instability of glasses ($T < T_g$)[14,15,16,17]. Since amorphous pharmaceuticals are typically stored as glasses, evaluation of such correlations in this state is of immense practical value.

The structural relaxation time in the supercooled state is typically $< 10^2$ s, whereas below T_g, the relaxation time can be very long. Thus experimental measurement of the structural relaxation time can be very challenging. As a result, in several compounds including nifedipine, griseofulvin, phenobarbital and sorbitol, structural relaxation times have been

estimated using different modifications of the Adam-Gibbs model[5,7,18,19,20]. In light of the potential limitations of this model[21,22], direct experimental measurement of the structural relaxation time would be useful. Experimental measurements rely on evaluating the kinetics of structural relaxation following an environmental perturbation[18,23,24]. Mechanical measurements (for example, stress relaxation) can provide insight into transport properties such as viscosity and relaxation time[25]. While this approach warrants further investigation, the brittle nature of pharmaceutical compounds may limit our ability to perform these measurements. Differential scanning calorimetry (DSC) provides an "average" measure of mobility but does not provide direct information about the contribution from different types of molecular motions. Dielectric spectroscopy (DES) allows direct measurement of molecular motions associated with dipole reorientation in the frequency range of 10^{-6} to 10^{12} Hz[24, 26]. Time domain dielectric techniques such as isothermal depolarization and thermally stimulated current have been employed to characterize molecular motions in glassy pharmaceuticals[27,28]. In this report, we have used a combination of time domain and frequency domain dielectric techniques to comprehensively map the molecular dynamics (i.e. α and β-relaxation) in glassy and supercooled states.

Recently, Cicerone et al[29] showed that protein stability in numerous sugar matrices (> 100) was directly linked to β-relaxation processes. A similar result was observed in naproxen glass wherein the Johari-Goldstein relaxation was shown to be responsible for the physical instability[30]. Crystallization in glassy fulvene and indomethacin has also been circumstantially linked to β-relaxation[14,17]. On the other hand, in several pharmaceutical glasses including nifedipine, griseofulvin, phenobarbital and sucrose, the

structural relaxation time below T_g was shown to be coupled to crystallization[3,5,18,19]. However, in these cases, the relaxation time was either an estimate obtained using the Adam-Gibbs model or was obtained using DSC. While both α and β-relaxations have been shown to influence the physical stability in the glassy state, very few studies have systematically and comprehensively characterized all the mobility modes which may influence crystallization in the temperature range of interest. We had two specific objectives in order to accomplish this goal: (i) comprehensively characterize the molecular mobility, i.e. both global and local motions, in supercooled and glassy states of two model compounds (celecoxib and indomethacin) and (ii) investigate the potential correlation between crystallization and the specific mobility mode in the glassy state. The model compounds were chosen since they can be readily rendered amorphous by melt quenching[14,31] and tend to crystallize rapidly in the glassy state[6,32]. This enabled the development of correlation models to predict crystallization in systems of interest. The ultimate aim is to enable the development of stabilization approaches by modulating the specific mobility correlated with the observed physical instability.

3.2 Experimental section

Preparation of amorphous materials. Celecoxib ($C_{17}H_{14}F_3N_3O_2S$, purity > 98%) and indomethacin ($C_{19}H_{16}ClNO_4$, purity > 98%; γ-form) were used as received. Amorphous samples were prepared by melting the crystalline powder followed by quench cooling on aluminum blocks precooled to -20 °C. The melt was lightly crushed using a mortar and pestle in a glove box at room temperature (< 5% relative humidity). The films were prepared in a similar manner by melting the powder between the two electrodes (sample assembly of the dielectric spectrometer) followed by quench cooling. Further handling

was done at room temperature under “dry conditions” (in a glove box maintained at < 5% RH).

Differential Scanning Calorimetry. A differential scanning calorimeter (Q2000, TA Instruments, New Castle, DE) equipped with a refrigerated cooling accessory was used. The instrument was calibrated with tin (SRM 741a, NIST). The sample was accurately weighed and sealed in hermetically sealed aluminum pans. All the measurements were done under dry nitrogen purge (50 ml/min) at a heating rate of 10 ºC/min following a cooling at the same rate. The T_g was determined as the midpoint of the glass transition region in the DSC curves.

X-ray diffractometry (XRD). A powder X-ray diffractometer (D8 ADVANCE; Bruker AXS, Madison, WI, USA) equipped with a variable temperature stage (TTK 450; Anton Paar, Graz-Straßgang, Austria) and Si strip one-dimensional detector (LynxEye™; Bruker AXS) was used. The isothermal crystallization kinetics, in the supercooled state, was evaluated at several temperatures. The powder samples were periodically exposed to Cu Kα radiation (40 kV & 40 mA), and the diffraction patterns were obtained under dry nitrogen purge by scanning over an angular range of 5 to 40° 2θ with a step size of 0.05° and a dwell time of 0.5 s.

Synchrotron XRD (SXRD; transmission mode). The enhanced sensitivity of this technique enabled us to monitor low levels of crystallization. Powdered samples, stored at several temperatures in the glassy state, were hermetically crimped in DSC pans and exposed to synchrotron radiation. Experiments were performed in the transmission mode in the 17-BM-B beamline at Argonne National Laboratory (Argonne, IL, USA). A monochromatic X-ray beam [wavelength 0.75009 Å; beam size 250 μm (horizontal) ×

160 μm (vertical)] and a two-dimensional area detector (XRD-1621, PerkinElmer) were used. Calibration was performed using an Al_2O_3 standard (SRM 674a, NIST). Using a stepper motor, the sample was oscillated (±1 mm from the center along the horizontal axis) during data collection. Each sample was scanned at 30 points, with an exposure time of 1 s for each scan (2 mm/30 seconds), and the results were averaged. The raw images were integrated to yield one dimensional d-spacing (Å) or 2θ (°) scans using the GSAS II software developed by Brian H. Toby and Robert B. Von Dreele at Argonne National Labs[33].

Quantification of XRD data. At each time point, crystallinity index was calculated using eq 1. The crystallinity index can be considered equivalent to the % crystallinity, if the total integrated intensity (amorphous + crystalline) remains constant throughout the isothermal crystallization experiment[34].

$$crystallinity\ index = \frac{intensity\ of\ crystalline\ peaks}{total\ diffracted\ intensity} \qquad (3.1)$$

To quantify the crystallinity index, a custom-built program (using Fortran 77) was used. In this program, the amorphous intensity contribution was based on the experimental XRD pattern of the amorphous "reference" material. The subtraction of the amorphous intensity from the total pattern yielded the intensity contribution from the crystalline peaks. The percent crystallinity was plotted as a function of time, and a characteristic crystallization time (t_c) was obtained for a desired level of crystallization. The time taken for 2.5% of the drug to crystallize was defined as the characteristic crystallization time (t_c) for both above and below T_g.

Dielectric spectroscopy (DES). The molecular mobility was comprehensively characterized using both time and frequency domain dielectric spectrometers. The film

samples, 50 μm thickness, were sandwiched between two round electrodes (stainless steel and copper electrodes were used in time and frequency domain setup respectively). The secondary relaxations were characterized using a high performance frequency analyzer (Novocontrol Alpha-A, Novocontrol Technologies, Germany). The isothermal dielectric measurements were carried out in the frequency range of 10^{-2} to 10^{7} Hz between -100 and 80 ºC.

The structural relaxation time, in both glassy and supercooled states, was measured using an in-house built time domain dielectric spectrometer[35]. For measurements in the supercooled state, the film sample was heated from room temperature to the temperature of interest. The voltage bias (200 V for 100 seconds) was applied as soon as the temperature stabilized (± 0.2 ºC). This was repeated for a series of temperatures above T_g. In the glassy state, the measurements were carried out in "*minimally aged glasses*". The sample was first heated to (T_g + 10 ºC) to remove the effect of thermal history and then cooled to the desired measurement temperature. In order to ensure that the dielectric probe is not influenced by the ongoing structural recovery, the measurement time (in this case 100 seconds) was less than 10% of the aging time[36]. Therefore, after thermal equilibration, the sample was aged for 1020 seconds and then pulsed. This cycle was repeated for a series of desired temperatures.

3.3 Data analysis

Frequency domain dielectric spectroscopy.

The secondary relaxations were fitted using the Cole - Cole[37] function (eq 3.2; an empirical function described in detail by Kremer[38]) to obtain the average relaxation time (τ_{FD}; FD - Frequency domain).

$$\varepsilon^*(\omega) = \varepsilon_\infty + \frac{\Delta\varepsilon}{(1+(i\omega\tau_{FD})^\gamma)} \qquad (3.2)$$

$$\varepsilon^*(\omega) = \varepsilon'(\omega) - i\varepsilon''(\omega) \qquad (3.3)$$

In eq 3.2, ω is the angular frequency, ε*(ω) is the complex dielectric permittivity (eq 3.3) consisting of real (ε') and imaginary components (ε") and Δε is the dielectric strength given by $\Delta\varepsilon = \varepsilon_s - \varepsilon_\infty$ where ε_s, static permittivity, gives the low frequency limit ($\omega \rightarrow 0$) of ε'(ω) and ε_∞ gives the high frequency limit ($\omega \rightarrow \infty$) of ε'(ω). The shape parameter (γ) can take values from 0 to 1 and accounts for the symmetrical broadening of the relaxation function in eq 3.2.

Time domain dielectric spectroscopy.

In this technique, a constant dielectric stress (application of an electric field) is applied and the resultant dielectric strain (dielectric compliance) is measured as a function of time. The dielectric compliance (ε) is given by the relationship[38]:

$$\varepsilon(t) = \frac{D(t)}{E\varepsilon_o} \leftrightarrow \frac{Dielectric\ strain}{Dielectric\ stress} \qquad (3.4)$$

where D is the dielectric displacement, E is the applied electric field and ε_o is the dielectric permittivity of vacuum.

The dielectric compliance behavior obtained could be described by the modified Kohlrausch[39] William-Watts[40] equation (KWW)[41] (eq 3.5), which includes the conductivity contribution.

$$\varepsilon(t) = \varepsilon_1 + \varepsilon_2(1 - e^{-(\frac{t}{\tau})^{\beta}}) + \frac{t}{\tau_c} \quad (3.5)$$

where ε_1 is the zero time compliance, $(\varepsilon_1 + \varepsilon_2)$ is the long time plateau compliance, β is related to the breadth of the relaxation spectrum, τ and τ_c are the relaxation and conductivity times respectively. If β remains constant with temperature, then the curves at different temperatures can be shifted horizontally to a reference curve thereby constructing a master curve in reduced time (t_{red}).

$$t_{red} = \frac{t}{a_T} \quad (3.6)$$

In eq 3.6, a_T is the temperature shift factor and is expressed as:

$$a_T = \frac{\tau_{TD}(T)}{\tau(T_{ref})} \quad (3.7)$$

wherein T_{ref} is the reference temperature. This is known as the time-temperature superposition (TTS) principle[42,43] an approach routinely used in polymer characterization[44]. Instead of using the KWW equation to fit each curve, and then estimating $\tau(T)$ and a_T, the master curve was constructed by manual shifting. First a reference curve was selected and then the rest of the profiles, obtained at different temperatures, were superimposed on the reference curve by shifting along the time axis. The $\tau_{TD}(T)$ was then determined as

$$\tau_{TD}(T) = a_T * \tau(T_{ref}) \quad (3.8)$$

where the $\tau(T_{ref})$ is determined from the fit to equation 3.5 for the data at $T_{ref.}$ At short times, the curves did not superimpose well due to presence of a weak β-relaxation (Figure

3.1). Only the data ascribed to the structural relaxation, separated from the β-relaxation, was considered in this calculation.

While the absolute relaxation times obtained from frequency and time domain dielectric measurements are not comparable, they exhibit the same temperature dependence.

3.4 Results and discussion

Baseline characterization. The amorphous materials were observed to be X-ray amorphous. The calorimetric glass transition temperatures ($T_{g,cal}$; celecoxib 55.3 ± 0.4 °C and indomethacin 45.1 ± 0.5 °C) were in good agreement with the literature values[23,45,46]. (DSC curves are included in Figure 3.10). The water content, determined by Karl Fischer titrimetry, was < 0.5% w/w.

Structural relaxation behavior. Figure 3.1a shows the dielectric response curves of celecoxib over a temperature range (39 to 65 °C) spanning the glassy and supercooled states. With a decrease in temperature, the observed shift in the dielectric response curves can be ascribed to an increase in relaxation time. The steep rise after the secondary plateau is attributed to dc conductivity[38]. Similar results were observed in case of indomethacin (Figure 3.1b).

Supercooled state. The average structural relaxation times (τ_{TD}), obtained by the TTS principle described earlier, were determined at several temperatures above T_g. The temperature dependence (Figure 3.2; black filled circles) was well described by the Vogel[47] - Fulcher[48] - Tamman[49] (VFT) model (eq 3.9)

$$\tau_{TD} = \tau_o \exp\left(\frac{DT_o}{T-T_o}\right) \qquad (3.9)$$

where T is the temperature and τ_o, D, T_o are constants, τ_o is the relaxation time of the unrestricted material (10^{-14} s, the quasi-lattice vibration period[50]), D is the strength

parameter[47,48,49] and T_o is the temperature of zero mobility (theoretical Kauzmann temperature). The VFT parameters are shown in Table 3.1 and are in agreement with literature values[6,45]. The fragility index[51,52], m, is related to D by eq 3.10[51] and the calculated values are provided in Table 3.1.

$$m = \frac{D}{ln10} * \frac{T_O}{T_g} * \frac{1}{(1-\frac{T_o}{T_g})\text{^}2} \quad (3.10)$$

These values (low D and high m) are indicative of fragile glass formers. The dielectric T_g values calculated using the VFT parameters, assuming a relaxation time of 100 s, were 49.5 ºC and 41.4 ºC for celecoxib and indomethacin respectively. These are in good agreement with the literature values of 54.8 ºC (celecoxib) and 41 ºC (indomethacin) obtained using dielectric spectroscopy[6,28]. Unless otherwise mentioned, we will use the $T_{g,cal}$ values.

Glassy state. In the glassy state, the structural relaxation slows down drastically, reflected by an increase in relaxation time. These motions appear to be "in equilibrium" up to (T_g – 6) and then diverge from the equilibrium supercooled line. The structural relaxation time increases by ~ 2.5 orders of magnitude as the temperature decreases from T_g to (T_g - 14) (Figure 3.2). The TTS principle enabled us to obtain the absolute structural relaxation time in the glassy state where the relaxation becomes extremely slow.

Secondary relaxations. Isothermal dielectric experiments. Isothermal frequency sweeps were carried out at several temperatures ranging from -100 to 80 ºC. A representative dielectric curve for celecoxib and indomethacin above T_g is shown in Figure 3.3. Interestingly, an excess wing was observed in the high frequency tail of the α-relaxation peak. This is a common feature of glasses, shown to be the high frequency flank of the β_{JG} relaxation, but masked by the α-relaxation contribution[53]. In an effort to check if the

excess wing is truly originating from the β_{JG} relaxation, we used the Ngai's coupling model[54,55]. This model considers the β_{JG} relaxation (referred to as independent relaxation, τ_o) to be the true precursor to α-relaxation (eq 3.11).

$$\tau_o = \tau_\alpha^{\beta_{KWW}} * \tau_c^{1-\beta_{KWW}} \qquad (3.11)$$

In this equation, β_{KWW} is a measure of the deviation from exponential decay of the α-relaxation peak and τ_c is the crossover time, typically ~2 ps in most glass formers[54]. The calculated primitive relaxation frequency ($f_o = 1/2\pi\tau_o$), in representative spectra of celecoxib and indomethacin, are shown in Figure 3.3. It can be seen that the calculated value of f_o lies in the frequency range where Havriliak Negami model for a single relaxation (α-), no longer adequately describes the data. Hence, the observed excess wing is truly characteristic of the hidden β_{JG} relaxation.

Temperature dependence of secondary relaxations in celecoxib. Three secondary relaxation peaks were observed between -90 and 50 ºC - the slowest β process, the faster γ process and the fastest δ process (Figure 3.4). As can be seen in Figure 3.2, the temperature dependence of these relaxations were well described by the Arrhenius equation:

$$\tau_{FD}(T) = \tau_\infty \, e^{\frac{\Delta E}{kT}} \qquad (3.12)$$

where τ_∞ is the pre-exponential factor, ΔE is the activation energy and k is the Boltzmann constant. The fitting parameters for the different relaxations are given below and are in reasonable agreement with the literature values[6]: log τ_∞ = -12.76, ΔE_β = 68 kJ/mol for β_{JG} relaxation; log τ_∞ = -14.64, ΔE_γ = 48 kJ/mol for γ relaxation and log τ_∞ = -9.52, ΔE_δ = 15 kJ/mol for δ relaxation.

Temperature dependence of secondary relaxations in indomethacin. Due to the weak β_{JG} relaxation signal in indomethacin, its temperature dependence could not be ascertained. The β_{JG} relaxation time is sensitive to pressure[56] while the temperature dependence of β_{JG} relaxation time remains unaffected by pressure as observed in sorbitol and xylitol[57,58]. The extent of correlation between the relaxation time and crystallization time depends on the temperature dependence rather than the absolute relaxation times. Therefore, we used the literature data for temperature dependence of β_{JG} relaxation time in indomethacin, obtained under high pressure[59]. The temperature dependence of γ- and δ- relaxation in glassy indomethacin could be reliably obtained (Figure 3.2b and 11). The fitted parameters are in excellent agreement with the literature values[59]: log τ_∞ = -10.54, ΔE_γ = 38 kJ/mol for γ relaxation and log τ_∞ = -13.69, ΔE_δ = 38 kJ/mol for δ relaxation.

Isothermal crystallization kinetics by XRD. *Supercooled and glassy state.* Crystallization occurred rapidly in the supercooled state and a laboratory source XRD was adequate to monitor crystallization kinetics. In the supercooled state, celecoxib crystallized as a mixture of forms I, II and III. As a representative example, the results obtained at 80 ºC are presented in Figure 3.5a and a peak unique to each form is pointed out[60]. The characteristic peaks appeared after 40 min, and their intensity progressively increased until crystallization was complete. Figure 3.5b shows the fraction of celecoxib crystallized at different temperatures. The isothermal crystallization data was well described by the modified Johnson-Mehl[61]-Avrami[62,63] (JMA) equation (eq 3.13):

$$\alpha(t) = \alpha_{max} - [(\alpha_{max} - \alpha_{min})e^{-(k(t-t_0))^n}] \quad (3.13)$$

where α(t) is the fraction crystallized at any time t, α_{max} is the fraction crystallized at t→∞, α_{min} is the fraction crystallized at t→0 and in this case it is fixed at 0 since there is

no crystal growth at t = 0, k is the rate constant, t_o is the crystallization onset time and n is the reaction order. Since crystallization was not complete, α_{max} was obtained by fitting the model to the crystallization data. The time taken for 2.5% of the drug to crystallize, t_c, was calculated from the fitted profile. By carrying out the experiments at several temperatures, the temperature dependence of t_c was obtained. Amorphous indomethacin was subjected to similar experiments. It crystallized in the α- and γ- forms in the supercooled and glassy states respectively (data not shown). For both indomethacin and celecoxib, the value of n (~ 1) remained constant in the temperature range studied.

The enhanced sensitivity of the synchrotron source at the Argonne National Laboratories enabled us to measure low levels of crystallization in both glassy celecoxib and indomethacin. The characteristic crystallization time, t_c, was taken as the time for 2.5% of the drug to crystallize (same as above T_g). Figure 6a contains representative SXRD patterns showing progressive drug crystallization in amorphous celecoxib at 45 ^oC. The 2D patterns were integrated to obtain the 1D XRD patterns, and t_c (Figure 3.6b). In the glassy state, only a mixture of forms II and III were observed.

Correlation between molecular mobility and crystallization. Assuming that molecular mobility is responsible for the observed physical instability, we attempted to identify the specific mobility responsible for crystallization. We therefore investigated the correlation between molecular mobility and crystallization behavior in amorphous celecoxib and indomethacin. In order to enable a visual comparison, the temperature dependence of different relaxations and the characteristic crystallization time (t_c, time taken for 2.5% crystallization) is plotted on the same graph (Figure 3.7). It is evident that crystallization in the glassy state is enhanced with respect to the prediction based on the extrapolation of

the data measured in the supercooled state. Similar results were reported by Ediger and Yu[64,65]. Above T_g, t_c and structural relaxation time show a similar temperature dependence. On the other hand, in the glassy state, the temperature dependence of t_c was markedly different from that of structural relaxation. The structural relaxation time appears to plateau off at ~ (T_g - 14) and the weak signal did not permit measurements below this temperature. It will be interesting to investigate the temperature dependence of structural relaxation and crystallization at temperatures << T_g. In the temperature range investigated in the glassy state, t_c and β_{JG} relaxation time showed a parallel relationship (Figure 3.7). The similar temperature dependence indicates that these two processes are coupled in the glassy state. Similar results were observed in indomethacin (Figure 12). One possible explanation is that, in the supercooled state transport properties (viscosity, diffusion) contribute to the observed crystal growth. Hence, we see a substantial correlation with structural relaxation time (discussed in more detail in the next paragraph). However, nucleation in the glassy state has been attributed to molecular motions involved in the Johari-Goldstein relaxation[66], a possible explanation for the observed correlation with the β_{JG} relaxation time.

In a log-log format, each regime (supercooled and glassy states) is well described by a linear relationship indicating a power law dependence of crystallization time (t_c) with relaxation time[67,68] (eq 3.14),

$$\log(t_c) = M\log(\tau) + A \quad (3.14)$$

wherein A is a constant and M is the value of the exponent. An exponent value of 1 indicates that the processes are completely coupled. The crystallization time versus average structural relaxation time plot in the supercooled state was linear (Figure 3.8).

The exponent value was determined to be ~ 0.8 in both celecoxib and indomethacin, indicating substantial but not complete coupling between crystallization time and structural relaxation time measured by dielectric spectroscopy. Thus factors other than molecular mobility (measured as structural relaxation time) are likely playing a role in the crystallization process. The time for 2.5% of the drug to crystallize was arbitrarily chosen since crystallization is slow in the glassy state. For the sake of consistency, we used the same level of crystallinity for the correlation plots in the supercooled state. The choice of different levels of crystallinity did not seem to affect the coupling coefficient (Figure 3.13). We have characterized the dielectric response due to the dipole reorientation. In the context of this discussion, rotational and translational modes of motion are of interest. These two motions decouple between T_g and 1.2 T_g, the temperature range of our studies, due to the breakdown of the Stokes - Einstein relationship[69]. However, in this temperature range, while the rotational motions and viscosity remain coupled, the crystal growth rates scale with $\eta^{-0.78}$. The translational diffusion coefficient and crystal growth rates exhibited the same temperature dependence in case of indomethacin, sorbitol and other small glass formers[12,70]. Since we did not observe complete coupling between rotational motions and crystallization time (M value of ~0.8; eq. 3.14), the physical stability in the temperature range of T_g to 1.2 T_g, may be better correlated to translational motions. Finally, we wanted to investigate if a specific molecular motion is coupled to the observed physical instability (crystallization) in the glassy state. We observed a poor correlation with the structural relaxation time (Figure 3.9a and 9b; celecoxib: 0.3, indomethacin: 0.2). This may be a manifestation of the enhanced decoupling, of the translational and rotational motions, due to the spatially

heterogeneous dynamics in deeply supercooled (i.e. at temperatures slightly above T_g) liquids[71]. The faster motions (γ- and δ- relaxations) originate from intramolecular motions of certain functional groups in celecoxib[72] and indomethacin. Therefore, their influence on physical instability is not considered significant. Finally, we wanted to consider the influence of β_{JG} relaxation on the crystallization process. In celecoxib, the β_{JG} relaxation time could not be experimentally obtained in the temperature range where crystallization was monitored. Since the β_{JG} relaxation exhibits an Arrhenius temperature dependence, we used the extrapolated relaxation times. Using equation 3.14, we observed a strong correlation between β_{JG} -relaxation and the characteristic crystallization time in glassy celecoxib and indomethacin (Figure 3.9c,d; celecoxib: 1.4, indomethacin: 1.1). Although the value of the exponent is expected to be between 0 and 1, the higher values may be attributed to experimental errors.

The β- relaxation process can be visualized as the motion of the entire molecule in these low density domains encaged by large cooperative regions which are relatively immobile[29]. It seems that the mobility in these local domains is sufficiently high to facilitate the right conformation to result in nucleation followed by growth. According to Hikima et al[73], the crystal-nucleation rate is determined by the β-molecular rearrangement and not by the α- mobility mode. Recently, the physical stability of amorphous celecoxib has been indirectly linked to β_{JG} relaxation[72]. The addition of octaacetylmaltose, while anti-plasticizing the β_{JG} relaxation (in this context, antiplasticization refers to an increase in β-relaxation time) had no significant effect on T_g and enhanced physical stability. Sibik et al[30] have also shown a strong correlation between fast dynamics and crystallization onset in several glass formers. In an exhaustive

study, a linear relationship between enzyme degradation rates and β- relaxation time in >100 plasticized (decrease in relaxation time) and antiplasticized sugar glasses was observed[29]. The degradation rate did not correlate with ($T-T_g$), a surrogate for structural relaxation time. The authors postulated that the anti-plasticization of fast motions caused stiffening of the glass matrix and decreased the degradation rate either by partial unfolding or reducing the exposure of highly reactive sites. In summary, our results reveal the strong influence of β_{JG} relaxation on crystallization in glassy indomethacin and celecoxib. It will be interesting and useful to investigate such a correlation in a wide variety of glassy pharmaceuticals. Once established, such correlation models can potentially be used to predict physical stability at temperatures of interest.

3.5 Conclusions

In this work, dielectric spectroscopy was used to comprehensively characterize the different modes of molecular mobility in supercooled and glassy celecoxib and indomethacin. Isothermal crystallization studies were carried out using a laboratory X-ray diffractometer whereas synchrotron source enabled similar studies in the glassy state. The structural relaxation time was coupled to the characteristic crystallization time in the supercooled state. However, we did not observe a similar correlation in the glassy state. Interestingly, a stronger correlation was observed between the β_{JG} relaxation time and physical instability in both glassy indomethacin and celecoxib. While limited to only two compounds, this study provides an avenue to predict the physical stability (measured as crystallization) of glassy pharmaceuticals. Antiplasticization of the β_{JG} relaxation can be a potential approach to enhance physical stability.

3.6 Acknowledgements

M.M. was partially supported by the Center for Pharmaceutical Processing and Research and Doctoral Dissertation Fellowship, University of Minnesota. The project was partially funded by the William and Mildred Peters endowment fund. The XRD studies were carried out at the College of Science and Engineering Characterization Facility, University of Minnesota, which receives partial support from NSF through the MRSEC program. Dr. Sunny Bhardwaj is thanked for helpful discussions and Karlis Bērziņš for helping with data analyses. This research used resources of the Advanced Photon Source, a U.S. Department of Energy (DOE) Office of Science User Facility operated for the DOE Office of Science by Argonne National Laboratory under Contract No. DE-AC02-06CH11357. We thank Dr. Gregory Halder for his help during the beamline experiment. Heelim Li is thanked for her help in sample preparation for synchrotron studies.

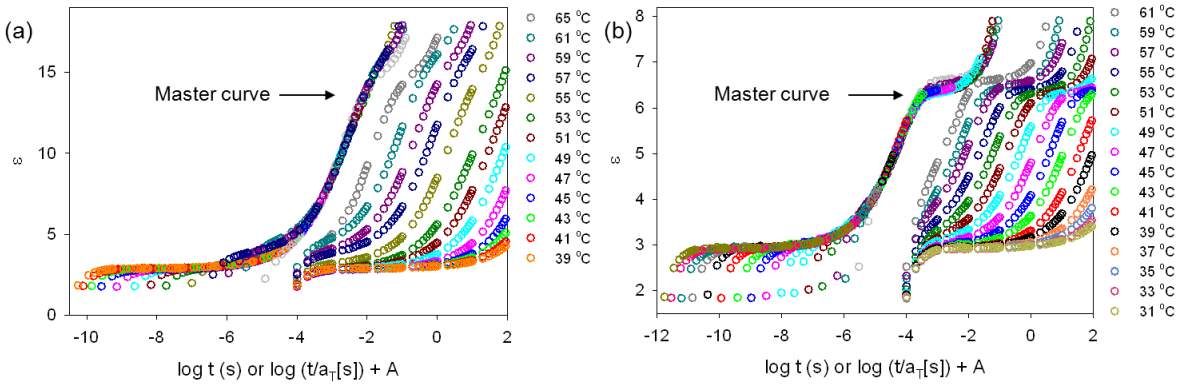

Figure 3-1 Dielectric compliance curves [ε(t)], where t is the duration of the voltage pulse, at different temperatures: (a) celecoxib and (b) indomethacin. The master curves were constructed with reference temperatures of 55 and 47°C for celecoxib and indomethacin respectively. For the sake of clarity, the master curve is offset by 3 decades for celecoxib and 4.5 decades for indomethacin.

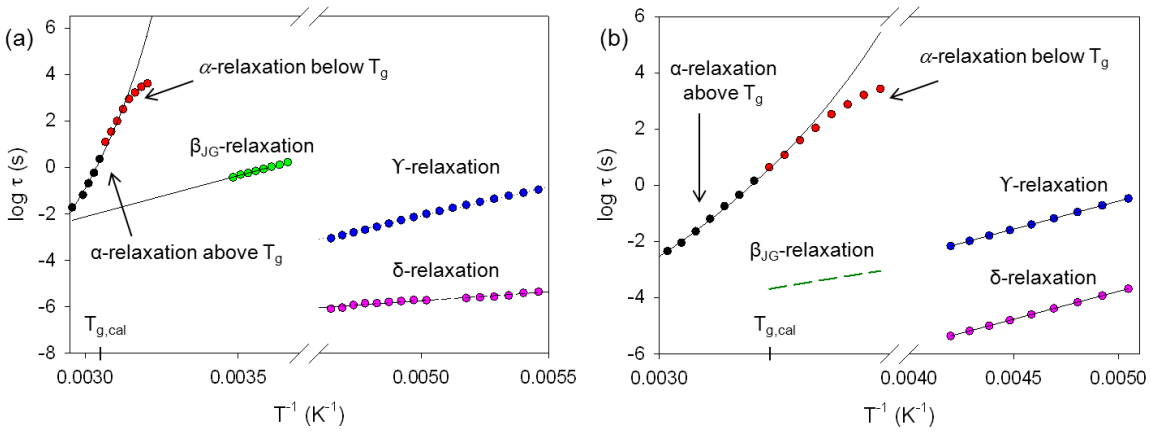

Figure 3-2 Plots of temperature dependence of relaxations in (a) celecoxib and (b) indomethacin. The β_{JG} values for indomethacin were obtained from the literature (reference 58). The black solid line describing the α-relaxation is the VFT fit obtained using eq. 3.9. The calorimetric T_g value is marked on the x-axis.

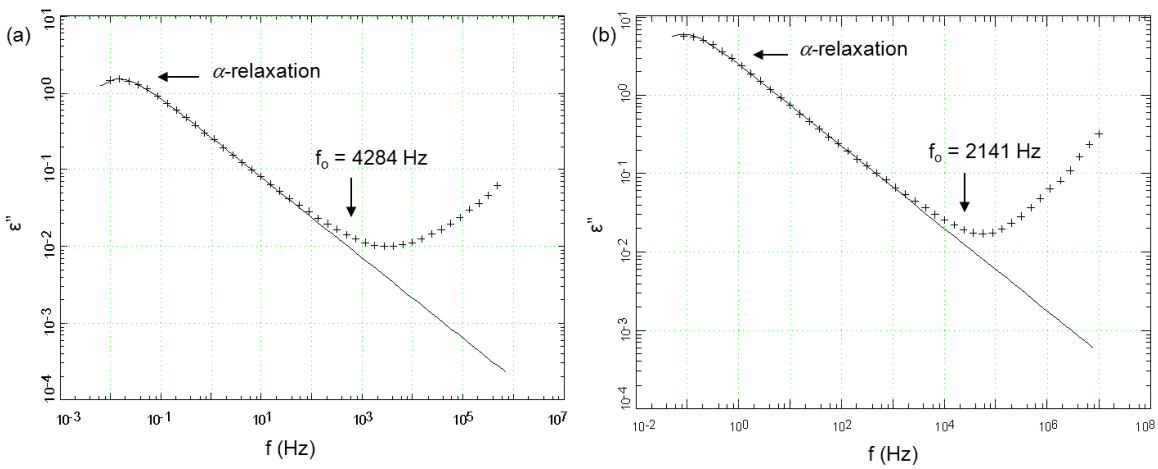

Figure 3-3 Plots of dielectric loss as a function of frequency in (a) celecoxib (at 60 °C) and (b) indomethacin (at 45 °C). Following the fitting of α-relaxation, the excess wing becomes evident. Vertical arrows indicate the position of f_o calculated using eq 3.11

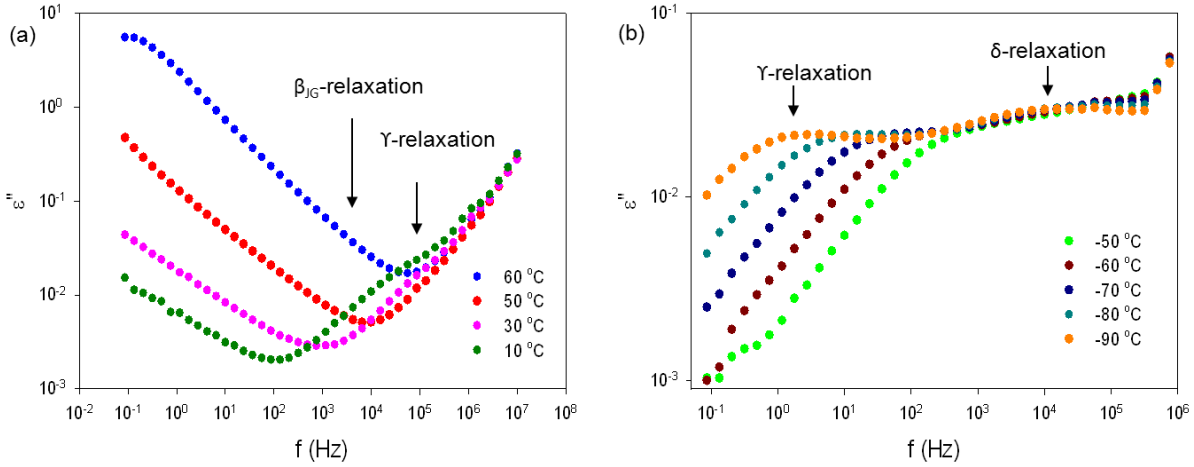

Figure 3-4 Dielectric loss spectra over the temperature range of (a) 10 to 60 °C and (b) -50 to -90 °C showing the presence of three secondary relaxations - β_{JG}, γ and δ- in amorphous celecoxib.

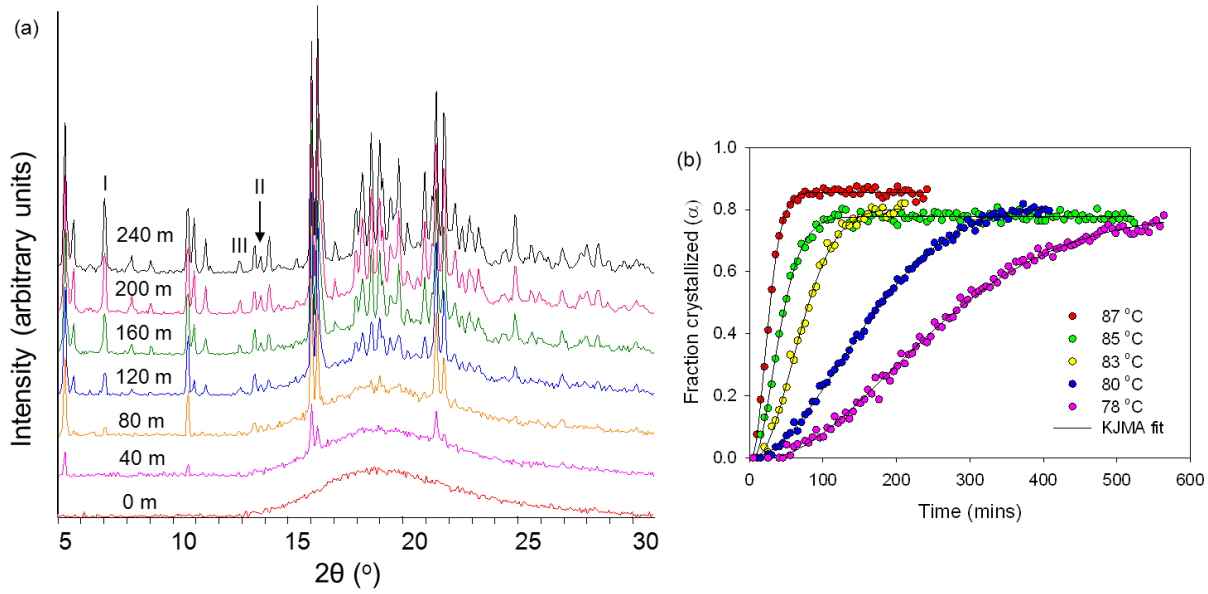

Figure 3-5 (a) Representative XRD patterns of amorphous celecoxib from 0 to 240 min (at 80 °C), and (b) fraction of celecoxib crystallized as a function of time at different temperatures. The solid lines are the fits obtained using eq. 3.13. A peak unique to each polymorph is pointed out.

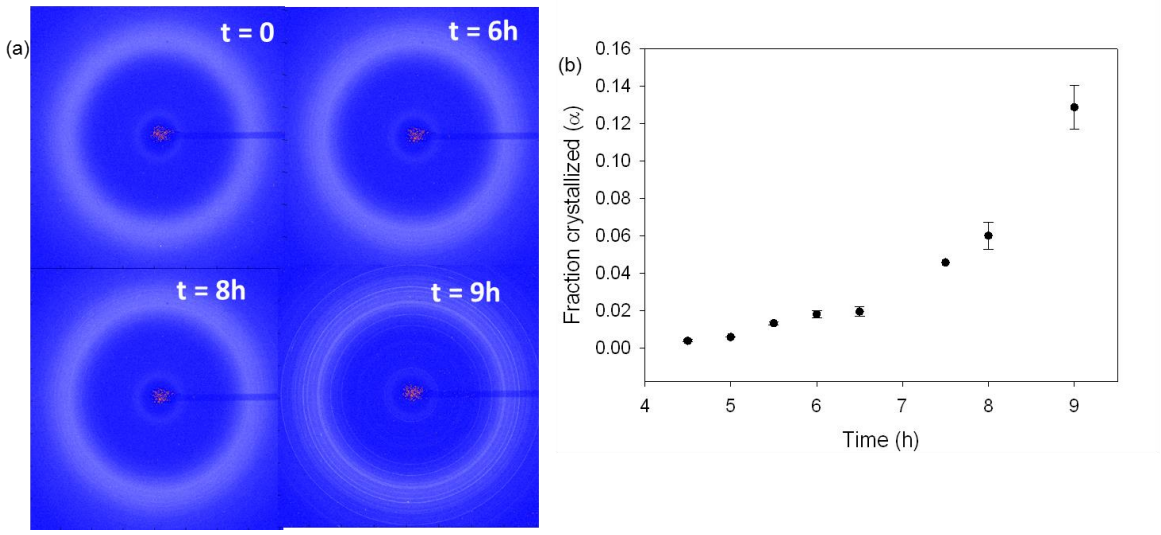

Figure 3-6 (a) Synchrotron XRD patterns of amorphous celecoxib at 45 °C as a function of time showing progressive crystallization, and (b) fraction of celecoxib crystallized as a function of time

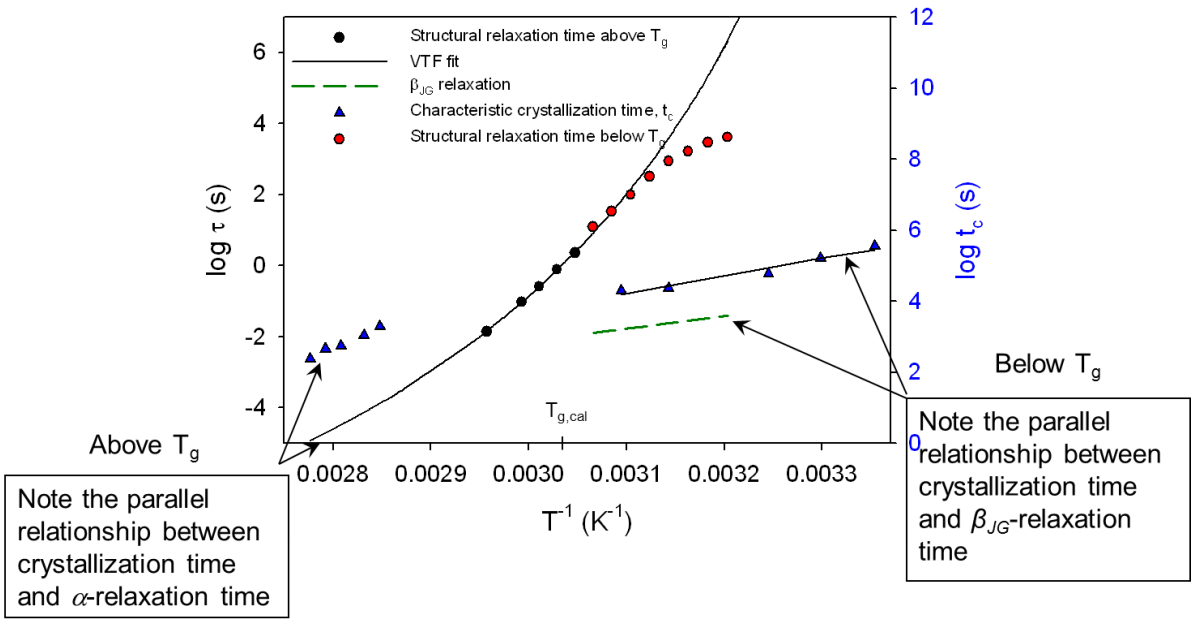

Figure 3-7 Temperature dependence of average relaxation time (left y-axis) and characteristic crystallization time (in blue, right y-axis) for different mobility modes in amorphous celecoxib. The β_{JG} -relaxation time was obtained by extrapolation since it shows an Arrhenius temperature dependence (Figure 3.2)

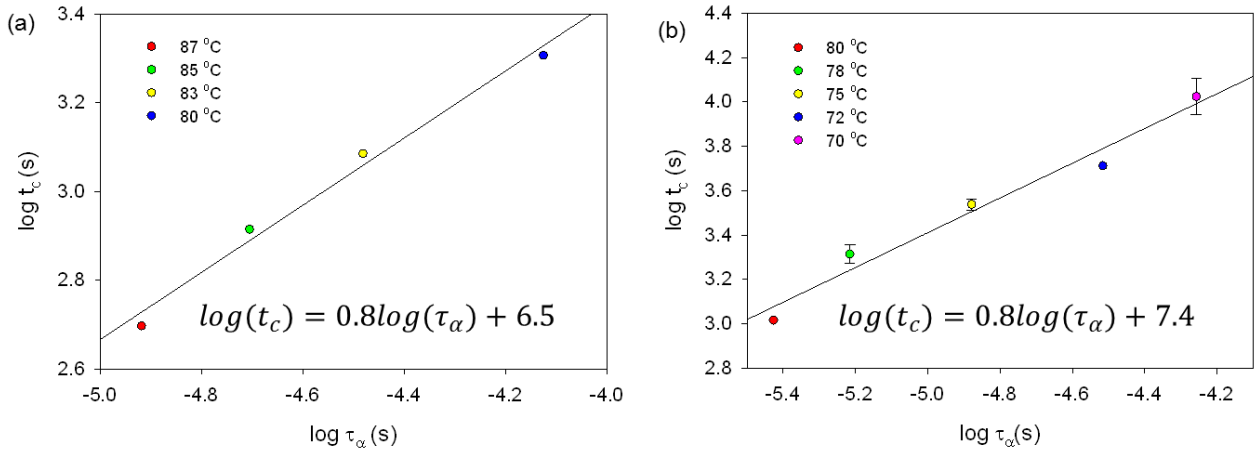

Figure 3-8 Plots of characteristic crystallization time (t_c, time taken for 2.5% crystallization) versus average α-relaxation time above T_g (measured using time domain dielectric spectroscopy) in (a) celecoxib and (b) indomethacin. The α-relaxation time was obtained by extrapolating the VFT fit to the temperature range of interest. Error bars are provided when n=3; otherwise the crystallization time is the average of two determinations.

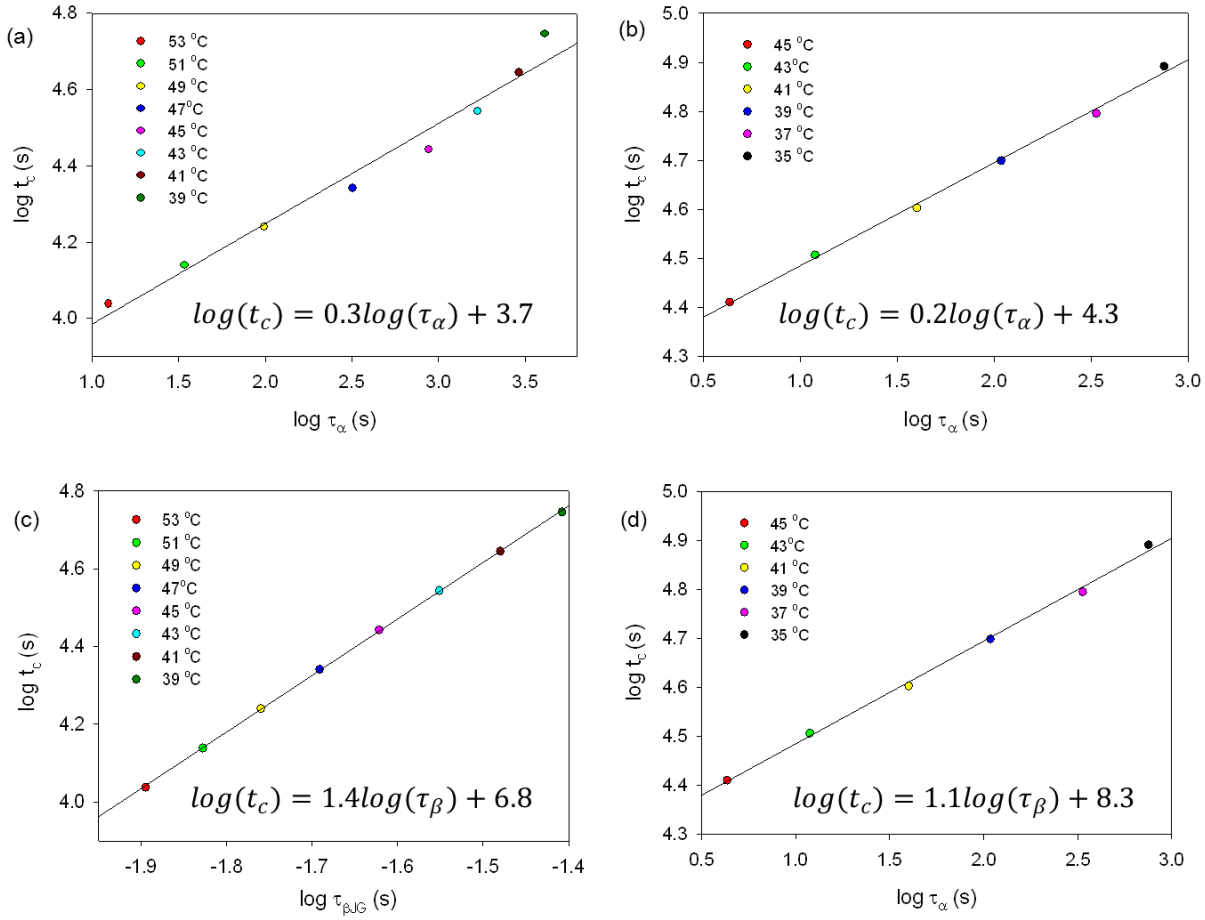

Figure 3-9 Plots of characteristic crystallization time (t_c, time taken for 2.5% crystallization; interpolated from figure 7 and 12) versus relaxation time below T_g in celecoxib (a & c) and indomethacin (b & d). Note - For celecoxib, the β_{JG} -relaxation time was obtained by extrapolation since it follows an Arrhenius temperature dependence. The β_{JG} -relaxation time, in indomethacin, has been digitized from ref. 59.

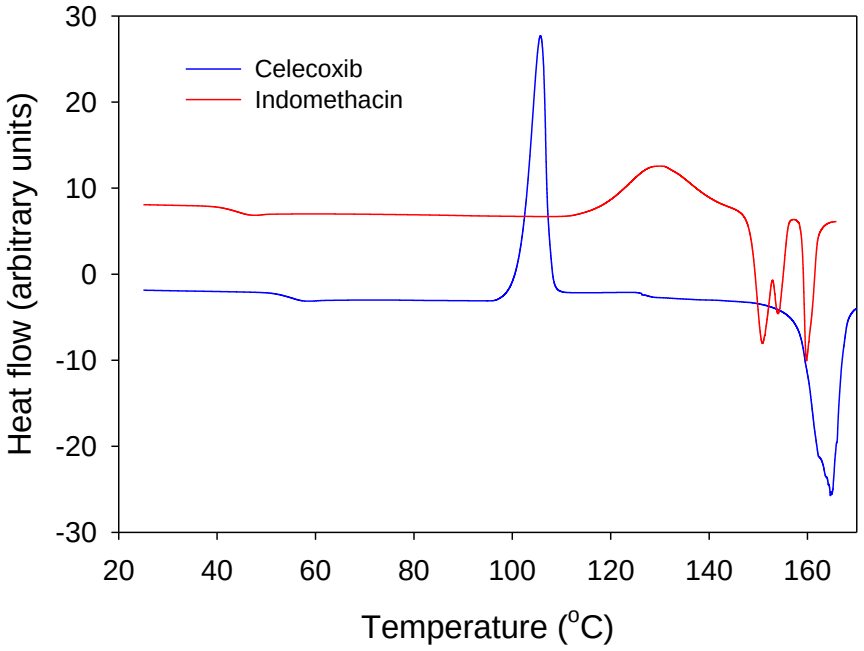

Figure 3-10 DSC heating curves (10 °C/min) of amorphous celecoxib and indomethacin

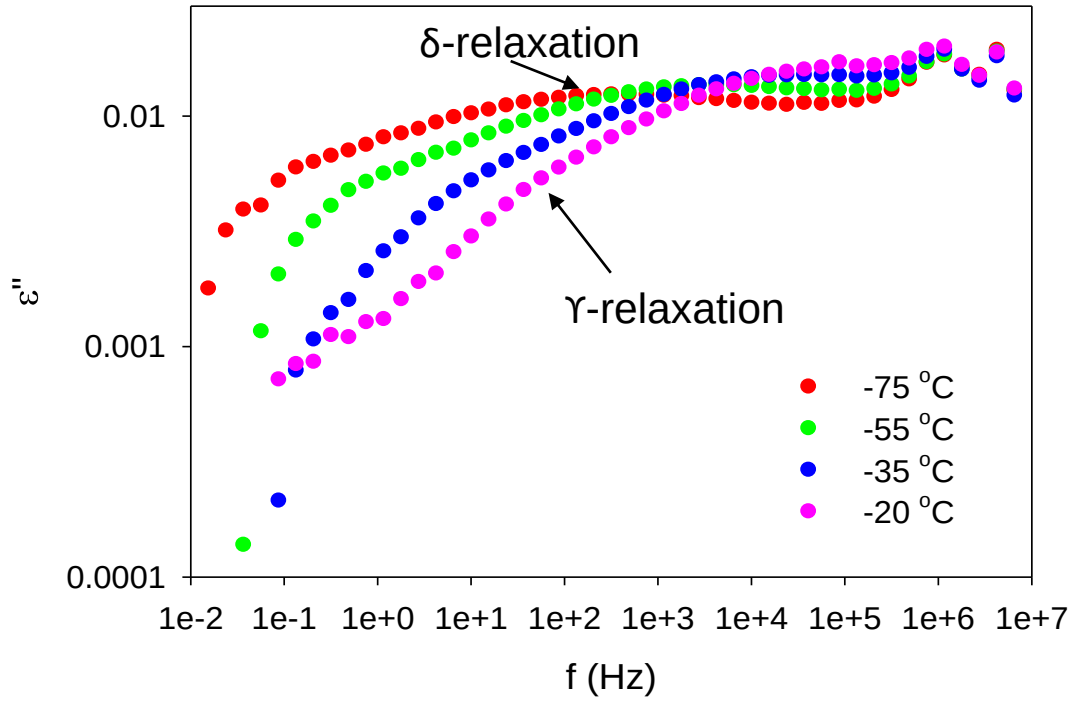

Figure 3-11 Dielectric loss spectra over the temperature range of -75 to -20 °C showing the presence of two secondary relaxations - δ and γ- in amorphous indomethacin

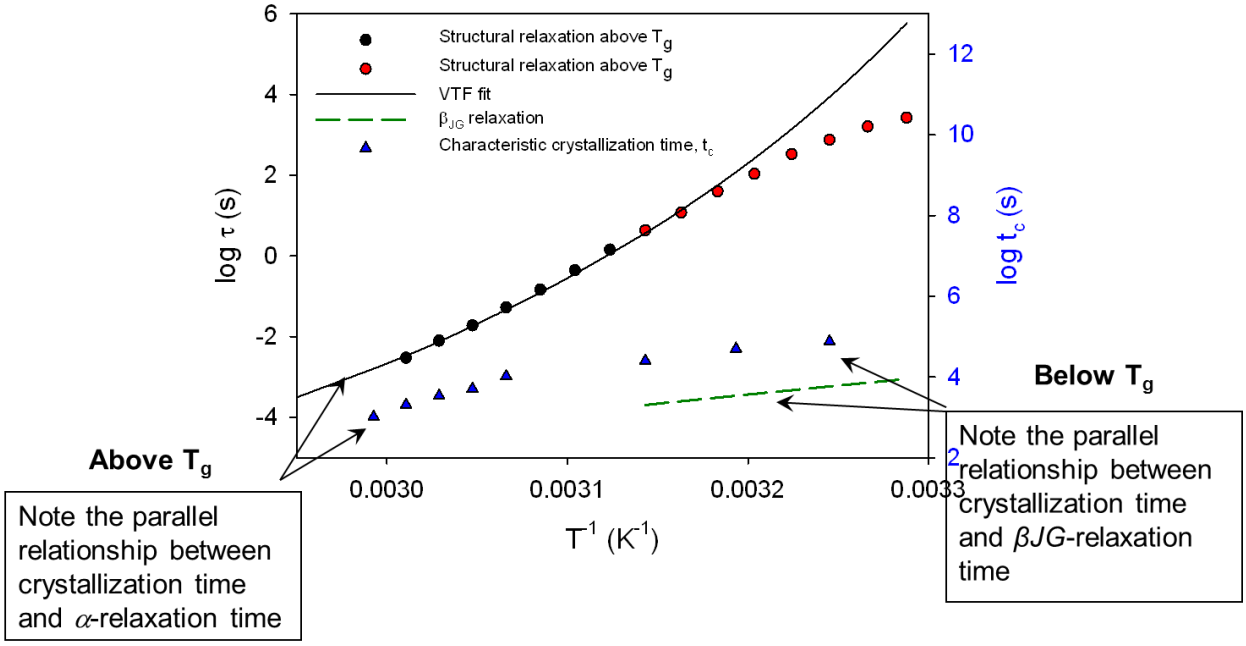

Figure 3-12 Temperature dependence of average relaxation time (left y-axis) and characteristic crystallization time (in blue, right y-axis) for different mobility modes in amorphous indomethacin.

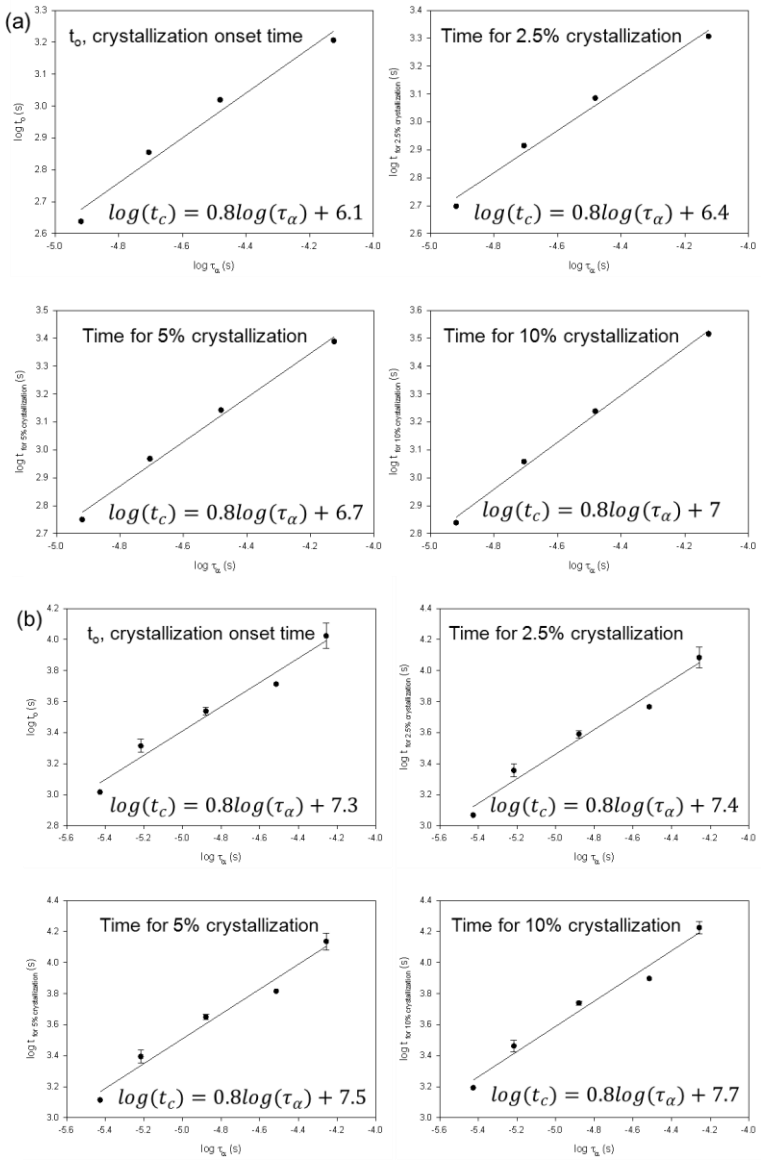

Figure 3-13 Plots of characteristic crystallization time (t_c) versus relaxation time above T_g in (a) celecoxib and (b) indomethacin for different levels of crystallization.

Table 3.1 VFT parameters (eq 3.9) obtained from model fitting of the relaxation time data

Sample	DT_o	T_o (K)	D	m
Celecoxib	1822 ± 69[a]	273 ± 2[a]	7	104
Indomethacin	1880 ± 30[a]	262 ± 1[a]	7	98

[a] Standard error of fitting

4 Molecular Mobility In Glassy Dispersions: Physical Stability Implications

4.1 Introduction

A large number of drug candidates under development suffer from the problem of aqueous insolubility. Among the numerous approaches, drug amorphization is an effective strategy to enhance the solubility and consequently the oral bioavailability of these new drug candidates. Solid dispersions, molecular drug − polymer mixtures, are known to physically stabilize amorphous drugs. However, the mechanism of stabilization by the polymer is not comprehensively understood. The role of thermodynamic and kinetic factors have been investigated in an effort to rationalize polymer selection[1,2,3,4]. The thermodynamic approach is of limited utility due to the typically low solubility of crystalline drugs in the polymers of interest[5,6,7]. Therefore, even at modest drug loading in a dispersion, the active pharmaceutical ingredient (API) is likely to be in a supersaturated state. Under such circumstances, crystallization inhibition is attributed to kinetic stabilization.

Molecular mobility can serve as a potential predictor of physical stability, in both amorphous drugs and their dispersions[8,9,10]. In the supercooled state, structural relaxation time (a measure of molecular mobility) was found to correlate with the crystallization time in nifedipine[11] (NIF) and itraconazole[10] solid dispersions. Drug-polymer interactions, by modulating molecular mobility, influence the physical stability of amorphous solid dispersions (ASDs)[12,13]. The hydrogen bonding interaction of NIF with poly(vinyl) pyrrolidone (PVP) was much stronger than with hydroxypropyl methylcellulose acetate succinate (HPMCAS). As a result, the reduction in molecular mobility was more pronounced in PVP dispersions leading to enhanced physical stability[8]. In ketoconazole ASDs prepared with different polymers, the strength of

interaction, the reduction in molecular mobility and crystallization inhibition followed the order: ionic > hydrogen bonding > dipole-dipole interaction[14]. Therefore, for preparing stable amorphous dispersions, molecular mobility can serve as a polymer selection tool. However, most of these studies were carried out in the supercooled state, i.e., at temperatures greater than the glass transition temperature T_g, rather than in the glassy state itself. The relationship between mobility and stability below T_g is warranted since ASDs are typically stored as glasses ($T < T_g$). In this work, we have investigated the structural relaxation behavior of glassy NIF dispersions prepared by mixing with either PVP or HPMCAS at different concentrations. As observed in the supercooled state[8], the strength of hydrogen bonding, structural relaxation time and crystallization followed the same order: NIF - PVP > NIF - HPMCAS > NIF. Thus the mechanism of physical stabilization in the glassy and supercooled states seems to be the same for these systems.

When the drug dose is high, ideally, the polymer should be effective at a low concentration so that the 'pill burden' is reasonable. Therefore, once a suitable polymer is selected, it is of immense practical interest to determine the minimum polymer concentration required to physically stabilize the drug during manufacture and storage. Previous work from our laboratory effectively employed molecular mobility as a tool to predict NIF crystallization in solid dispersions[15] (described later). Based on the observed crystallization kinetics in ASDs with low polymer concentration, the model enabled prediction of crystallization behavior at higher polymer concentrations. All of these investigations were carried out in the supercooled state. In order to extend this approach to the glassy state, it is necessary to directly measure the structural relaxation time (typically > 10^2 s). The time-temperature superposition (TTS) principle has been used to

obtain the relaxation time in pharmaceuticals[16,17,18,19] and polymers[20,21]. We hypothesize that this principle would be valid in ASDs and allow the calculation of temperature dependence of structural relaxation time in glassy dispersions. Interference from the β-relaxation can result in the potential breakdown of TTS[22,23,24,25,26]. This is often not readily evident in viscoelastic measurements because of their narrow dynamic range[20]. However, since dielectric spectroscopy covers a wide dynamic range, both α- and β-relaxations are more readily observed. In this work we have used dielectric spectroscopy, to perform TTS in NIF dispersions. We also evaluated the validity of time-temperature-concentration superposition. This provided a relationship between structural relaxation time and polymer concentration in the solid dispersions. To the best of our knowledge, this is the first application of the TTS principle to characterize structural relaxation in glassy dispersions. Secondly, the time-temperature-concentration superposition provides an avenue to predict the effect of polymer concentration on molecular mobility and, by extension, on the physical stability.

4.2 Experimental section

Materials. NIF ($C_{17}H_{18}N_2O_6$; Laborate Pharmaceutical Ltd, India), PVP (K12 grade; M_w ~ 2000 - 3000 g mol^{-1}; BASF, USA) and HPMCAS - HF (M_w ~ 18000 g mol^{-1} ; Shin-Etsu Chemicals, Japan) were used as received.

Preparation of amorphous drug and solid dispersions. Amorphous NIF was prepared by melting the crystalline powder and then quenching on an aluminum block precooled to -20 °C. The NIF dispersions were prepared by solvent evaporation followed by melt-quenching. For each polymer system, a physical mixture of NIF and polymer was dissolved in an appropriate solvent (acetone, methanol or dichloromethane). The solvent

was evaporated at 40 °C under reduced pressure in a rotary evaporator (IKA-HB10, Werke GmbH and Co., Germany). The samples were dried overnight, at room temperature, to remove excess solvent. PVP solid dispersions contained between 10 and 20% w/w polymer while the HPMCAS concentration was kept at 10% w/w. The powder was then heated to 5 °C above the melting point of NIF and quenched to -20 °C. The melt was lightly crushed using a mortar and pestle in a glove box at room temperature (< 5% relative humidity). The powders were stored at -20 °C in desiccators containing anhydrous calcium sulfate until further use. The films were prepared in a similar manner by melting the powder between the two electrodes (sample assembly of the dielectric spectrometer) followed by quench cooling.

Differential Scanning Calorimetry. A differential scanning calorimeter (Q2000, TA Instruments, New Castle, DE) equipped with a refrigerated cooling accessory was used. The instrument was calibrated with tin (SRM 741a, NIST). In a glovebox, accurately weighed samples were hermetically sealed in aluminum pans. All the measurements were done under dry nitrogen purge (50 ml/min) at a heating rate of 10 °C/min following a cooling step at the same rate.

Synchrotron XRD (SXRD; transmission mode). The enhanced sensitivity of the technique enabled us to monitor low levels of crystallization in select systems. Powdered samples were hermetically crimped in DSC pans and exposed to synchrotron radiation. Experiments were performed in the transmission mode in the 17-BM-B beamline at Argonne National Laboratory (Argonne, IL, USA). A monochromatic X-ray beam [wavelength 0.75009 Å; beam size 250 μm (horizontal) × 160 μm (vertical)] and a two-dimensional area detector (XRD-1621, PerkinElmer) was used. Calibration was

performed using an Al_2O_3 standard (SRM 674a, NIST). Using a stepper motor, the sample was continuously moved (±1 mm from the center along the horizontal axis) during data collection. Each sample was scanned at 30 points, with an exposure time of 1 s for each scan (2 mm/30 seconds), and the results were averaged.

Dielectric spectroscopy. The structural relaxation time was obtained using an in-house built time domain dielectric spectrometer[27,28]. For measurements in the supercooled state, the film sample was heated from room temperature to the temperature of interest, after the temperature stabilized (± 0.2 ^oC), the voltage bias (200 V for 100 s) was applied. This was repeated at several temperatures above T_g. The measurements below T_g were carried out in "*minimally aged glasses*", i.e., the dielectric measurements in the glassy state were carried out isochronally at a constant aging time (in this case 1020 seconds)[29]. The sample was first heated to (T_g + 10 ^oC) to remove the effect of thermal history and then cooled to the desired measurement temperature. In order to ensure that the dielectric probe is not influenced by the ongoing structural recovery, the measurement time (in this case 100 seconds) was less than 10% of the aging time[30].

4.3 Data analysis

Dielectric response data. The dielectric compliance behavior is often well represented by the modified Kohlrausch[31]-William-Watts[32] equation (KWW) (eq 4.1)[28], which includes the conductivity contribution.

$$\varepsilon(t) = \varepsilon_1 + \varepsilon_2\left(1 - e^{-\left(\frac{t}{\tau}\right)^{\beta}}\right) + \frac{t}{\tau_c} \quad (4.1)$$

where ε_1 is the zero time dielectric compliance, (ε_1 + ε_2) is the long time plateau compliance, β is related to the breadth of the relaxation spectrum, τ and τ_c are the relaxation and conductivity times respectively. Our previous study showed that, in the

temperature range of 31 to 62.5 ^{o}C, the time-aging time[33] and time-temperature[34] superpositions hold true in NIF[17].

Time-temperature and time-concentration superposition. The superposition principle is based on the assumption that the shape of the response curve (permittivity versus log time in this case) is independent of temperature or concentration. Thus, the curves can be shifted horizontally to a reference curve thereby constructing a master curve in reduced time (t_{red}).

$$t_{red} = \frac{t}{a(i)} \qquad (4.2)$$

where a(i) is the horizontal shift factor and is determined by

$$a(i) = \frac{\tau(i)}{\tau(i)_r} \qquad (4.3)$$

In eq (4.3) i can represent either temperature (T) or concentration and $\tau(i)_r$ is the reference relaxation time. Instead of using the KWW equation to fit each curve, and then estimating $\tau(i)$ and a(i), the master curve was constructed by manual shifting. First a reference curve was selected and then the rest of the profiles, obtained at different temperatures, were superimposed on the reference curve by shifting along the time axis. The τ(i) was then determined as

$$\tau(i) = a(i) * \tau(i)_r \quad (4.4)$$

The curves superimposed very well except at short and long times (Figure 4.1). At short times, this observation is attributed to the appearance of a weak β-relaxation. The lack of superposition at longer time scales is due to interference from dc conductivity. Only the data ascribed to the structural relaxation, separated from the β-relaxation, was considered in this calculation.

4.4 Results and discussion

Characterization of PVP and HPMCAS dispersions

Glass transition temperature. The calorimetric T_g ($T_{g,cal}$) values of NIF and the dispersions (10% w/w polymer) prepared with each PVP and HPMCAS were 45.7 ± 0.2, 46.2 ± 0.2 and 46.7 ± 0.2 °C respectively. The calorimetric T_g values were almost identical despite differences in their relaxation times (discussed later). The T_g values calculated using the Gordon - Taylor equation[35] (eq 4.5) for NIF - PVP and NIF - HPMCAS dispersions were 48.3 and 48.9 °C respectively [reported density (g/cm^3) values used for calculation: NIF (1.36)[36], PVP (1.23)[37], HPMCAS (1.29)[4]].

$$T_{g,mix} = \frac{w_1 + Kw_2 T_{g,2}}{w_1 + Kw_2} \qquad (4.5)$$

In this equation, w is the weight fraction and the value of K is given by $\rho_1 T_{g,1} / \rho_2 T_{g,2}$ [38]. The free volume additivity does not hold and the experimental T_g values were lower than those predicted using ideal mixing. The negative deviation can be attributed to a net loss in the degree of hydrogen bonding on mixing the two components[39].

Structural relaxation time. Dielectric spectroscopy was used to characterize the structural relaxation, both in the supercooled and glassy states. With an increase in temperature, the observed shift in the dielectric response curves can be ascribed to a decrease in relaxation time (Figure 4.1). The sharp increase in permittivity after the secondary plateau is attributed to dc conductivity[40,41]. The addition of the polymers caused a pronounced increase in conductivity, an effect attributable to ionic impurities in the polymers.

The effect exerted by PVP and HPMCAS on the molecular mobility is evident from the dielectric profiles shown in Figure 4.2. The rise in permittivity (ε), reflecting dipole

alignment, was most pronounced in NIF while NIF - HPMCAS and NIF – PVP showed similar and weaker increase in ε than pure NIF at long times. The time taken to reach the secondary plateau appears to increase in the following order: NIF < NIF - HPMCAS < NIF - PVP. That is, the dipoles seem to take slightly longer to orient in the NIF - PVP than in the corresponding HPMCAS dispersions. These observations indicate that the molecular mobility increases in the following order: NIF - PVP < NIF - HPMCAS < NIF (Figure 4.3). Though the differences between the NIF-PVP and NIF-HPMCAS systems do not appear very large in Figure 4.2, the quantitative analysis of the retardation times in Figure 4.3 shows this ordering clearly above the glass transition (Figure 4.3a), while the NIF and NIF-HPMCAS seem similar in the glassy state (Figure 4.3b).

At the selected "reference temperature", the relaxation time (τ) and shape parameter (β_{KWW}) were obtained using the modified KWW equation (eq 4.1). Assuming β remains constant, the relaxation times at the other temperatures of interest were calculated using the TTS principle. The relaxation time distribution is slightly broader in dispersions (β_{KWW} of 0.5 and 0.6 for PVP and HPMCAS dispersions respectively) as compared to NIF (0.7). The relative broadening of the segmental relaxation peak in polymer blends has been correlated to their ΔT_g values (difference between the T_g values of drug and polymer) i.e. the peak becomes broader as the ΔT_g increases (ΔT_g = 44 and 76 °C for the PVP and HPMCAS dispersion respectively)[42]. This effect can be attributed to the significant difference in mobility between the two components.

The average relaxation time, in the glassy and supercooled states, could be rank ordered as NIF - PVP > NIF - HPMCAS > NIF (Figure 4.3). The time-temperature superposition (TTS) principle described earlier was used to calculate the relaxation time. Kothari et al[8]

observed a similar trend in these systems in the supercooled state. The temperature dependence in the supercooled state was non-linear and well described by the Vogel[43] - Fulcher[44] - Tamman[45] (VFT) model (eq 4.6)

$$\tau = \tau_o \exp\left(\frac{DT_o}{T-T_o}\right) \qquad (4.6)$$

where T is the temperature, τ_o is the relaxation time of the unrestricted material (10^{-14} s, the quasi-lattice vibration period[46]), D is the strength parameter, and T_o is the temperature of zero mobility (theoretical Kauzmann temperature). Table 4.1 contains the parameters obtained by fitting the VFT model to the data and are in agreement with the literature values[8]. The low strength parameter (D) values are indicative of a fragile glass former. The fragility index[47,48], m, is related to D by eq 7[47] and the calculated values are provided in Table 4.1

$$m = \frac{D}{ln10} * \frac{T_0}{T_g} * \frac{1}{(1-\frac{T_o}{T_g})\text{^}2} \qquad (4.7)$$

The addition of polymer, at 10% w/w, does not seem to influence the fragility measures (m and D values) of the systems. This is perhaps not surprising since there was only a small change in the T_g values[49]. The calculated dielectric T_g, assuming a relaxation time of 100 s, typically exceeds the calorimetric T_g by 2 to 3 degrees[50] and a similar behavior is exhibited by these systems. Unless otherwise mentioned, any reference to glass transition temperatures will implicitly assume $T_{g,cal}$ values.

Physical stability. To study the influence of polymer type on the physical stability in the glassy state, the systems were held isothermally at 45 °C, and the crystallization was monitored using synchrotron radiation. PVP was more effective than HPMCAS in inhibiting NIF crystallization. After 21 days of storage, crystallization, based on appearance of Debye rings, was observed only in the HPMCAS dispersion and not in the

PVP dispersions (Figure 4.4). On the other hand, NIF (in the absence of polymer) showed substantial crystallization after 5 days. Thus the most pronounced crystallization inhibition was observed with PVP. These dispersions also showed the longest relaxation time (i.e. slowest mobility; Figure 4.3b).

In supercooled dispersions, PVP, through hydrogen bonding interactions with NIF, decreased the mobility of the dispersion[8]. Similarly in the glassy state, the longer relaxation times observed in the PVP dispersion when compared to HPMCAS, can be attributed to its stronger interaction with NIF (Figure 4.3b). To our knowledge this is the first report of the link between molecular mobility, strength of drug-polymer interactions and physical stability in glassy dispersions.

Effect of PVP concentration

Glass transition. In the investigated PVP concentration range (10 - 20% w/w), DSC revealed a single T_g in agreement with literature reports of miscible dispersions[51]. As expected, the T_g of the system increased with PVP concentration (Figure 4.5). The system exhibited a negative deviation from the T_g values predicted by the Gordon - Taylor equation[35] (eq 4.5). This has been attributed to the stronger drug-polymer interactions compared to the drug-drug hydrogen bonding interactions[52]. Similar behavior is seen in felodipine (a structural analogue of NIF) - PVP systems[52].

Structural relaxation behavior. Dielectric spectroscopy was used to study the effect of polymer concentration on structural relaxation behavior in the supercooled and glassy states. With an increase in polymer concentration the dielectric response curves shifted to the right, an effect ascribed to an increase in relaxation time (Figure 4.6). The longer "lag time" is likely due to an increase in viscosity which causes the dipoles to take longer

to orient in the direction of the electric field. As shown earlier, a decrease in temperature showed a similar effect (Figure 4.1). At this point, it is also instructive to point out the effect of polymer concentration on the dielectric constant (Figure 4.1). A small decrease in the dielectric compliance value at the secondary plateau, indicative of the dielectric constant of the system, is observed with an increase in polymer concentration. This is attributed to the low dielectric constant of PVP[53].

The TTS master curves for each system, referenced to a temperature at which $\tau = 1$ s, are shown in Figure 4.7a. When we compare the dispersion profiles, only the master curve of the 20% w/w polymer dispersion, referenced to $\tau = 1$ s, did not superimpose with the other dispersions (inset of Figure 4.7a). In this instance, we believe that the modified KWW function does not adequately describe the relaxation behavior at long time scales due to a pronounced conductivity contribution. As a result, the obtained relaxation times may be unreliable leading to a discrepancy in the superposition of master curves at the nominal 1 second T_g. We therefore manually shifted (along the time axis) the master curve for the 20% polymer system resulting in superposition with the master curves at the other polymer concentrations (Figure 4.7a). Thus, in the investigated polymer concentration range, time-temperature concentration superposition holds. However, the NIF master curve does not superimpose with that of the dispersions. This is not surprising since the dispersions, unlike the drug, are binary systems. While there are examples of polymer – small molecule/solvent mixtures exhibiting time-concentration superposition[54,55], this is not universal[56]. The β_{KWW} value also provides insight into the lack of superposition. With an increase in polymer concentration from 0 to 20% w/w, the β_{KWW} value decreased from 0.6 to 0.4. The consequent "stretching" of the exponential

function can explain the lack of superposition. The decrease in β_{KWW} value, indicative of increased heterogeneity, can be attributed to concentration fluctuations[57] resulting in nanodomains with different T_g values and consequently different relaxation times[42].

Figure 4.7b contains the shift factors used to construct the master curves for the drug and the NIF - PVP dispersions shown in Figure 4.7a. The VFT model (eq 4.8), in the framework of the TTS principle, describes the temperature dependence of shift factors:

$$\ln a_T = \frac{B}{T - T_{ref}} \quad (4.8)$$

where a_T is the horizontal shift factor required to shift the curve at temperature (T) relative to the reference temperature (T_{ref}) and B is a constant. The temperature dependence of the shift factor, and therefore the fragility of the system, appears to be unaffected over a PVP concentration range of 0 to 20% w/w.

The temperature dependence of relaxation time (τ) obtained from the shift factors, spanning the supercooled and glassy states, is shown in Figure 4.8a. As expected, with an increase in polymer concentration, the relaxation times become longer (i.e. mobility decreases). At 43 °C (glassy state), there is a ~ two fold increase in relaxation time as the polymer concentration increases from 0 to 10% w/w. This effect is more dramatic (~ 80 fold) at a higher polymer concentration (20% w/w). Similar findings have been reported in the supercooled state[15].

Influence of polymer concentration on physical stability in the glassy state. Synchrotron XRD enabled us to detect NIF crystallization in solid dispersions stored at 45 °C (Figure 4.9). In the absence of polymer (drug alone), NIF crystallization was evident after 24 hours of storage. The addition of polymer caused a pronounced stabilization. In dispersions containing 10% w/w polymer, following storage for 50 days,

drug crystallization was readily evident. In contrast, when the polymer concentration was increased to 25% w/w, no drug crystallization was observed. Thus, increasing polymer concentration has similar effects on structural relaxation behavior (Figure 4.1) and physical stability (Figure 4.9) - an increase in relaxation time and a delay in crystallization.

In summary, at $T < T_g$, an increase in structural relaxation time was accompanied by an enhancement in physical stability. However, other factors may influence devitrification deep in the glassy state[11,58]. At ~ 50 °C below T_g, where the α-relaxation is thought to be insignificant, it has been suggested that the β-relaxation may control the crystallization process[59]. At temperatures between T_g and (T_g - 35), Brian and Yu for example observed that the surface crystal growth rate of nifedipine correlated with the surface diffusion[60].

4.5 Significance.

The widespread use of ASDs in solid dosage forms hinges on our ability to (i) retain the API in the amorphous state during the entire shelf-life of the product, and (ii) to identify the polymer concentration needed to yield a physically stable product. Drug crystallization, by the attendant solubility decrease, can adversely affect the product performance. It is well recognized that physical stability of the drug is likely to increase as a function of polymer concentration. However, practical considerations may limit the polymer concentration. As a result, identifying the optimum polymer concentration is of great practical importance.

In a log-log format, a power law dependence of crystallization time (t_c) with relaxation time (τ) is observed (eq 4.9). This relationship has been used to predict crystallization in amorphous drugs as well as their dispersions[9,11,15].

$$\log(t_c) = M\log(\tau) + A \quad (9)$$

where A is a constant and M is the exponent value. The exponent value provides a quantitative measure of the role of molecular mobility on crystallization behavior. Kothari et al[15] observed a linear relationship between relaxation time (or crystallization time) and polymer concentration and hence assumed the exponent value to be independent over a polymer concentration range of 0 to 20% w/w. In supercooled dispersions, the crystallization times predicted using this approach were in excellent agreement with the experimental results. Since amorphous pharmaceuticals are typically stored below the glass transition temperature, extending this approach to glasses is of immense practical value. This is possible if: (i) molecular mobility and physical stability are coupled and (ii) the relationship between relaxation time (or crystallization time) and polymer concentration is linear[15]. While we observed a non-linear relationship between relaxation time and polymer concentration (Figure 8b), the link between mobility and crystallization needs to be established. Performing crystallization studies, especially at high polymer concentrations, is very time consuming and would be the subject of a future investigation. These preliminary studies serve as a starting point to test the feasibility of this approach in glassy pharmaceuticals. Our ultimate aim is to predict crystallization in dispersions with high polymer loading at temperatures of pharmaceutical interest.

4.6 Conclusions

Time domain dielectric spectroscopy enabled a comprehensive characterization of the structural relaxation in glassy solid dispersions. Strong drug - polymer hydrogen bonding interactions improved the physical stability (i.e. absence of crystallization) by reducing the molecular mobility in these systems. An increase in polymer concentration, by further

reducing molecular mobility, enhanced the physical stability. Thus, molecular mobility can serve as a potential polymer selection tool. Our next objective is to use molecular mobility as the basis to predict crystallization in glassy dispersions.

4.7 Acknowledgements

M.M. was partially supported by the Center for Pharmaceutical Processing and Research and Doctoral Dissertation Fellowship, University of Minnesota. Part of this work was supported by the William and Mildred Peters endowment fund. The XRD studies were carried out at the College of Science and Engineering Characterization Facility, University of Minnesota, which receives partial support from NSF through the MRSEC program. Heelim Li is thanked for her help in sample preparation for synchrotron studies. This research used resources of the Advanced Photon Source, a U.S. Department of Energy (DOE) Office of Science User Facility operated for the DOE Office of Science by Argonne National Laboratory under Contract No. DE-AC02-06CH11357. We thank Dr. Gregory Halder for his help during the beamline experiments.

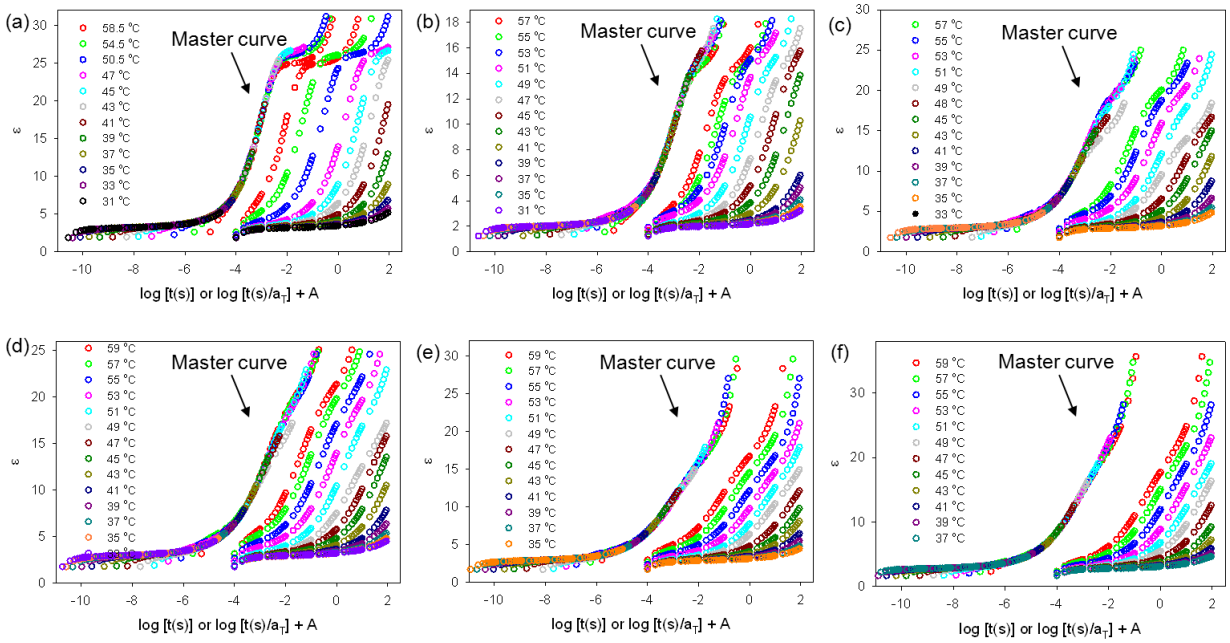

Figure 4-1 Dielectric compliance curves [ε(t)], where t is the duration of the voltage bias, at different temperatures in (a) NIF (b) NIF - HPMCAS dispersions and NIF - PVP dispersions containing (c) 10% (d) 15% (e) 17.5% and (f) 20% w/w polymer. For the sake of clarity, the master curve is offset by 3 decades (denoted by A).

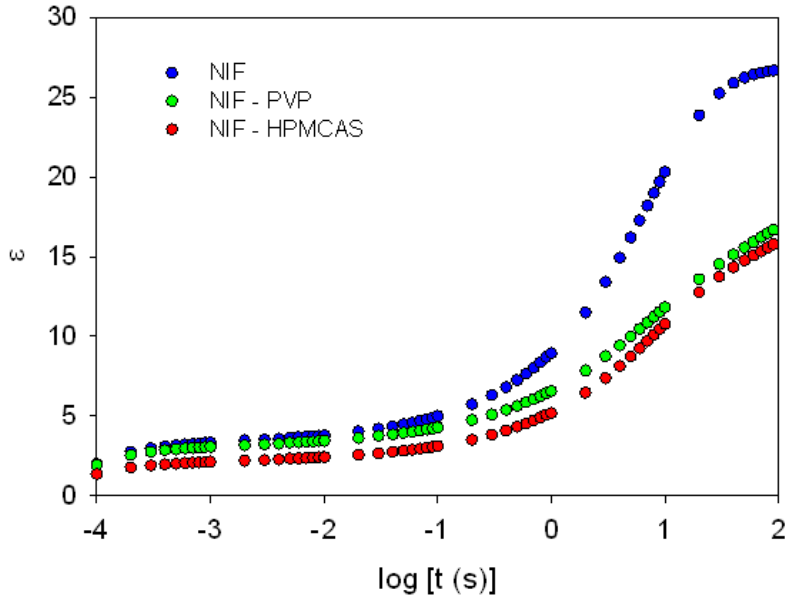

Figure 4-2 Dielectric compliance curves obtained at 45 ºC in NIF and its dispersions with each PVP and HPMCAS (at 10% w/w polymer loading).

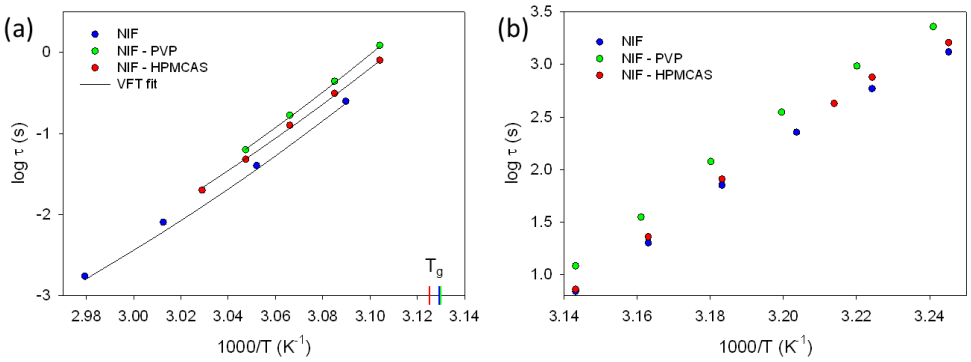

Figure 4-3 Temperature dependence of relaxation time in (a) supercooled and (b) glassy state of NIF and its dispersions prepared with each PVP and HPMCAS at 10% w/w polymer loading. The calorimetric T_g of each system is marked on the x-axis.

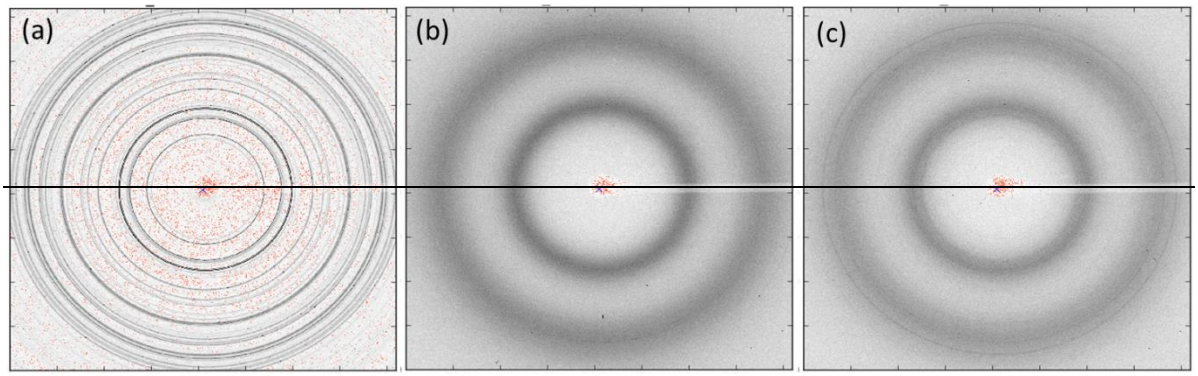

Figure 4-4 SXRD patterns of (a) NIF (day 5) (b) NIF – PVP (day 21) and (c) NIF – HPMCAS (day 21) solid dispersions at 45 °C

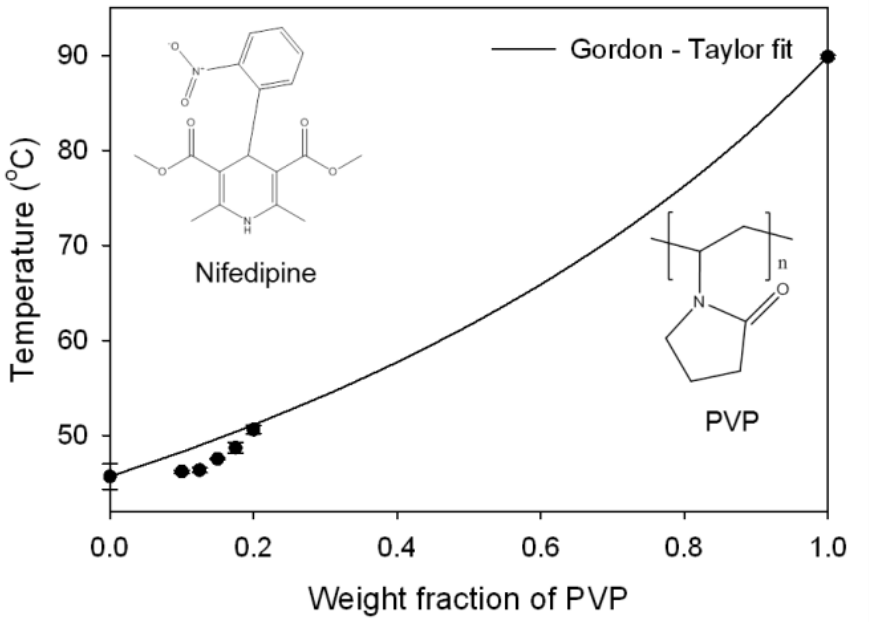

Figure 4-5 Calorimetric T_g as a function of polymer concentration.

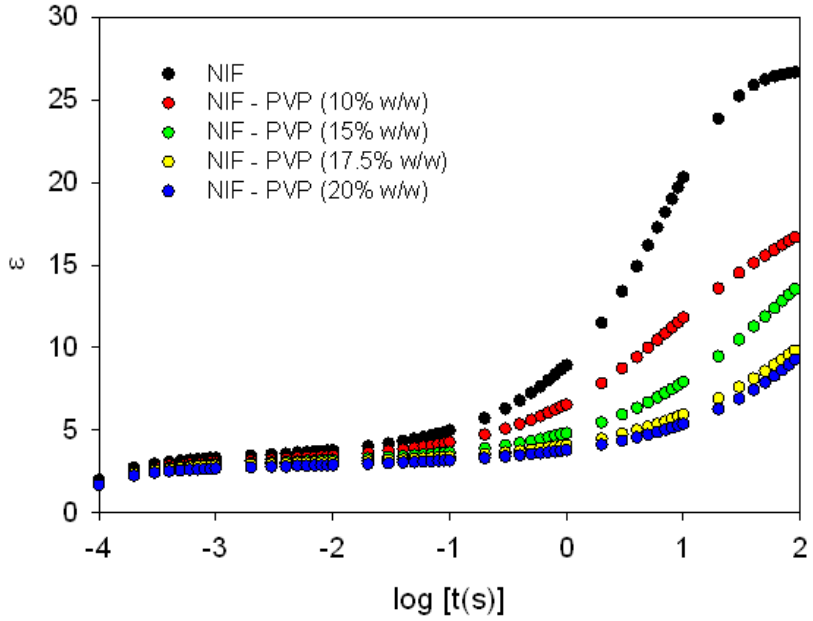

Figure 4-6 Dielectric compliance curves of NIF and its dispersions with 10%, 15%, 17.5% and 20% w/w polymer loading at 45 ^{o}C

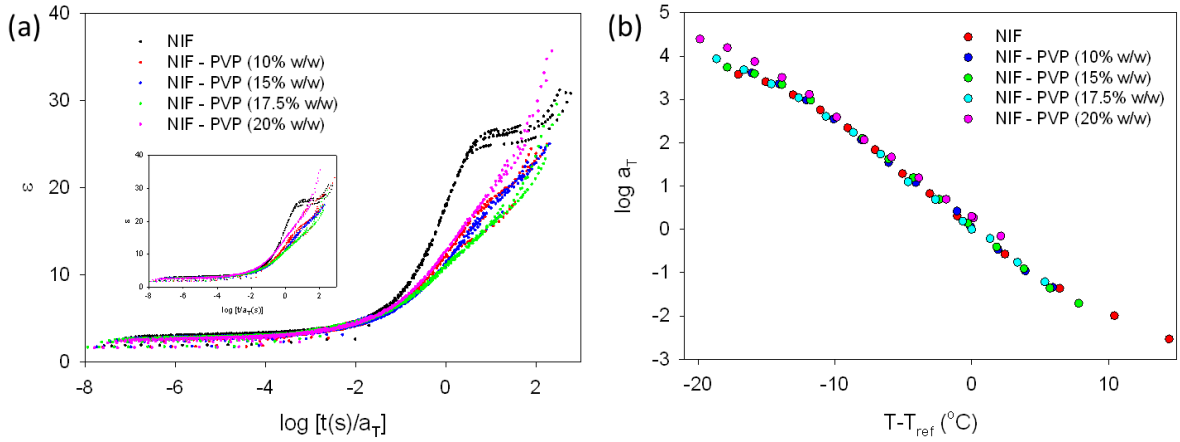

Figure 4-7 (a) Overlay of the master curves, referenced to a T (τ = 1 s), of NIF and NIF – PVP dispersions with 10%, 15% and 17.5%. The master curve of 20% w/w polymer loading was manually shifted by 0.3 decades to superimpose with other curves. The inset shows the superposition of master curves without the manual shifting of the 20% w/w polymer loading master curve, and (b) Temperature shift factors (a_T) as a function of ($T-T_{ref}$) in NIF and NIF – PVP dispersions.

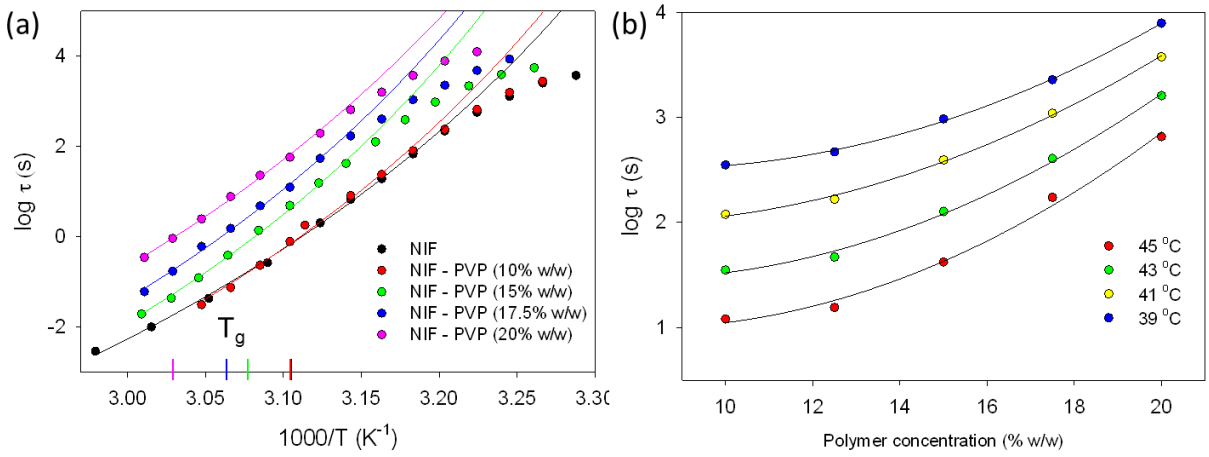

Figure 4-8 (a) Temperature dependence of relaxation time in NIF and NIF – PVP dispersions. The calorimetric T_g of each system is marked in the x-axis. The relaxation times, below the indicated calorimetric T_g, were obtained by performing isochronal dielectric measurements at an aging time of 1020 seconds. (b) Relaxation time as a function of polymer concentration at different temperatures in glassy NIF – PVP dispersions. The solid lines are drawn to assist in visualizing the trend.

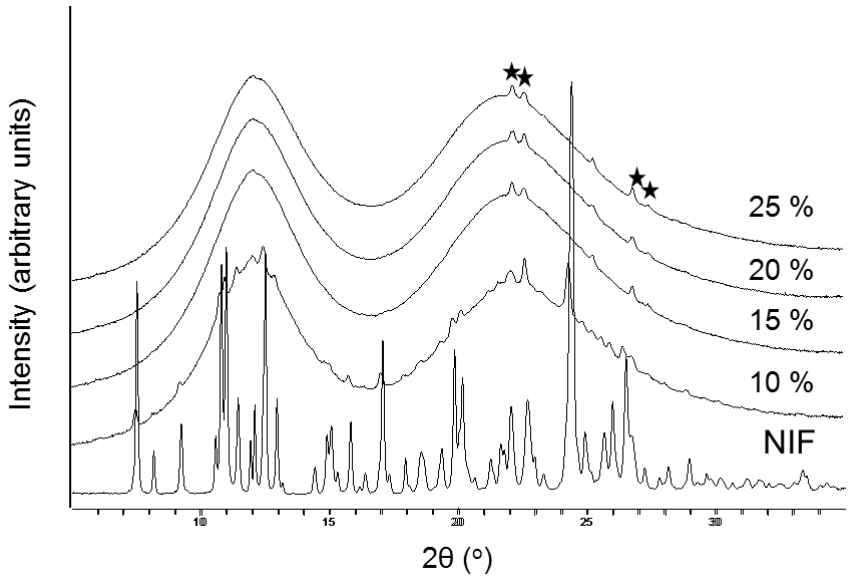

Figure 4-9 Synchrotron XRD patterns of NIF (day 1) and NIF – PVP dispersions (day 50) stored at 45 °C. Peaks due to the sample holder are marked with *.

Table 4.1 VFT parameters (eq 4.6) obtained from model fitting of the relaxation time data.

Sample	T_o (K)	DT_o	D	m	T_g (^oC)	
					Dielectric	Calorimetric
NIF	262 ± 1[a]	1898 ± 42[a]	7	97	41	46 ± 0.2[b]
NIF - PVP	262 ± 1[a]	1962 ± 23[a]	8	95	42	46 ± 0.2[b]
NIF - HPMCAS	259 ± 1[a]	2011 ± 24[a]	8	92	41	47 ± 0.2[b]

[a] Standard error of fitting
[b] Standard deviation from experimental measurements; n=3

5 Effect Of Water On Molecular Mobility And Physical Stability Of Amorphous Pharmaceuticals*

http://pubs.acs.org/doi/abs/10.1021/acs.molpharmaceut.5b00950

5.1 Introduction

Amorphous systems are typically characterized by a pronounced tendency to sorb water. Water, by increasing the free volume[1], plasticizes the system leading to an increase in mobility. This can potentially increase the risk of physicochemical instability in amorphous materials[2,3,4]. Therefore, it is important to tightly control the water vapor pressure in the atmosphere. However, during the manufacture and storage of amorphous pharmaceuticals, there are practical limits to the extent to which the ambient water vapor pressure can be reduced. Thus, it is important to understand the role of sorbed water content on molecular mobility and consequently the crystallization behavior of amorphous pharmaceuticals.

Water sorption has been shown to decrease the physical stability of both single and binary amorphous systems. The increase in water content accelerated crystallization in amorphous sucrose and glucose[5]. It was attributed to the decrease in viscosity leading to increased probability of nucleation followed by crystallization. In amorphous lactose, with increasing water sorption, there was a progressive decrease in the peak crystallization temperature[6]. With an increase in affinity to water (hygroscopicity), there was a reduction in the ability of a polymer to inhibit drug crystallization[7].

The influence of water on molecular mobility has been investigated by dielectric spectroscopy, nuclear magnetic resonance spectroscopy (NMR) and isothermal calorimetry[8,9,10]. In colyophilized sucrose-PVP mixtures, based on NMR, water sorption caused no change in molecular mobility either in the PVP side chain or pyranose/furanose ring in sucrose[9]. On the other hand, in melt quenched nifedipine-excipient mixtures, a small increase in mobility was observed as a function of water

content[11]. In amorphous indomethacin, an increase in water concentration from ~1.2 to ~2.3% w/w, resulted in a pronounced increase in mobility (measured by dielectric spectroscopy)[8]. Similar results were observed in amorphous glucose[12]. While these investigations have qualitatively evaluated the effect of water sorption on mobility, there is no quantitative and comprehensive investigation of the effect of water on molecular mobility and consequently, physical stability.

The objectives of this study were to systematically vary the water content in a model amorphous system and determine the effects on (i) molecular mobility, and (ii) crystallization behavior. These investigations were conducted using nifedipine - polyvinylpyrrolidone vinyl acetate 64 (NIF - PVP) as a model solid dispersion. Our initial goal was to carry out a comprehensive investigation encompassing both the glassy and supercooled states. Unfortunately, the studies in the glassy state had to be discontinued since the crystallization was much too slow. However, using griseofulvin as a model drug, we were able to study the influence of water on the crystallization behavior in the glassy state. Thus these results provide insight into the role of water in both the glassy and supercooled states.

5.2 Experimental section

Preparation of amorphous phases. The NIF - PVP dispersions were prepared, at 15% w/w polymer loading, by solvent evaporation followed by melt-quenching. The physical mixture was dissolved in methanol and the solvent was evaporated at 40 °C under reduced pressure in a rotary evaporator (IKA-HB10, Werke GmbH, Germany). In an effort to remove any residual solvent, the samples were dried overnight, at room temperature. The powder was heated to 5 °C above the melting point of nifedipine and

quenched to -20 ºC. The melt was lightly crushed using a mortar and pestle in a glove box at room temperature (< 5% relative humidity). Amorphous griseofulvin was prepared by melting the crystalline powder and then quenching on an aluminum block precooled to -20 °C. The powders were stored at -20 °C in desiccators containing anhydrous calcium sulfate until further use. The water contents of the dispersion and the amorphous griseofulvin were consistently < 0.2 and 0.4% w/w respectively. The 'as prepared' amorphous phases are hereafter referred to as 'dry' dispersion or griseofulvin.

Samples containing sorbed water. NIF - PVP dispersions containing 0.6, 0.9 and 1.5% w/w water were prepared by storing in chambers maintained at 32.8, 52.8 and 75.3% RH (25 °C) for two hours. Amorphous griseofulvin sorbed 0.75% w/w water when stored at 75.3% RH (25 °C) for one hour. The desired RH values were obtained using saturated salt solutions[13].

Karl Fischer Titrimetry. The water content was determined coulometrically using a Karl Fischer titrimeter (DL36, Mettler Toledo, Columbus, OH). Approximately 50 - 100 mg of the powdered sample was added to the titration cell and the water content was determined.

Differential Scanning Calorimetry. A differential scanning calorimeter (Q2000, TA Instruments, New Castle, DE) equipped with a refrigerated cooling accessory was used. The instrument was calibrated with tin (SRM 741a, NIST). Accurately weighed sample was hermetically sealed in aluminum pans. All the measurements were done under dry nitrogen purge (50 ml/min) at a heating and a cooling rate of 10 °C/min. The T_g was determined as the midpoint of the temperature range of the transition.

X-ray diffractometry (XRD). A powder X-ray diffractometer (D8 ADVANCE; Bruker AXS, Madison, WI, USA) equipped with a variable temperature stage (TTK 450; Anton Paar, Graz-Straßgang, Austria) and Si strip one-dimensional detector (LynxEye™; Bruker AXS) was used. The powder samples were exposed to Cu Kα radiation (40 kV & 40 mA), and the diffraction patterns were obtained by scanning over an angular range of 5 to 40° 2θ with a step size of 0.05° and a dwell time of 1 s.

Synchrotron XRD (SXRD; transmission mode). For the isothermal crystallization studies, amorphous griseofulvin samples, either dry or containing 0.75% w/w water, were sealed in Mylar pouches and stored at selected temperatures. The samples, retrieved at selected time points, were hermetically crimped in DSC pans and exposed to synchrotron radiation. Experiments were performed in the transmission mode in the 17-BM-B beamline at Argonne National Laboratory (Argonne, IL, USA). A monochromatic X-ray beam [wavelength 0.72910 Å; beam size 250 μm (horizontal) × 160 μm (vertical)] and a two-dimensional area detector (XRD-1621, PerkinElmer) were used. Calibration was performed using an Al_2O_3 standard (SRM 674a, NIST). The synchrotron experiments were conducted at room temperature. The two-dimensional (2D) data were integrated to yield 1D d-spacing (Å) or 2θ (°) scans using the FIT2D software developed by A. P. Hammersley of the European Synchrotron Radiation Facility[14,15]

Quantification of XRD data. At each time point, crystallinity index was calculated using eq 1. The crystallinity index can be considered equivalent to the % crystallinity, if the total integrated intensity (amorphous + crystalline) remains constant throughout the isothermal crystallization experiment[16].

$$crystallinity\ index = \frac{intensity\ of\ crystalline\ peaks}{total\ diffracted\ intensity} \qquad (5.1)$$

To quantify the crystallinity index, a custom-built program (using Fortran 77) was used. In this program, the amorphous intensity contribution was based on the experimental XRD pattern of the amorphous "reference" material. The subtraction of the amorphous intensity from the total pattern yielded the intensity contribution from the crystalline peaks. The percent crystallinity was plotted as a function of time, and a characteristic crystallization time (t_c) was obtained for a desired level of crystallization (0.5% in this study).

Dielectric spectroscopy (DES). A broadband dielectric spectrometer (Novocontrol Alpha-AK high performance frequency analyzer, Novocontrol Technologies, Germany) was used over a frequency range of 10^{-2} to 10^{7} Hz. About 100 mg of powder sample was placed between two round copper electrodes (20 mm diameter) and a PTFE spacer. The PTFE spacer (thickness, 1 mm; area, 59.69 mm^2; and capacitance, 1.036 pF) was used to keep the sample confined between electrodes at high temperatures and also to minimize errors due to stray capacitance or edge effects. Powdered samples containing sorbed water were sealed between electrodes using Permatex® High-Temp Red RTV Silicone to retain the water during the dielectric measurement. The water content determined, before and after the dielectric measurement, did not reveal any difference.

The Havriliak-Negami function (eq 5.2) was used to fit the dielectric data to obtain the average relaxation time (τ) and the shape parameters (α_{HN} and β_{HN}).

$$\varepsilon^*(\omega) = \varepsilon_\infty + \frac{\Delta\varepsilon}{(1+(i\omega\tau)^{\alpha_{HN}})^{\beta_{HN}}} \qquad (5.2)$$

$$\varepsilon^*(\omega) = \varepsilon'(\omega) - i\varepsilon''(\omega) \qquad (5.3)$$

In eq 5.2, ω is the angular frequency, $\varepsilon^*(\omega)$ is the complex dielectric permittivity (eq 5.3) consisting of real (ε') and imaginary components (ε'') and $\Delta\varepsilon$ is the dielectric strength

given by $\Delta\varepsilon = \varepsilon_s - \varepsilon_\infty$ where ε_s, static permittivity, gives the low frequency limit ($\omega \rightarrow 0$) of $\varepsilon'(\omega)$ and ε_∞ gives the high frequency limit ($\omega \rightarrow \infty$) of $\varepsilon'(\omega)$. The shape parameters (α_{HN} and β_{HN}) account for the symmetric and asymmetric broadening of the spectrum respectively, and $0 < \alpha$ (or β) < 1.

5.3 Results

NIF – PVP dispersion

Baseline characterization. The dispersion was observed to be X-ray amorphous both before and after water sorption. As expected, with increasing water content, there was a progressive decrease in the glass transition temperature (T_g) of the NIF - PVP dispersions (Figure 5.1a).

Effect of water content on molecular mobility in supercooled dispersions. Dielectric spectroscopy was used to characterize the molecular mobility in ASDs containing different amounts of sorbed water. In the dry dispersions, isothermal frequency sweeps were conducted at several temperatures ranging from 40 to 90 ºC. In systems containing water, the experiments were conducted only over a temperature range of 30 to 60 ºC to minimize water loss during measurement. In the supercooled state, irrespective of the water content, well resolved α-relaxation peaks were observed (Figure 5.2). This mobility mode, also referred to as global motion, is cooperative in nature and responsible for glass transition. As the temperature was increased, the peak moved to a higher frequency indicating a decrease in the relaxation time i.e. an increase in the global mobility of the system. At a given temperature, the effect of water on molecular mobility was evident from the position of the dielectric loss peak (Figure 5.1b). At a modest water content of

1.5% w/w, when compared with the spectrum of the dry sample, the dielectric loss peak exhibited a pronounced shift to a higher frequency, indicating a pronounced increased in molecular mobility. In Figure 5.2d, an additional loss peak at low frequency is observed at elevated temperatures. This is attributed to the interfacial polarization, known as the Maxwell-Wagner polarization[17,18].

The α-relaxation times (τ) were obtained by fitting the Havriliak - Negami equation (eq 5.2) to the dielectric loss data. Figure 5.3a shows the temperature dependence of relaxation time in NIF – PVP dispersion with increasing water content. Addition of 0.6% and 1.5% w/w water resulted, respectively, in approximately 1.5 and 3 orders of magnitude decrease in relaxation time. The temperature dependence was non-linear and well described by the Vogel[19] - Fulcher[20] - Tamman[21] (VFT) model (eq 5.4):

$$\tau = \tau_o \exp\left(\frac{DT_o}{T - T_o}\right) \qquad (5.4)$$

In eq 5.4, τ is the relaxation time at temperature T, τ_o is the relaxation time of the unrestricted material (10^{-14} s, the quasi-lattice vibration period[22]), D is the strength parameter and T_o is the zero mobility temperature. The VFT parameters are provided in Table 5.1. The strength parameter (D value)[19,20,21], irrespective of the water content, was ~ 8, indicative of a fragile glass former. Sorbed water content, up to 1.5% w/w, does not seem to influence the fragility of the dispersion. The plots of relaxation time versus T_g /T are shown in Figure 5.3b. Here, T_g is defined as the temperature at which τ = 100 seconds. The temperature scaling (T_g/T) allowed us to simultaneously evaluate the effects of water content and temperature on the relaxation time. It is evident that once scaled, the relaxation times of the systems with different water contents overlap. This implies that the observed increase in mobility can be simply explained by the “plasticization” effect

of water. This is in agreement with the results obtained with several other compounds[8,23,24]. However, over a wider concentration range, water may influence the fragility of the system[25,26].

Influence of water content on the crystallization behavior of supercooled dispersion. We had earlier reported that, with increasing water content, there was a progressive lowering in T_g (Figure 5.1a). DSC (Figure 5.4) revealed that this was accompanied by a decrease in crystallization onset temperature (T_c). The depression in T_g, due to the plasticizing effect of water, is known to accelerate crystallization[6,27]. With increasing water content, there was a progressive lowering of the melting point (T_m) (Figure 5.4). This can be explained by the melting point depression of the polymer brought about by diluent[28]. It is attributed to the decrease in chemical potential of the melt phase through entropy of mixing[29]. Similar results have been reported in polymer-solvent[28,30] and API-polymer systems[31]. Zhou et al[32] introduced the concept of reduced temperature, $(T_c - T_g)/(T_m - T_g)$, which provides an estimate of the crystallization tendency in the supercooled state. This value allows a comparison of crystallization propensities of compounds with different T_g and T_m values (Table 5.2). The lower the value, stronger is the crystallization propensity. The reduced temperature value seemed to be unaffected by the water content. Thus a decrease in crystallization onset temperature can be explained by depression in T_g brought about by water. Similar findings have been reported in amorphous disaccharides[3,27,4].

In summary, in the supercooled state, water content, in a concentration dependent manner, increases the mobility and accelerates crystallization - effects attributable to plasticization.

Amorphous griseofulvin

Baseline characterization. Griseofulvin was observed to be X-ray amorphous both before and after water sorption. Dry amorphous griseofulvin was characterized by a T_g of 89 ^oC, while sorption of 0.75% w/w water reduced the T_g to 75 ^oC.

Sorbed water – effect on crystallization of glassy griseofulvin. The crystallization behavior of dry powder was compared with a sample containing 0.75% w/w sorbed water. The studies were conducted at several temperatures, ranging from 25 to 45 ^oC. Irrespective of the storage temperature, sorbed water accelerated crystallization as is evident from the earlier appearance and the increase in intensity of the Debye rings (Figure 5.5). When crystallization was monitored as a function of time, at 45 ^oC, again the crystallization was substantially accelerated in presence of water (Figure 5.6). The time taken for 0.5% of griseofulvin to crystallize, t_c, was determined at several temperatures. The temperature dependence of t_c showed an Arrhenius relationship (Figure 5.7a).

The temperature scaling (T_g /T) allowed us to simultaneously evaluate the effects of water content and temperature on the crystallization behavior. A single linear relationship explained the temperature dependence of t_c in both the dry powder and in griseofulvin containing 0.75% w/w water (Figure 5.7b). This implies that the observed decrease in t_c can be explained by the "plasticization" effect of water. We had earlier observed the same effect of water in the supercooled state (Table 5.2). The linear profile also indicates that the activation energy of crystallization is unaffected in the presence of water. Similar results have been reported in lamotrigine mesylate[27] and in a proprietary spray dried dispersion[4].

To summarize the results, in supercooled nifedipine dispersions containing sorbed water, both the mobility and crystallization onset temperature were observed to scale with T_g. Similarly, in glassy griseofulvin, the plasticization effect of water could explain the decrease in crystallization time. Unfortunately, our efforts to determine the molecular mobility of the griseofulvin with sorbed water were not successful. This was due to the difficulty in retaining the sorbed water *during* the dielectric measurement.

Effect of water content on molecular mobility in the glassy state. While a direct measurement of molecular mobility in griseofulvin would have been ideal, based on literature, we expect the mobility to scale with T_g. In both indomethacin and in poly-L-asparagine, D (a measure of kinetic fragility) remained unchanged in presence of water[23,24]. We obtained similar results in the NIF-PVP dispersion (Figure 5.3b). The fragility index, m, is related to D by eq 5.5[33]

$$m = 16 + \frac{590}{D} \qquad (5.5)$$

The fragility or steepness index (m) is defined as the characteristic slope of the plot of log τ versus T_g/T, and at T_g, the slope is given by eq 5.6[33].

$$m = \left[\frac{d\log\left[\tau_\alpha(s)\right]}{d\left(\frac{T_g}{T}\right)}\right] at\ T = T_g \qquad (5.6)$$

In the glassy state, the temperature dependence of α-relaxation is often described by the Adam - Gibbs model[34]

$$\tau = \tau_o \exp\left(\frac{DT_0}{T\left(1-\frac{T_0}{T_f}\right)}\right) \qquad (5.7)$$

where T_f denotes fictive temperature and is defined as the temperature at which a non-equilibrium property *p* (enthalpy or entropy) of a glass, *in excess with respect to the*

stable crystalline state, would have the same value as in the equilibrium supercooled liquid. Eq 5.7 can be rewritten as:

$$\tau = \tau_o \exp\left(\frac{D(T_o/T_g)}{(T/T_g)(1-\frac{T_o}{T_f})}\right) \quad (5.8)$$

where

$$\frac{T_o}{T_g} = \left(1 - \frac{m_{min}}{m}\right) \quad (5.9)$$

In eq 5.9, m_{min} is the lower limit of fragility and is ~ 16[33]. At low water content, since D is unaffected, T_o/T_g can be assumed to be constant. At temperatures close to T_g, $T_f \approx T_g$ and therefore $T_o/T_f \approx T_o/T_g$. Thus, eq 5.8 becomes

$$\tau = \tau_o \exp\left(A\frac{T_g}{T}\right) \quad (5.10)$$

where A is a constant

$$A = \frac{D(T_o/T_g)}{(1-\frac{T_o}{T_f})}$$

Thus, we anticipate the data points in a plot of log τ vs T_g/T to overlap and therefore described by a single relationship[4]. Hence, mobility, along with crystallization time (shown earlier), is expected to scale with T_g in the glassy state. This has been observed in amorphous raffinose with different water contents (2.0 to 6.3% w/w)[10]. The relaxation times were close to one another, when plotted against ($T_g - T_a$) where T_a is the annealing temperature. These experiments were conducted over ($T_g - T_a$) spanning 50 degrees.

However, the use of the Adam Gibbs model has limitations. In the literature, T_f is often assumed to be equal to T_g[35,36]. This is only possible if the annealing temperature is very close to T_g or the heat capacity of the crystalline and the glassy states are very close. However, since the heat capacity of a glass is always higher than that of its crystalline counterpart, $T_f < T_g$. The magnitude of this difference can be obtained by comprehensive

measurements in the glassy state. In spite of these limitations, the Adam Gibbs model provides an avenue to estimate the effect of water on the mobility in the glassy state with experimental data obtained in the supercooled state.

5.4 Significance.

It is well known that amorphous systems have a strong tendency to sorb solvents including water. Thus it is very difficult to "completely dry" amorphous pharmaceuticals (drug substance as well as dispersions). Sorbed water, in a concentration dependent manner, caused a pronounced increase in molecular mobility. This increase, as well as the faster crystallization, could be completely explained by the plasticizing effect of water.

Our results should be viewed with caution since they are qualitative and based on two model systems. The next step will be to systematically investigate the effect of plasticization on both mobility and stability in a single model system. While the correlation between mobility and stability has been established in "dry" systems[37,38,39], we do not know the impact of sorbed water on this correlation.

5.5 Conclusions

The influence of sorbed water on the physical stability (crystallization) in a model drug (griseofulvin) and a dispersion (NIF - PVP) was investigated. Water sorption led to a decrease in both the relaxation (increase in mobility) and crystallization times - effects attributed to "plasticization" by water.

5.6 Acknowledgements

Parts of this work were supported by the William and Mildred Peters endowment fund. The XRD studies were carried out at the College of Science and Engineering

Characterization Facility, University of Minnesota, which receives partial support from NSF through the MRSEC program. Khushboo Kothari and Vishard Ragoonanan are generously thanked for providing the griseofulvin data and helpful discussions. This research used resources of the Advanced Photon Source, a U.S. Department of Energy (DOE) Office of Science User Facility operated for the DOE Office of Science by Argonne National Laboratory under Contract No. DE-AC02-06CH11357. We thank Dr. Gregory Halder for his help during the beamline experiments.

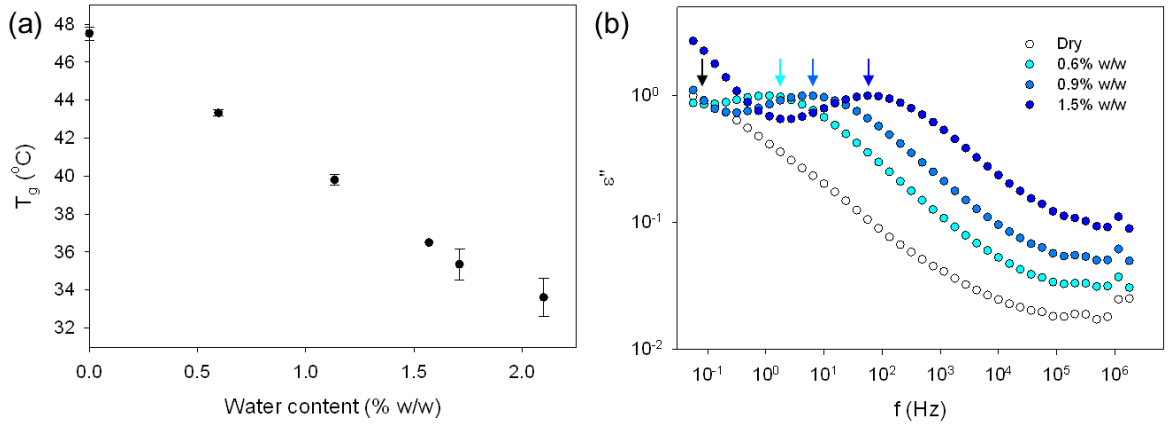

Figure 5-1 The effect of water content on the (a) T_g (mean ± SD; n = 3) and (b) dielectric loss behavior of NIF-PVP dispersions at 50 °C. The arrows show the progressive shift in the loss peak, to higher frequencies, with increasing water content.

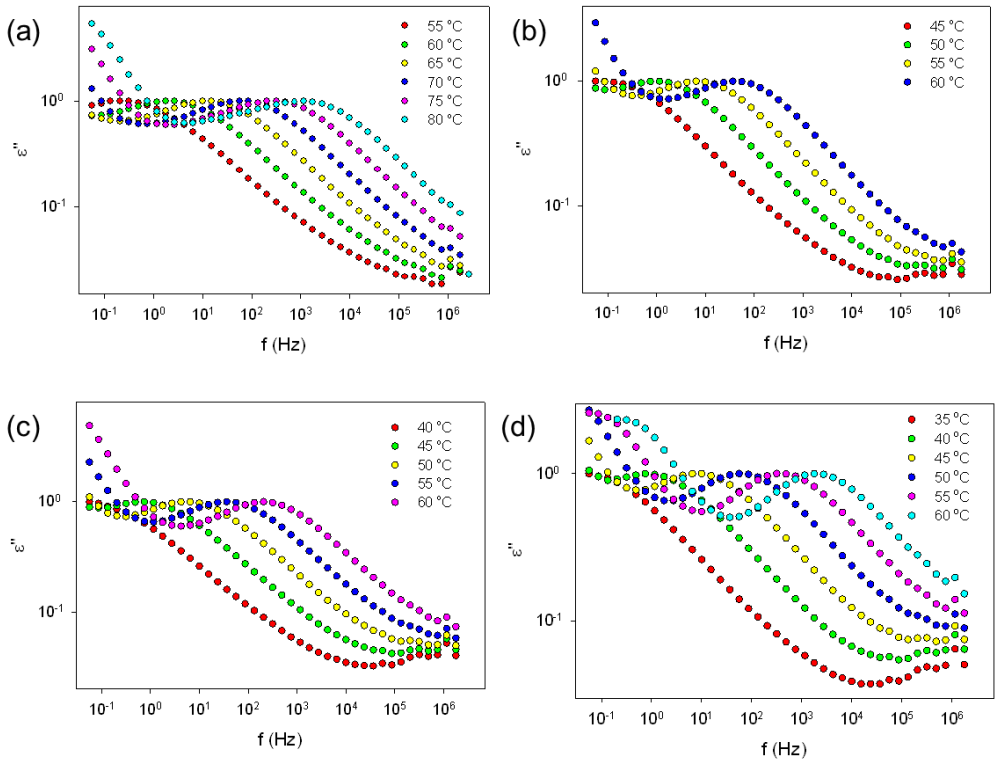

Figure 5-2 Dielectric loss spectra of NIF - PVP dispersion, (a) in the dry state and containing (b) 0.6%, (c) 0.9% and (d) 1.5% w/w water respectively. The loss curves have been normalized to the maximum loss value.

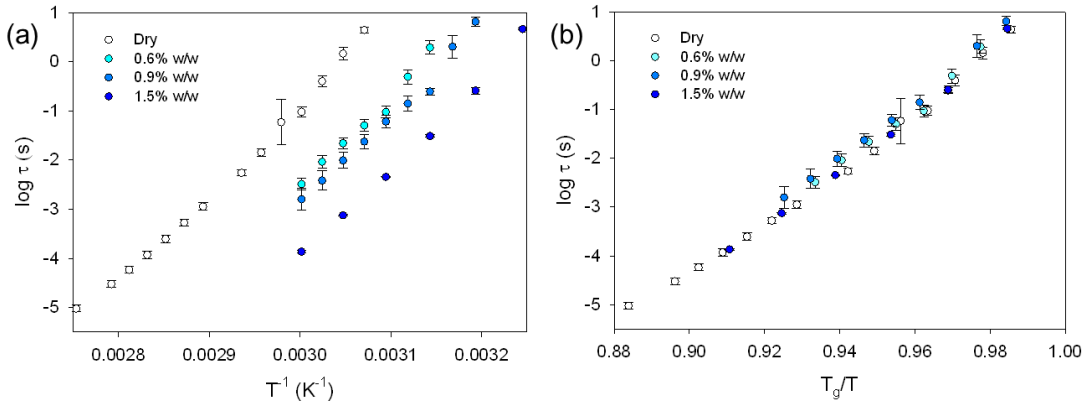

Figure 5-3 Plots of relaxation time (mean ± SD; n = 3) as a function of (a) inverse temperature, and (b) T_g/T in NIF-PVP dispersions.

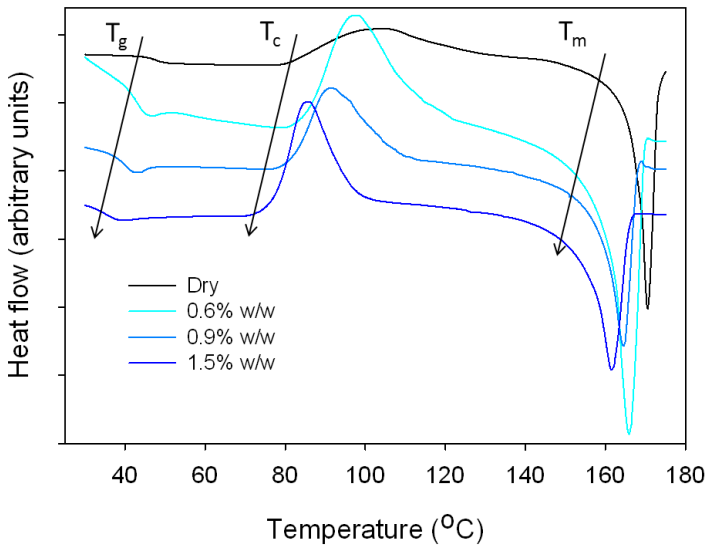

Figure 5-4 DSC curves of NIF – PVP dispersion. The water content ranged from 0.6 to 1.5% w/w.

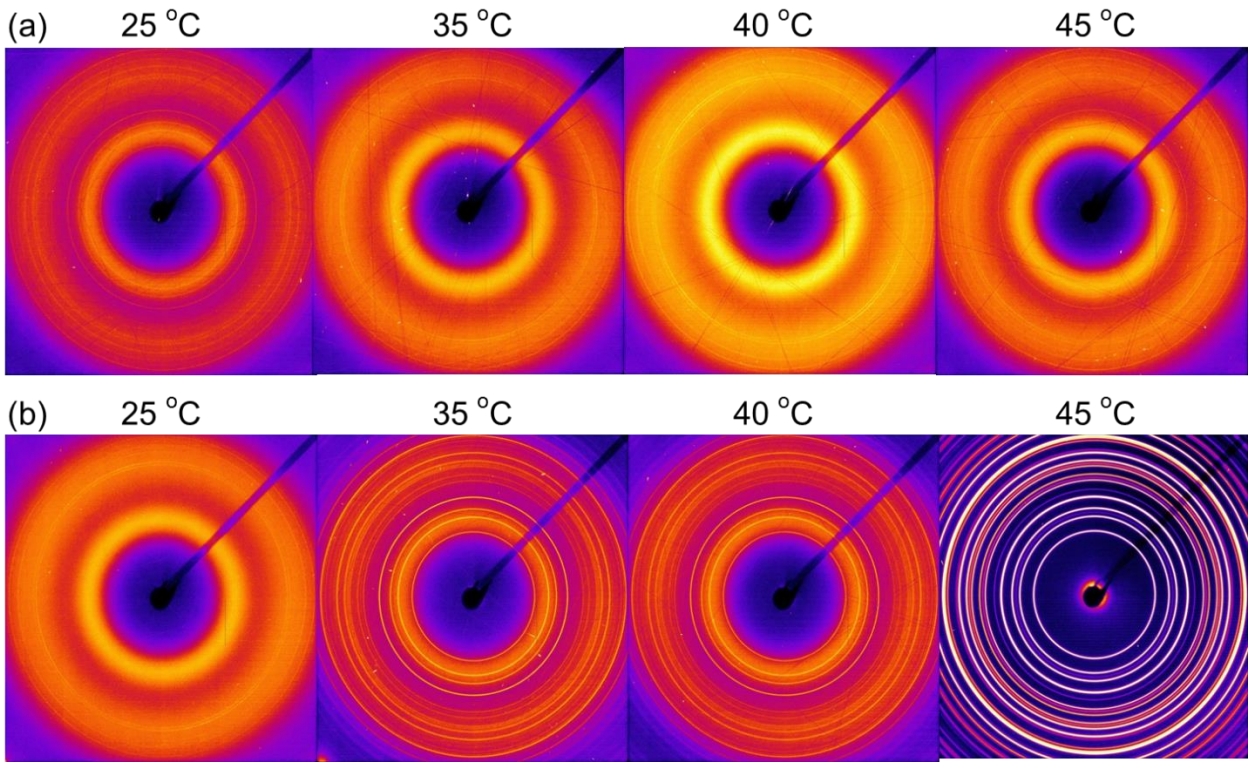

Figure 5-5 Synchrotron XRD patterns of amorphous griseofulvin after 12 hours of storage at the indicated temperature. (a) Dry powder and (b) sample containing 0.75% w/w water.

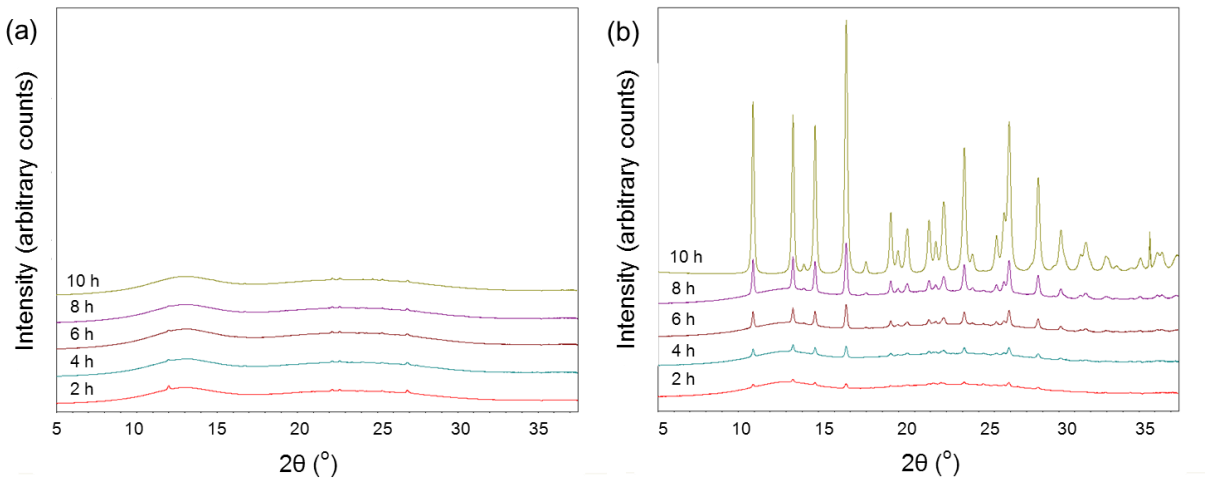

Figure 5-6 XRD patterns obtained following storage at 45 °C of (a) dry griseofulvin and (b) sample containing 0.75% w/w water. The 1D patterns were obtained by integrating the 2D synchrotron images.

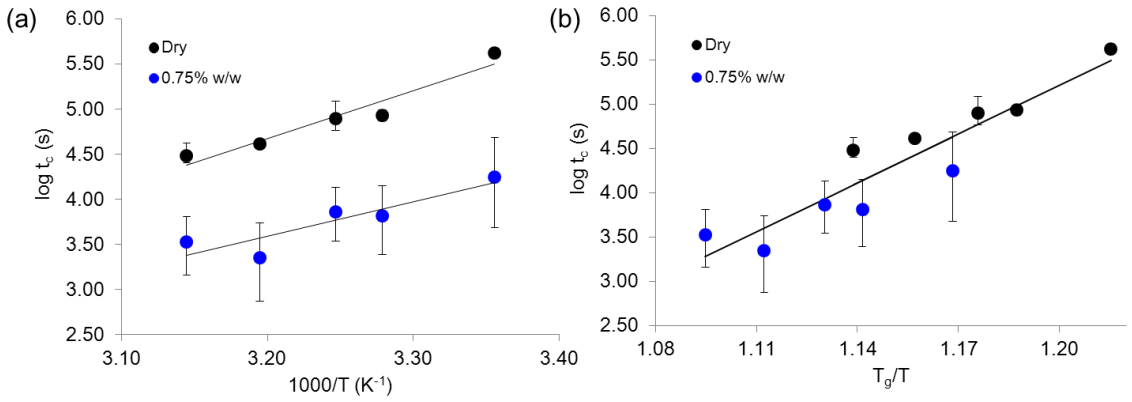

Figure 5-7 Plot of crystallization time, t_c, as a function of (a) inverse temperature, and (b) scaled temperature (T_g/T) in amorphous griseofulvin (mean ± relative error). The powder was either dry or contained 0.75% w/w water.

Table 5.1 VFT parameters for the NIF-PVP dispersions. The values were obtained from fitting eq. 5.4 to the relaxation time data. The dielectric and calorimetric T_g values are also tabulated.

Water content (% w/w)	DT_o	T_o (°C)	D	T_g (°C)	
				Dielectric	Calorimetric
Dry[a]	2017.6 (21.5)[b]	-7.0 (0.8)[b]	7.6	47.8	47.5 (0.4)[c]
0.6	2104.0 (95.1)[b]	-19.4 (3.1)[b]	8.3	37.8	37.8 (0.2)[c]
0.9	2161.0 (79.0)[b]	-23.7 (2.6)[b]	8.7	35.1	
1.5	1926.9 (27.5)[b]	-22.2 (0.9)[b]	7.7	30.2	36.5

[a] Water content less than 0.2% w/w
[b] Standard error of fitting
[c] Standard deviation from experimental measurements; n=3

Table 5.2 Non-isothermal crystallization behavior of NIF – PVP dispersion with different water contents

Water content (% w/w)	Crystallization temperature, T_c (°C)	$\frac{T_c - T_g}{T_m - T_g}$
Dry[a]	102.2	0.44
0.6	97.9	0.44
1.2	91.1	0.39
1.7	84.9	0.41

[a] Water content less than 0.2% w/w

6 Accelerated stability testing method of amorphous dispersions

6.1 Introduction

One of the major challenges in the development of amorphous formulations is the reliable prediction of long term physical stability. Studying degradation kinetics at elevated temperatures and extrapolating to room temperature, an approach classically used for predicting chemical stability, cannot be used for physical stability (crystallization) prediction. Molecular mobility has been used to build predictive models for crystallization in both dry amorphous drugs[1,2,3] and dispersions[4,5]. This may not be practically feasible in systems with high polymer loading, since crystallization is extremely slow. It will therefore be useful to develop an accelerated stability (physical) testing method enabling crystallization prediction under practical storage conditions.

Our goal, much like in chemical degradation studies, is to accelerate drug crystallization from amorphous dispersions. This can be accomplished by monitoring the properties following storage under elevated temperature or by increasing the water content in the dispersions. Exposing the ASD to elevated temperatures is not a desirable approach for at least two reasons. (i) There is potential for chemical degradation, particularly if the temperature is substantially higher than room temperature. (ii) If the studies are conducted in the supercooled state (as is likely to be the case), extrapolation of the results to the glassy state may lead to erroneous conclusion. This is because of the discontinuity in the temperature dependence of the properties of interest. Water sorption decreases the T_g of the dispersion and can consequently facilitate crystallization[6]. This plasticization effect of water allows the accelerated stability studies to be conducted at or close to room temperature.

The combined effects of temperature and sorbed water content on the crystallization behavior of amorphous pharmaceuticals have been investigated. Miyazaki et al studied the crystallization behavior of supercooled nilvadipine with different water contents[7]. Irrespective of the water concentration, the plots of crystallization time vs T_g/T overlapped, attributable to the plasticizing effect of water. Similar results were observed in lamotrigine mesylate[8] and in an amorphous solid dispersion[9]. In our earlier investigation, we evaluated the effect of water sorption on the molecular mobility in NIF dispersions. The increase in molecular mobility was explained by the plasticization effect of water. Interestingly the temperature dependence of the α-relaxation time was independent of the water content. In several model systems, we have documented a correlation between molecular mobility and crystallization (both onset and kinetics) (reference). However, these studies were restricted to system with very negligible water content. Therefore, a logical extension will be to determine the influence of water content on the correlation between mobility and crystallization. *We hypothesize that the extent of coupling between molecular mobility and crystallization time would remain unaffected in dispersions.* If the hypothesis is valid, then the use of the coupling coefficient obtained from studying the stability of dispersions with different water contents can be used to predict crystallization in dry systems. If our approach is successful, this has the potential to predict the physical stability of dispersions and thereby reduce the time for solid dispersion development.

6.2 Experimental section

Preparation of amorphous solid dispersion. FEL ($C_{18}H_{19}Cl_2NO_4$) and PVP (K17 grade) were used as received. The FEL - PVP solid dispersions were prepared, at 10%

w/w polymer loading, by solvent evaporation followed by melt-quenching. A physical mixture of drug and polymer was dissolved in methanol and the solvent was evaporated at 40 °C under reduced pressure in a rotary evaporator (IKA-HB10, Werke GmbH, Germany). The samples were dried overnight, at room temperature. The powder was heated to 150 °C (5 degrees above the melting point of felodipine) and immediately quenched to -20 ºC and then transferred to a glove box at room temperature (< 5% relative humidity). The quenched sample was lightly crushed using a mortar and pestle and stored at −20 °C in desiccators containing anhydrous calcium sulfate. The water contents of the dispersion was consistently < 0.2 w/w. The 'as prepared' amorphous dispersion is hereafter referred to as 'dry' dispersion.

Samples containing sorbed water. Solid dispersions containing 0.9, 1.5 and 1.8% w/w water were prepared by storing in chambers maintained at 32.8, 75.3 and 93.0% RH (25 °C) for two hours. Chambers of desired RH were obtained using saturated salt solutions[10].

Karl Fischer Titrimetry. The water content was determined coulometrically using a Karl Fischer titrimeter (DL36, Mettler Toledo, Columbus, OH). Approximately 50 - 100 mg of the powdered sample was added to the titration cell and the water content was determined.

Differential Scanning Calorimetry. A differential scanning calorimeter (Q2000, TA Instruments, New Castle, DE) equipped with a refrigerated cooling accessory was used. The instrument was calibrated with tin (SRM 741a, NIST). Accurately weighed powder was hermetically sealed in aluminum pans and heated (or cooled) at 10 °C/min under dry nitrogen purge (50 ml/min). The T_g was determined as the midpoint of the temperature range of the transition.

Dielectric spectroscopy (DES). A broadband dielectric spectrometer (Novocontrol Alpha-AK high performance frequency analyzer, Novocontrol Technologies, Germany) was used over a frequency range of 10^{-2} to 10^{7} Hz and between 40 and 60 °C. About 100 mg of powder sample was placed between two round copper electrodes (20 mm diameter) and a PTFE spacer. The spacer (thickness, 1 mm; area, 59.69 mm^2; and capacitance, 1.036 pF) was used to keep the sample confined between electrodes at high temperatures and also to minimize errors due to stray capacitance or edge effects. Powdered samples containing sorbed water were sealed between electrodes using a silicone gasket (Permatex® High-Temp Red RTV Silicone). There was no measurable difference in the water content determined, before and after the dielectric measurement.

The Havriliak-Negami function (eq 6.1) was used to fit the dielectric data to obtain the average relaxation time (τ) and the shape parameters (α_{HN} and β_{HN}).

$$\varepsilon^*(\omega) = \varepsilon_\infty + \frac{\Delta\varepsilon}{(1+(i\omega\tau)^{\alpha_{HN}})^{\beta_{HN}}} \qquad (6.1)$$

$$\varepsilon^*(\omega) = \varepsilon'(\omega) - i\varepsilon''(\omega) \qquad (6.2)$$

In eq 6.1, ω is the angular frequency, ε*(ω) is the complex dielectric permittivity (eq 6.2) consisting of real (ε') and imaginary components (ε") and Δε is the dielectric strength given by $\Delta\varepsilon = \varepsilon_s - \varepsilon_\infty$ where ε_s, static permittivity, gives the low frequency limit ($\omega \rightarrow 0$) of ε'(ω) and ε_∞ gives the high frequency limit ($\omega \rightarrow \infty$) of ε'(ω). The shape parameters (α_{HN} and β_{HN}) account for the symmetric and asymmetric broadening of the spectrum respectively, and $0 < \alpha$ (or β) < 1.

X-ray diffractometry (XRD). A powder X-ray diffractometer (D8 ADVANCE; Bruker AXS, Madison, WI, USA) equipped with a variable temperature stage (TTK 450; Anton Paar, Graz-Straßgang, Austria) and Si strip one-dimensional detector (LynxEye™; Bruker AXS) was used. The powder samples were exposed to Cu Kα radiation (40 kV & 40 mA), and the diffraction patterns were obtained by scanning over an angular range of 5 to 40° 2θ with a step size of 0.05° and a dwell time of 1 s.

Synchrotron XRD (SXRD; transmission mode). Isothermal crystallization studies were carried out, *in situ*, in the beamline (17-BM-B) at Argonne National Laboratory (Argonne, IL, USA). The powder samples were hermetically sealed in DSC pans and placed in a specially designed temperature stage. A monochromatic X-ray beam [wavelength 0.72910 Å; beam size 250 μm (horizontal) × 160 μm (vertical)] and a two-dimensional area detector (XRD-1621, PerkinElmer) were used. Calibration was performed using an Al_2O_3 standard (SRM 674a, NIST). The raw images were integrated to yield one dimensional d-spacing (Å) or 2θ (°) scans using the GSAS II software (developed by Brian H. Toby and Robert B. Von Dreele at Argonne National Labs)[11].

Quantification of XRD data. At each time point, the crystallinity index was calculated using eq 6.3. The crystallinity index is equivalent to % crystallinity, if the total integrated intensity (amorphous + crystalline) remains constant throughout the isothermal crystallization experiment[12].

$$crystallinity\ index = \frac{intensity\ of\ crystalline\ peaks}{total\ diffracted\ intensity} \qquad (6.3)$$

To quantify the crystallinity index, a custom-built program (using Fortran 77) was used. The subtraction of the amorphous intensity from the total pattern yielded the intensity contribution from the crystalline peaks. The amorphous intensity contribution was based on the experimentally obtained XRD of the amorphous FEL – PVP dispersion. The percent crystallinity was plotted as a function of time, and a characteristic crystallization time (t_c) was obtained for a desired level of crystallization (1% in this study).

6.3 Results and discussion

Baseline characterization. The FEL - PVP dispersions were found to be X-ray amorphous with a calorimetric T_g of 49.1 ± 0.2 °C. With an increase in water content, there was a progressive decrease in T_g. Sorption of 0.9, 1.5 and 1.8% w/w water decreased the T_g to 46.0 (± 0.4), 37.2 (± 0.3) and 31.9 °C respectively. The dispersions continued to be X-ray amorphous after water sorption.

Influence of water content on molecular mobility. FEL - PVP dispersions, with different water contents, were subjected to dielectric spectroscopy. In order to avoid water loss during the experiment, the measurements were restricted to temperatures below 60 °C. The dielectric spectra revealed well resolved α-relaxation peaks (Figure 6.1). This relaxation mode represents cooperative motions responsible for glass transition. With an increase in temperature or water content, the relaxation peak shifted to

higher frequency indicating a decrease in relaxation time i.e. an increase in molecular mobility (Figures 6.1 and 6.2). This was also accompanied by an increased contribution of dc conductivity to the low frequency region of the spectrum (Figure 6.1).

To obtain the relaxation times (τ), the Havriliak - Negami equation (eq 6.1) was used to fit the dielectric profiles. Figure 6.3a shows the temperature dependence of relaxation time in FEL - PVP dispersion with different water contents. As expected, the α-relaxation exhibited a non-Arrhenius temperature dependence and was well described by the Vogel[13] - Fulcher[14] - Tamman[15] (VFT) model:

$$\tau = \tau_o \exp\left(\frac{DT_o}{T - T_o}\right) \qquad (6.4)$$

In this expression, T is temperature, τ_o is the relaxation time of the unrestricted material (10^{-14} s, the quasi-lattice vibration period[16]), D (the strength parameter) is a measure of the kinetic fragility and T_o is the zero mobility temperature. The VFT parameters are provided in Table 6.1. The strength parameter (D)[13,14,15] value was ~ 11, both in dry state and dispersions containing sorbed water, reflecting the fragile nature of the glass former.

Figure 6.3b shows the relaxation time as a function of temperature scaled for dielectric T_g (defined as the temperature at which τ = 100 seconds). The data spans ~ 3 orders of magnitude of relaxation time and covers the temperature domain where the Angell plot[17] exhibits a strong curvature typical of fragile liquids. Water contents up to 1.8% w/w, do not seem to influence the fragility of the FEL - PVP dispersion. This implies that the increase in mobility caused by water is explained by its "plasticization" effect. We reported similar results in NIF - PVP dispersions earlier in Chapter 5.

Sorbed water - effect on crystallization. Our next objective was to study the influence of water content on the physical stability in the supercooled state. Above T_g, the

isothermal crystallization was carried out in the temperature range of T_g to (T_g + 53). The effect of water content on the isothermal crystallization behavior is evident from Figure 6.4. From the intensity of the Debye rings, it is readily apparent that the crystallinity increased as a function of water content. The 2D patterns were integrated to obtain the 1D XRD patterns, and the % crystallinity was calculated (equation 6.3). Figure 6.5, a representative example, is a plot of fraction of drug crystallized as a function of time. These experiments were carried out isothermally at several temperatures. The time taken for 1% of the drug to crystallize, t_c, was used as a measure of physical instability.

A similar set of experiments carried out in dispersions with different water contents, This provided a measure of the effect of water content on the temperature dependence of t_c (Figure 6.6). Crystallization time, t_c, shows an Arrhenius temperature dependence for different water contents. The crystallization time, t_c, decreases as the temperature and water content increase. The slopes of the line appear parallel to each other implying activation energy remains unchanged at low water content. Similar results have been reported in amorphous drug[8] and dispersions[9,7].

Correlation between molecular mobility and crystallization. The classical crystallization rate[18], G(T), is given by

$$G(T) = D(T) \times f(T) \qquad (6.5)$$

or often approximated by

$$G(T) = \frac{f(T)}{\eta(T)} \qquad (6.6)$$

where D(T), η(T) is the temperature dependence of molecular diffusion and viscosity respectively. f(T) represents the nucleation/crystal growth free energy term. Eq 6.6 is used whenever D(T) is unavailable or is limited in scope. The temperature dependence of

D(T) and η(T) is only comparable at small supercooling[18-19], due to the breakdown of the Stokes - Einstein relationship at large supercooling (between T_g and 1.2 T_g)[20]. As a result, pronounced enhancement of D over η is observed at temperatures close to T_g. The decoupling factor, ξ, between D and η is expressed as

$$D(T) \propto \frac{T}{\eta^{\xi}} \propto \frac{T}{\tau_{\alpha}^{\xi}} \qquad (6.7)$$

where τ_α is the α-relaxation time. η and τ_α can be used interchangeably since they exhibit a similar temperature dependence. The coupling model, based on eq 6.6 and 6.7, provides a relationship between crystallization time, t_c, and the relaxation time, τ (eq 6.8)

$$\log(t_c) = M log(\tau) + A \quad (6.8)$$

wherein M is the exponent value and A is a constant. The constant, A, is related to the free energy term in eq 6.6 and is a measure of the thermodynamic barrier to crystallization. An M value of 1 indicates complete coupling between the two processes. The log-log plot of crystallization and relaxation time in dry dispersion was linear (Figure 6.7). The exponent value, M, was determined to be 0.63 indicating partial coupling between the two processes. This is attributed to the decoupling between the translational and rotational motions in the temperature range of T_g to 1.2 T_g. Similar M value ~0.67 was reported in nifedipine - PVP dispersions (nifedipine - structural analogue of felodipine)[5]. The relationship between crystallization time and relaxation time, in dry dispersions, could be expressed as

$$\log(t_c) = 0.63 log(\tau) + 6.03 \quad (6.9)$$

Since both t_c and τ showed a similar temperature dependence in the water content range studied, we expected the exponent value to remain unchanged in presence of water. Indeed, the M value remained approximately the same in dispersions containing sorbed

water. We obtained an M value of 0.64 and 0.67 for dispersions containing 1.5% and 1.8% w/w water respectively. The value of constant A decreases very slightly, at low water content, indicating a decrease in free energy barrier for crystallization. These studies show that the extent of coupling between crystallization and molecular mobility remains the same in presence of water.

6.4 Significance

ASD's will find extensive use if their potential for crystallization can be successfully predicted. Molecular mobility is an effective predictor of drug crystallization, as shown in amorphous drugs[1,2,] and dispersions[4,5]. However, extending this approach to commercial ASD's and developing a model relating the drug crystallization from solid dispersion to molecular mobility may be practically challenging. The reason is, extremely slow crystallization in timescales of interest due to high polymer loading and storage conditions - typically in the glassy state. In this study, we observed that the correlation between molecular mobility and crystallization remains approximately the same in dispersions, at low water contents. As a first step towards predicting crystallization, we propose the use of "water sorption" to accelerate crystallization in slow crystallizing systems (high polymer loading dispersions). Thereafter, measuring the molecular mobility in presence of water would enable us to determine the exponent value (M value). We can calculate the value of constant A in eq 6.8, by carrying out crystallization studies in dry dispersions at an elevated temperature (rapid crystallization). This would allow the use of "water sorption" to build a model to predict crystallization in slow crystallizing systems. Since most amorphous pharmaceuticals are stored below the T_g, it will be of great practical interest to extend this approach in the glassy state. Time domain

dielectric spectroscopy can be used to experimentally measure α-relaxation or the Adam-Gibbs[2] model can be employed to estimate the relaxation time below T_g. However, in the glassy state the contribution from the β-relaxation will also need to be considered.

6.5 Conclusions

An increase in water content led to a decrease in relaxation time and consequently the physical stability of FEL - PVP dispersions. A good correlation was observed between crystallization time and α-relaxation time (a measure of molecular mobility) in supercooled dispersions. The extent of coupling between the two processes remained the same at low water contents. This information can be exploited to employ "water sorption" as an approach to predict crystallization in systems that crystallize slowly in practical timescales of interest.

6.6 Acknowledgments

Part of this work was carried out at the College of Science and Engineering Characterization Facility, University of Minnesota, which receives partial support from NSF through the MRSEC program. This research used resources of the Advanced Photon Source, a U.S. Department of Energy (DOE) Office of Science User Facility operated for the DOE Office of Science by Argonne National Laboratory under Contract No. DE-AC02-06CH11357. We thank Dr. Gregory Halder for his help during the beamline experiments. Vishard Ragoonanan is thanked for his help with writing the program for XRD quantification.

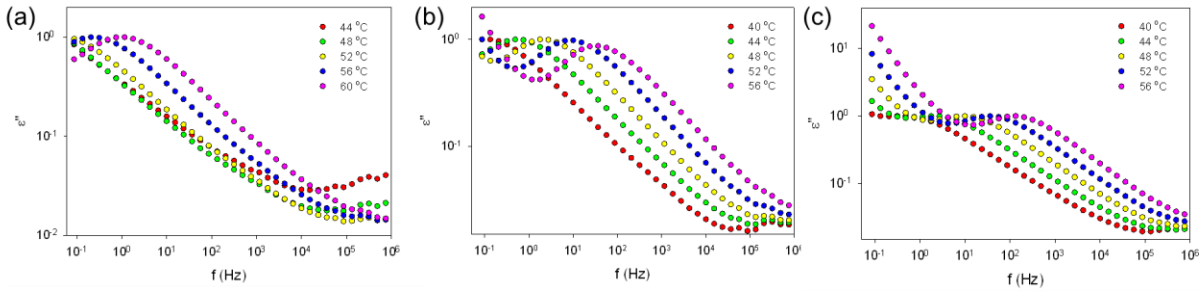

Figure 6-1 Dielectric loss spectra of FEL - PVP dispersion, (a) in the dry state and containing (b) 1.5%, and (c) 1.8% w/w water respectively. The loss curves have been normalized to the maximum loss value.

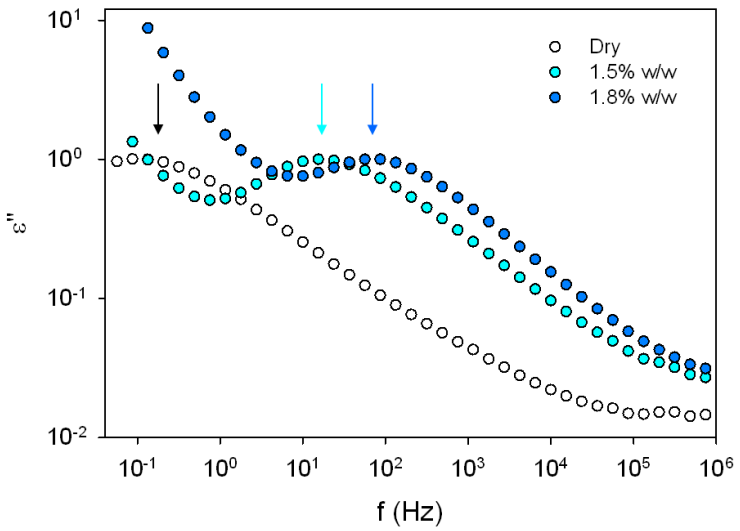

Figure 6-2 Dielectric loss spectra of FEL – PVP dispersion showing α-relaxation at 54 °C. The arrows show the progressive shift in the loss peak, to higher frequencies, with increasing water content.

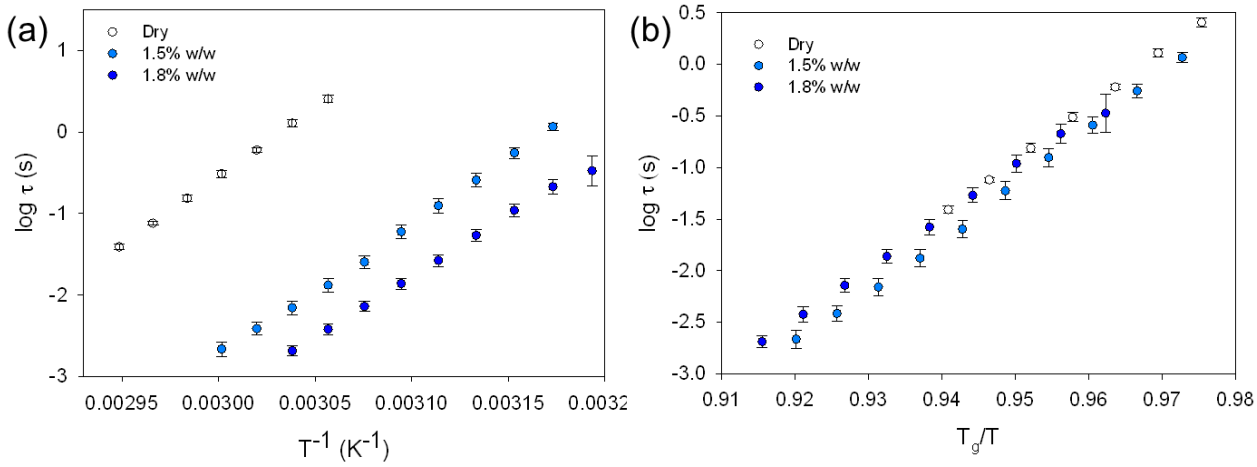

Figure 6-3 Plots of relaxation time (mean ± SD; n = 3) as a function of (a) inverse temperature, and (b) T_g/T in FEL-PVP dispersions.

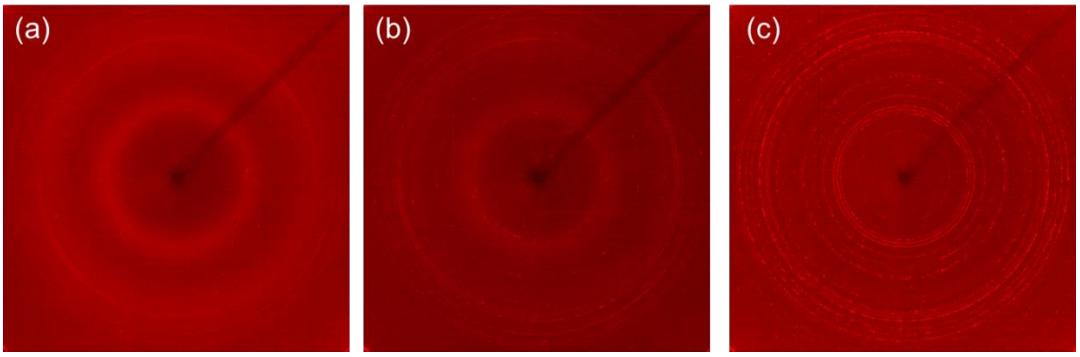

Figure 6-4 Two dimensional synchrotron XRD patterns of FEL – PVP dispersion, (a) in the dry state and containing (b) 0.6% and (c) 1.8% w/w water respectively, after holding at 85 °C for 12 hours.

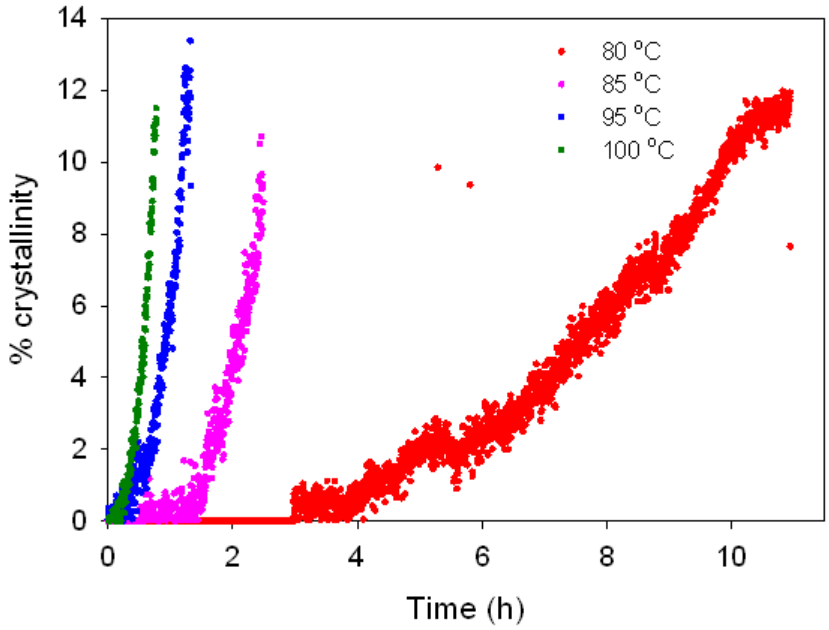

Figure 6-5 Representative plot of fraction of FEL crystallized from FEL – PVP dispersion, in the dry state, as a function of time at several temperatures

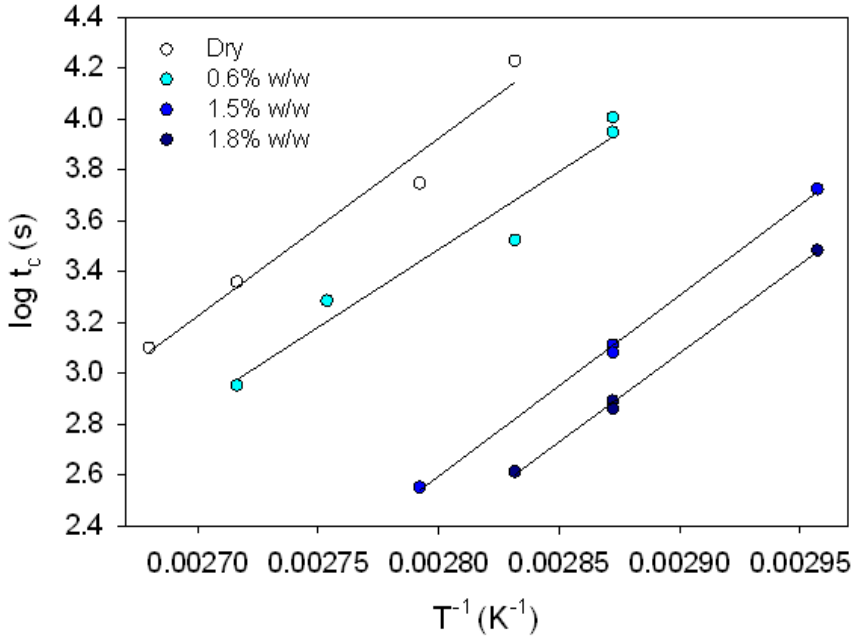

Figure 6-6 Plot of crystallization time, t_c, as a function of temperature in FEL – PVP dispersion, (a) in the dry state and containing (b) 0.6%, (c) 1.5% and (c) 1.8% w/w water respectively.

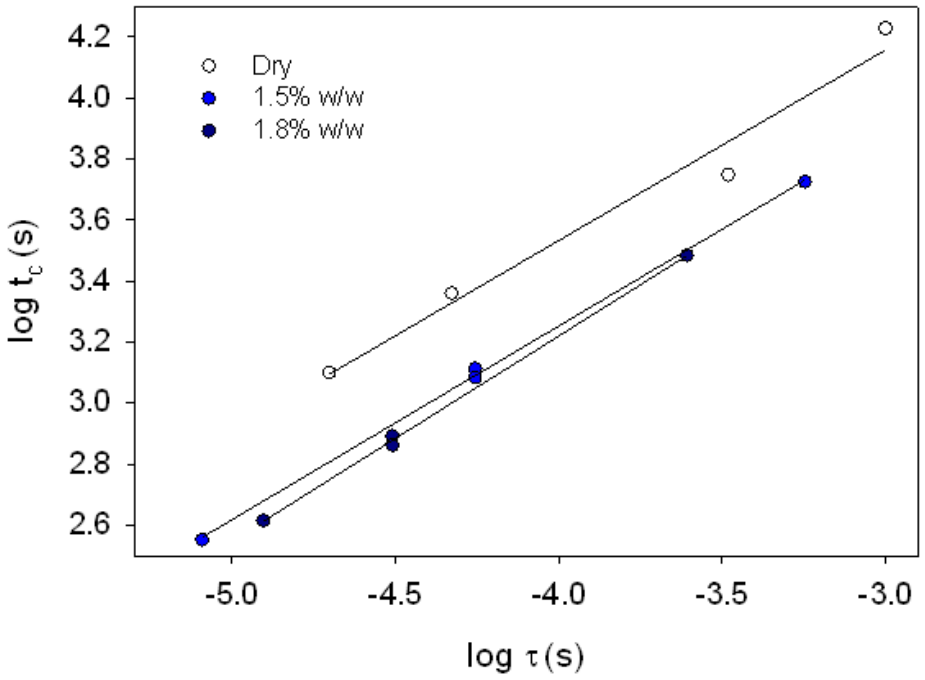

Figure 6-7 Plot of log crystallization time versus log average relaxation time in FEL – PVP dispersion

Table 6.1 VFT parameters for the FEL - PVP dispersion with different water contents. The values were obtained from fitting eq. 6.4 to the relaxation time data.

Water content (% w/w)	DT_o	T_o (K)	D	T_g (°C)	
				Dielectric	Calorimetric
Dry[a]	2766.3 (29.5)[b]	243.9 (1.3)[b]	11.3	45.9	49.1 (0.2)[c]
1.5	2390.4 (27.4)[b]	241.6 (0.9)[b]	9.9	33.4	37.2 (0.3)[c]
1.8	2517.6 (64.3)[b]	232.9 (2.2)[b]	10.8	28.2	31.9

[a] Water content less than 0.2% w/w
[b] Standard error of fitting
[c] Standard deviation from experimental measurements; n=3

7 Summary

Previous investigators from our laboratory have established a correlation between structural relaxation time and crystallization behavior in the supercooled state. However, amorphous pharmaceuticals are usually stored below the glass transition temperature. Thus, evaluation of such correlations in the glassy state is of immense practical value. The extremely long time scale of these motions and the non-ergodic nature of glasses, pose a challenge in experimentally characterizing the structural relaxation. The work in Chapter 2 was aimed at using time domain dielectric spectroscopy to comprehensively characterize both the time and temperature dependence of structural relaxation in the glassy state. Nifedipine (NIF), an antihypertensive, was used as a model compound in this study. Time - aging time and time - temperature superposition principle enabled us to calculate the time and temperature dependence of relaxation time. To the best of our knowledge, this is the first comprehensive investigation of structural relaxation behavior in a pharmaceutical glass.

In Chapter 3, the correlation between molecular mobility and physical stability in the glassy state was investigated. The molecular mobility (both global and local) in the model systems (celecoxib and indomethacin) was comprehensively characterized using a combination of time and frequency domain dielectric spectroscopy. In both the compounds, in the supercooled state, a coupling coefficient of ~0.8 between structural relaxation time and crystallization time was obtained. The crystallization kinetics in the glassy state was monitored using synchrotron radiation. Interestingly in the glassy state, the β_{JG} relaxation was better coupled to the crystallization time (coupling coefficient - celecoxib: 1.4 and indomethacin: 1.1). On the other hand, no correlation was observed between structural relaxation and physical stability in the glassy state.

Chapter 4 was aimed at characterizing the structural relaxation in glassy dispersions of nifedipine with each poly(vinyl) pyrrolidone (PVP) and hydroxypropyl methylcellulose acetate succinate (HPMCAS) with the goal of understanding the effect of type of polymer and polymer concentration on physical stability. For pure NIF as well as the dispersions, the validity of the time-temperature superposition principle was established. This enabled the calculation of the long relaxation times in these systems. The strength of hydrogen bonding, structural relaxation time and crystallization followed the order: NIF-PVP > NIF-HPMCAS > NIF. With an increase in polymer concentration, the relaxation times were longer indicating a decrease in molecular mobility. This is the first application of the superposition principle to characterize structural relaxation in glassy pharmaceutical dispersions.

Amorphous systems are typically characterized by a pronounced tendency to sorb water. This can potentially increase their physicochemical instability. In Chapter 5, we systematically varied the water content in model systems to determine the effects on (i) molecular mobility, and (ii) crystallization behavior. These investigations were conducted using nifedipine - polyvinylpyrrolidone vinyl acetate 64 (NIF - PVP) as a model solid dispersion and griseofulvin as a model drug substance. The observed increase in mobility and the decrease in crystallization onset temperature brought about by water could be explained by the “plasticization” effect of water. Similar results were observed in the glassy drug substance. A single linear relationship was observed between crystallization time and T_g/T in both dry and water containing systems. Since fragility is unaffected by modest amounts of water, much like crystallization time, the mobility in the glass is expected to scale with T_g.

One of the major challenges in the development of amorphous formulations is the reliable prediction of long term physical stability. Studying degradation kinetics at elevated temperatures and extrapolating to room temperature, an approach classically used for predicting chemical degradation, cannot be used for physical stability (crystallization) prediction. In Chapter 6, we are proposing the use of “water sorption” as an accelerated stability approach to predict crystallization in “dry” slow crystallizing systems (high polymer loading dispersions). Felodipine - PVP (FEL - PVP) dispersion was used as the model system. Similar to our earlier results in NIF - PVP system, both the increase in molecular mobility and a faster crystallization onset could be explained by the plasticization effect. The manifestation of this effect - a similar coupling coefficient, as in dry systems, was observed between molecular mobility and crystallization time in presence of water. Based on these findings, we are proposing the use of “water sorption” to build predictive models for crystallization in slow crystallizing drug dispersions.

8 Future work

Both the time and temperature dependence of structural relaxation was characterized using dielectric spectroscopy (Chapter 2). The structural relaxation behavior in the glassy state can be modeled using the Tool-Narayanaswamy-Moynihan (TNM) framework. This framework should then be extended to predict the structural relaxation behavior, using the model parameters, under any given thermal history. The predictions should be validated with the experimental results for several thermal histories. This would be valuable in determining the influence of processing and storage conditions on the structural relaxation behavior of amorphous pharmaceuticals. Annealing, in other words deliberate physical aging, has been shown to reduce the water sorption potential and improve the chemical stability of small molecule glasses. Physical aging studies could provide a mechanistic insight into this behavior and determine its correlation to properties of interest such as water sorption tendency and physical stability.

In Chapter 3, molecular mobility (both global and local) was studied in model systems and its correlation with physical stability in the glassy state was established. Correlation models were successfully developed based on the coupling between local mobility (β_{JG} relaxation) and stability. Validation of the developed models (for crystallization) at relevant temperatures would be practically valuable. Thus, the comparison of the predicted values (determined using the mobility values from time domain dielectric spectrometer) with the observed physical instability would validate the developed models demonstrating their practical utility. It will be useful to investigate such a correlation in a wide variety of glassy pharmaceuticals to draw a general conclusion. Studies determining the mechanism of crystallization i.e. whether it is diffusion or nucleation limited would be useful. The expectation is that β_{JG} relaxation may play a dominant role in nucleation

limited mechanism as compared to diffusion limited. These studies also need to be extended to amorphous solid dispersions to identify the specific mobility mode responsible for physical instability. Bulk diffusion measurements, if possible, can shed light on the decoupling between rotational and translational motions in the glassy state. It would be interesting to evaluate the role of diffusion on the crystallization behavior in glasses.

In Chapter 4, the effect of polymer additive/concentration on the structural relaxation behavior in glassy NIF dispersions was evaluated. Only the data ascribed to the structural relaxation, separated from the β-relaxation, was considered in the calculation. It would be worthwhile to tease out the contribution from the β-relaxation in order to gain a better understanding of the influence of polymer additive/concentration on the local mobility in these systems. Crystallization studies should be carried out at several temperatures in the glassy dispersions so to identify the specific mobility mode responsible for the observed physical instability. Such an approach would enhance our mechanistic understanding of the physical stabilization brought about by the addition of polymer in the glassy state.

In Chapters 5 & 6, the influence of water content on the molecular mobility and crystallization behavior in supercooled dispersions was investigated. Our results demonstrate that coupling between mobility and crystallization time remains unaffected in presence of water. The next step would be to use the developed model to predict crystallization in "dry" dispersions. Once this approach is validated, then it should be extended to the glassy state. The influence of water on glassy state dynamics (both global and local) needs to be evaluated to determine a correlation with physical stability. It is experimentally challenging to retain water in the systems. Therefore, using a non-volatile

small molecule glass former such as glycerol may be more practically feasible for these studies.

9 Bibliography

Chapter 1

1. Lipp, R., The Innovator Pipeline: Bioavailability Challenges And Advanced Oral Drug Delivery Opportunities. *American Pharmaceutical Review* **2013,** *16* (3).
2. Shah, N.; Iyer, R. M.; Mair, H.-J.; Choi, D. S.; Tian, H.; Diodone, R.; Fähnrich, K.; Pabst Ravot, A.; Tang, K.; Scheubel, E., Improved Human Bioavailability Of Vemurafenib, a practically insoluble drug, Using An Amorphous Polymer Stabilized Solid Dispersion Prepared By A Solvent Controlled Coprecipitation Process. *J. Pharm. Sci* **2013,** *102* (3), 967-981.
3. Bhugra, C.; Rambhatla, S.; Bakri, A.; Duddu, S. P.; Miller, D. P.; Pikal, M. J.; Lechuga Ballesteros, D., Prediction Of The Onset Of Crystallization Of Amorphous Sucrose Below The Calorimetric Glass Transition Temperature From Correlations With Mobility. *J. Pharm. Sci* **2007,** *96* (5), 1258-1269.
4. Bhardwaj, S. P.; Suryanarayanan, R., Molecular Mobility As An Effective Predictor Of The Physical Stability Of Amorphous Trehalose. *Mol. Pharm.* **2012,** *9* (11), 3209-3217.
5. Kothari, K.; Ragoonanan, V.; Suryanarayanan, R., Influence Of Molecular Mobility On The Physical Stability of Amorphous Pharmaceuticals in the Supercooled and Glassy States. *Mol. Pharm.* **2014,** *11* (9), 3048-3055.
6. Grzybowska, K.; Paluch, M.; Grzybowski, A.; Wojnarowska, Z.; Hawelek, L.; Kolodziejczyk, K.; Ngai, K. L., Molecular Dynamics And Physical Stability Of Amorphous Anti-Inflammatory Drug: Celecoxib. *J. Phys. Chem. B.* **2010,** *114* (40), 12792-12801.
7. Aso, Y.; Yoshioka, S.; Kojima, S., Molecular Mobility Based Estimation Of The Crystallization Rates Of Amorphous Nifedipine And Phenobarbital In Poly (vinylpyrrolidone) Solid Dispersions. *J. Pharm. Sci* **2004,** *93* (2), 384-391.
8. Johari, G. P.; Goldstein, M., Viscous Liquids And The Glass Transition. II. Secondary Relaxations In Glasses Of Rigid Molecules. *J. Chem. Phys.* **1970,** *53* (6), 2372-2388.
9. Johari, G. P., Intrinsic Mobility Of Molecular Glasses. *J. Chem. Phys.* **1973,** *58* (4), 1766-1770.
10. Bhardwaj, S. P.; Arora, K. K.; Kwong, E.; Templeton, A.; Clas, S.-D.; Suryanarayanan, R., Correlation Between Molecular Mobility And Physical Stability Of Amorphous Itraconazole. *Mol. Pharm.* **2013,** *10* (2), 694-700.
11. Dantuluri, A. K. R.; Amin, A.; Puri, V.; Bansal, A. K., Role Of α-relaxation On Crystallization Of Amorphous Celecoxib Above T_g Probed By Dielectric Spectroscopy. *Mol. Pharm.* **2011,** *8* (3), 814-822.
12. Swallen, S. F.; Ediger, M. D., Self-diffusion Of The Amorphous Pharmaceutical Indomethacin Near T_g. *Soft. Matter.* **2011,** *7* (21), 10339-10344.
13. Johari, G. P.; Goldstein, M., Molecular Mobility In Simple Glasses. *J. Phys. Chem.* **1970,** *74* (9), 2034-2035.
14. Vyazovkin, S.; Dranca, I., Physical Stability And Relaxation Of Amorphous Indomethacin. *J. Phys. Chem. B.* **2005,** *109* (39), 18637-18644.
15. Hikima, T.; Adachi, Y.; Hanaya, M.; Oguni, M., Determination Of Potentially Homogeneous Nucleation Based Crystallization In o-terphenyl And An Interpretation Of The Nucleation Enhancement Mechanism. *Phys. Rev. B.* **1995,** *52* (6), 3900.

16. Sun, Y.; Xi, H.; Ediger, M. D.; Yu, L., Diffusionless Crystal Growth From Glass Has Precursor In Equilibrium Liquid. *J. Phys. Chem. B.* **2008,** *112* (3), 661-664.
17. Alig, I.; Braun, D.; Langendorf, R.; Voigt, M.; Wendorff, J. H., Simultaneous Ageing And Crystallization Processes Within The Glassy State Of A Low Molecular Weight Substance. *J. Non-Cryst. Solids.* **1997,** *221* (2), 261-264.
18. (a) Bhardwaj, S. P.; Suryanarayanan, R., Use Of Dielectric Spectroscopy To Monitor Molecular Mobility In Glassy And Supercooled Trehalose. *J. Phys. Chem. B.* **2012,** *116* (38), 11728-11736; (b) Kremer, F., Dielectric Spectroscopy - Yesterday, Today and Tomorrow. *J. Non-Cryst. Solids.* **2002,** *305* (1), 1-9.
19. Alie, J.; Menegotto, J.; Cardon, P.; Duplaa, H.; Caron, A.; Lacabanne, C.; Bauer, M., Dielectric Study Of The Molecular Mobility And The Isothermal Crystallization Kinetics Of An Amorphous Pharmaceutical Drug Substance. *J. Pharm. Sci* **2004,** *93* (1), 218-233.
20. Correia, N. T.; Ramos, J. J. M.; Descamps, M.; Collins, G., Molecular Mobility And Fragility In Indomethacin: A Thermally Stimulated Depolarization Current Study. *Pharm. Res.* **2001,** *18* (12), 1767-1774.
21. Miyazaki, T.; Yoshioka, S.; Aso, Y.; Kojima, S., Ability of Polyvinylpyrrolidone and Polyacrylic acid To Inhibit the Crystallization of Amorphous Acetaminophen. *J. Pharm. Sci* **2004,** *93* (11), 2710-2717.
22. Konno, H.; Taylor, L. S., Influence Of Different Polymers On The Crystallization Tendency Of Molecularly Dispersed Amorphous Felodipine. *J. Pharm. Sci* **2006,** *95* (12), 2692-2705.
23. Shamblin, S. L.; Zografi, G., Enthalpy Relaxation In Binary Amorphous Mixtures Containing Sucrose. *Pharm. Res.* **1998,** *15* (12), 1828-1834.
24. Kilburn, D.; Townrow, S.; Meunier, V.; Richardson, R.; Alam, A.; Ubbink, J., Organization And Mobility Of Water In Amorphous And Crystalline Trehalose. *Nat. Mater.* **2006,** *5* (8), 632-635.
25. Ohtake, S.; Shalaev, E., Effect of water on the chemical stability of amorphous pharmaceuticals: I. Small molecules. *J. Pharm. Sci* **2013,** *102* (4), 1139-1154.
26. Heljo, V. P.; Nordberg, A.; Tenho, M.; Virtanen, T.; Jouppila, K.; Salonen, J.; Maunu, S. L.; Juppo, A. M., The effect of water plasticization on the molecular mobility and crystallization tendency of amorphous disaccharides. *Pharm. Res.* **2012,** *29* (10), 2684-2697.
27. Greco, S.; Authelin, J.-R.; Leveder, C.; Segalini, A., A practical method to predict physical stability of amorphous solid dispersions. *Pharm. Res.* **2012,** *29* (10), 2792-2805.
28. Mullin, J. W., *Crystallization*. Butterworth-Heinemann: 2001.
29. Bhugra, C.; Pikal, M. J., Role of Thermodynamic, Molecular and Kinetic Factors In Crystallization From The Amorphous State. *J. Pharm. Sci.* **2008,** *97* (4), 1329-1349.
30. Turnbull, D.; Fisher, J. C., Rate of nucleation in condensed systems. *The Journal of Chemical Physics* **1949,** *17*, 71.
31. (a) Andronis, V.; Zografi, G., Crystal nucleation and growth of indomethacin polymorphs from the amorphous state. *Journal of non-crystalline solids* **2000,** *271* (3), 236-248; (b) Gutzow, I.; Schmelzer, J., *The vitreous state: thermodynamics, structure, rheology, and crystallization*. Springer Berlin: 1995.
32. (a) Avrami, M., Kinetics of phase change. I General theory. *The Journal of Chemical Physics* **1939,** *7*, 1103; (b) Avrami, M., Kinetics of phase change. II

transformation-time relations for random distribution of nuclei. *The Journal of Chemical Physics* **1940,** *8*, 212; (c) Avrami, M., Granulation, phase change, and microstructure kinetics of phase change. III. *The Journal of Chemical Physics* **1941,** *9*, 177; (d) Maffezzoli, A.; Kenny, J.; Torre, L., On the physical dimensions of the Avrami constant. *Thermochimica acta* **1995,** *269*, 185-190; (e) Woldt, E., The relationship between isothermal and non-isothermal description of Johnson-Mehl-Avrami-Kolmogorov kinetics. *Journal of Physics and Chemistry of Solids* **1992,** *53* (4), 521-527.

33. (a) Aso, Y.; Yoshioka, S.; Kojima, S., Molecular mobility-based estimation of the crystallization rates of amorphous nifedipine and phenobarbital in poly (vinylpyrrolidone) solid dispersions. *Journal of pharmaceutical sciences* **2004,** *93* (2), 384-391; (b) Mehta, M.; Bhardwaj, S. P.; Suryanarayanan, R., Controlling the Physical form of Mannitol in Freeze-Dried Systems. *European Journal of Pharmaceutics and Biopharmaceutics* **2013,** *85* (2), 207-213; (c) Bhardwaj, S. P.; Suryanarayanan, R., Molecular Mobility as an Effective Predictor of the Physical Stability of Amorphous Trehalose. *Molecular pharmaceutics* **2012,** *9* (11), 3209-3217; (d) Zhou, D.; Zhang, G. G.; Law, D.; Grant, D. J.; Schmitt, E. A., Physical stability of amorphous pharmaceuticals: Importance of configurational thermodynamic quantities and molecular mobility. *Journal of pharmaceutical sciences* **2002,** *91* (8), 1863-1872.

34. (a) Aso, Y.; Yoshioka, S.; Kojima, S., Explanation of the crystallization rate of amorphous nifedipine and phenobarbital from their molecular mobility as measured by 13C nuclear magnetic resonance relaxation time and the relaxation time obtained from the heating rate dependence of the glass transition temperature. *Journal of pharmaceutical sciences* **2001,** *90* (6), 798-806; (b) Ngai, K.; Magill, J.; Plazek, D., Flow, diffusion and crystallization of supercooled liquids: Revisited. *The Journal of Chemical Physics* **2000,** *112*, 1887.

35. Yoshioka, S.; Aso, Y., Correlations between molecular mobility and chemical stability during storage of amorphous pharmaceuticals. *Journal of pharmaceutical sciences* **2007,** *96* (5), 960-981.

36. (a) Bhugra, C.; Rambhatla, S.; Bakri, A.; Duddu, S. P.; Miller, D. P.; Pikal, M. J.; Lechuga-Ballesteros, D., Prediction of the onset of crystallization of amorphous sucrose below the calorimetric glass transition temperature from correlations with mobility. *Journal of pharmaceutical sciences* **2007,** *96* (5), 1258-1269; (b) Korhonen, O.; Bhugra, C.; Pikal, M. J., Correlation between molecular mobility and crystal growth of amorphous phenobarbital and phenobarbital with polyvinylpyrrolidone and L-proline. *Journal of pharmaceutical sciences* **2008,** *97* (9), 3830-3841.

37. (a) Bhugra, C.; Shmeis, R.; Krill, S. L.; Pikal, M. J., Predictions of onset of crystallization from experimental relaxation times I-correlation of molecular mobility from temperatures above the glass transition to temperatures below the glass transition. *Pharmaceutical research* **2006,** *23* (10), 2277-2290; (b) Bhugra, C.; Shmeis, R.; Krill, S. L.; Pikal, M. J., Prediction of onset of crystallization from experimental relaxation times. II. Comparison between predicted and experimental onset times. *Journal of pharmaceutical sciences* **2008,** *97* (1), 455-472; (c) Caron, V.; Bhugra, C.; Pikal, M. J., Prediction of onset of crystallization in amorphous pharmaceutical systems: Phenobarbital, nifedipine/PVP, and phenobarbital/PVP. *Journal of pharmaceutical sciences* **2010,** *99* (9), 3887-3900.

38. (a) Andronis, V.; Yoshioka, M.; Zografi, G., Effects of sorbed water on the crystallization of indomethacin from the amorphous state. *Journal of pharmaceutical sciences* **1997,** *86* (3), 346-351; (b) Miyazaki, T.; Yoshioka, S.; Aso, Y.; Kojima, S., Ability of polyvinylpyrrolidone and polyacrylic acid to inhibit the crystallization of amorphous acetaminophen. *Journal of pharmaceutical sciences* **2004,** *93* (11), 2710-2717; (c) Saleki-Gerhardt, A.; Zografi, G., Non-isothermal and isothermal crystallization of sucrose from the amorphous state. *Pharmaceutical research* **1994,** *11* (8), 1166-1173; (d) Shamblin, S. L.; Huang, E. Y.; Zografi, G., The effects of co-lyophilized polymeric additives on the glass transition temperature and crystallization of amorphous sucrose. *Journal of Thermal Analysis and Calorimetry* **1996,** *47* (5), 1567-1579.
39. (a) Bhattacharya, S.; Suryanarayanan, R., Molecular motions in sucrose-PVP and sucrose-sorbitol dispersions: I. Implications of global and local mobility on stability. *Pharmaceutical research* **2011,** *28* (9), 2191-2203; (b) Marsac, P. J.; Konno, H.; Taylor, L. S., A comparison of the physical stability of amorphous felodipine and nifedipine systems. *Pharmaceutical research* **2006,** *23* (10), 2306-2316.
40. Johari, G. P., Intrinsic mobility of molecular glasses. *The Journal of Chemical Physics* **1973,** *58*, 1766.
41. (a) Hodge, I. M., Strong and fragile liquids—a brief critique. *Journal of non-crystalline solids* **1996,** *202* (1), 164-172; (b) Shamblin, S. L.; Tang, X.; Chang, L.; Hancock, B. C.; Pikal, M. J., Characterization Of The Time Scales Of Molecular Motion In Pharmaceutically Important Glasses. *J. Phys. Chem. B.* **1999,** *103* (20), 4113-4121.
42. Adam, G.; Gibbs, J. H., On The Temperature Dependence of Cooperative Relaxation Properties in Glass-Forming Liquids. *J. Chem. Phys.* **1965,** *43* (1), 139-146.
43. Narayanaswamy, O., Stress and structural relaxation in tempering glass. *J. Am. Ceram. Soc* **1978,** *61* (3-4), 146-152.
44. Shamblin, S. L.; Hancock, B. C.; Pikal, M. J., Coupling between chemical reactivity and structural relaxation in pharmaceutical glasses. *Pharmaceutical research* **2006,** *23* (10), 2254-2268.
45. Aso, Y.; Yoshioka, S.; Kojima, S., Explanation Of The Crystallization Rate Of Amorphous Nifedipine And Phenobarbital From Their Molecular Mobility As Measured By ^{13}C Nuclear Magnetic Resonance Relaxation Time And The Relaxation Time Obtained From The Heating Rate Dependence Of The Glass Transition Temperature. *J. Pharm. Sci* **2001,** *90* (6), 798-806.
46. Narayanaswamy, O., A Model of Structural Relaxation in Glass. *J. Am. Ceram. Soc* **1971,** *54* (10), 491-498.
47. Moynihan, C. T.; Macedo, P. B.; Montrose, C. J.; Gupta, P. K.; DeBolt, M. A.; Dill, J. F.; Dom, B. E.; Drake, P. W.; Easteal, A. J.; Elterman, P. B., Structural Relaxation in Vitreous Materials*. *Ann. Ny. Acad. Sci.* **1976,** *279* (1), 15-35.
48. Sobieski, J. W., PhD Dissertation - Structural Recovery in Polymer Glasses. **1999**.
49. (a) Bhardwaj, S. P.; Suryanarayanan, R., Molecular Mobility as a Predictor of the Water Sorption by Annealed Amorphous Trehalose. *Pharmaceutical research* **2012**, 1-7; (b) Surana, R.; Pyne, A.; Rani, M.; Suryanarayanan, R., Measurement of enthalpic relaxation by differential scanning calorimetry—effect of experimental conditions. *Thermochimica acta* **2005,** *433* (1), 173-182; (c) Weuts, I.; Kempen, D.; Six, K.; Peeters, J.; Verreck, G.; Brewster, M.; Van den Mooter, G., Evaluation of different calorimetric methods to determine the glass transition temperature and molecular mobility below< i>

T</i>< sub> g</sub> for amorphous drugs. *International journal of pharmaceutics* **2003,** *259* (1), 17-25.
50. Andronis, V.; Zografi, G., Molecular mobility of supercooled amorphous indomethacin, determined by dynamic mechanical analysis. *Pharmaceutical research* **1997,** *14* (4), 410-414.
51. Aso, Y.; Yoshioka, S.; Kojima, S., Relationship between the crystallization rates of amorphous nifedipine, phenobarbital, and flopropione, and their molecular mobility as measured by their enthalpy relaxation and 1H NMR relaxation times. *Journal of pharmaceutical sciences* **2000,** *89* (3), 408-416.
52. (a) Johari, G. P.; Goldstein, M., Viscous liquids and the glass transition. II. Secondary relaxations in glasses of rigid molecules. *The Journal of Chemical Physics* **1970,** *53* (6), 2372-2388; (b) Paluch, M.; Pawlus, S.; Hensel-Bielowka, S.; Kaminski, K.; Psurek, T.; Rzoska, S.; Ziolo, J.; Roland, C., Effect of glass structure on the dynamics of the secondary relaxation in diisobutyl and diisoctyl phthalates. *Physical Review B* **2005,** *72* (22), 224205; (c) Sixou, B.; Faivre, A.; David, L.; Vigier, G., Intermolecular and intramolecular contributions to the relaxation process in sorbitol and maltitol. *Molecular physics* **2001,** *99* (22), 1845-1850.
53. De Gusseme, A.; Carpentier, L.; Willart, J.; Descamps, M., Molecular mobility in supercooled trehalose. *The Journal of Physical Chemistry B* **2003,** *107* (39), 10879-10886.
54. Ngai, K., An extended coupling model description of the evolution of dynamics with time in supercooled liquids and ionic conductors. *Journal of Physics: Condensed Matter* **2003,** *15* (11), S1107.
55. Bhardwaj, S. P.; Arora, K. K.; Kwong, E.; Templeton, A.; Clas, S.-D.; Suryanarayanan, R., Mechanism Of Amorphous Itraconazole Stabilization In Polymer Solid Dispersions: Role Of Molecular Mobility. *Mol. Pharm.* **2014,** *11* (11), 4228-4237.
56. Alegria, A.; Guerrica-Echevarria, E.; Goitiandia, L.; Telleria, I.; Colmenero, J., . alpha.-Relaxation in the Glass Transition Range of Amorphous Polymers. 1. Temperature Behavior across the Glass transition. *Macromolecules* **1995,** *28* (5), 1516-1527.
57. (a) Vyazovkin, S.; Dranca, I., Effect of physical aging on nucleation of amorphous indomethacin. *The Journal of Physical Chemistry B* **2007,** *111* (25), 7283-7287; (b) Masuda, K.; Tabata, S.; Sakata, Y.; Hayase, T.; Yonemochi, E.; Terada, K., Comparison of molecular mobility in the glassy state between amorphous indomethacin and salicin based on spin-lattice relaxation times. *Pharmaceutical research* **2005,** *22* (5), 797-805.
58. Vyazovkin, S.; Dranca, I., Physical stability and relaxation of amorphous indomethacin. *The Journal of Physical Chemistry B* **2005,** *109* (39), 18637-18644.
59. Vyazovkin, S.; Dranca, I., Probing beta relaxation in pharmaceutically relevant glasses by using DSC. *Pharmaceutical research* **2006,** *23* (2), 422-428.
60. (a) Strickley, R. G.; Anderson, B. D., Solid-state stability of human insulin I. Mechanism and the effect of water on the kinetics of degradation in lyophiles from pH 2–5 solutions. *Pharmaceutical research* **1996,** *13* (8), 1142-1153; (b) Strickley, R. G.; Anderson, B. D., Solid-state stability of human insulin II. Effect of water on reactive intermediate partitioning in lyophiles from pH 2–5 solutions: Stabilization against covalent dimer formation. *Journal of pharmaceutical sciences* **1997,** *86* (6), 645-653; (c) Wang, B.; Tchessalov, S.; Cicerone, M. T.; Warne, N. W.; Pikal, M. J., Impact of sucrose

level on storage stability of proteins in freeze-dried solids: II. Correlation of aggregation rate with protein structure and molecular mobility. *Journal of pharmaceutical sciences* **2009,** *98* (9), 3145-3166; (d) Yoshioka, S.; Miyazaki, T.; Aso, Y., β-relaxation of insulin molecule in lyophilized formulations containing trehalose or dextran as a determinant of chemical reactivity. *Pharmaceutical research* **2006,** *23* (5), 961-966.
61. Hodge, R.; Bastow, T.; Edward, G.; Simon, G.; Hill, A., Free volume and the mechanism of plasticization in water-swollen poly (vinyl alcohol). *Macromolecules* **1996,** *29* (25), 8137-8143.
62. (a) Aso, Y.; Yoshioka, S.; Kojima, S., Relationship between water mobility, measured as nuclear magnetic relaxation time, and the crystallization rate of amorphous nifedipine in the presence of some pharmaceutical excipients. *Chemical and pharmaceutical bulletin* **1996,** *44* (5), 1065-1067; (b) Greco, S.; Authelin, J.-R.; Leveder, C.; Segalini, A., A practical method to predict physical stability of amorphous solid dispersions. *Pharmaceutical research* **2012,** *29* (10), 2792-2805; (c) Hancock, B. C.; Zografi, G., The relationship between the glass transition temperature and the water content of amorphous pharmaceutical solids. *Pharmaceutical research* **1994,** *11* (4), 471-477; (d) Schmitt, E.; Davis, C.; Long, S., Moisture-dependent crystallization of amorphous lamotrigine mesylate. *Journal of pharmaceutical sciences* **1996,** *85* (11), 1215-1219.
63. Makower, B.; Dye, W., Sugar crystallization, equilibrium moisture content and crystallization of amorphous sucrose and glucose. *Journal of Agricultural and Food Chemistry* **1956,** *4* (1), 72-77.
64. Kedward, C.; MacNaughtan, W.; Mitchell, J., Crystallization kinetics of amorphous lactose as a function of moisture content using isothermal differential scanning calorimetry. *Journal of food science* **2000,** *65* (2), 324-328.
65. (a) Andronis, V.; Zografi, G., The molecular mobility of supercooled amorphous indomethacin as a function of temperature and relative humidity. *Pharmaceutical research* **1998,** *15* (6), 835-842; (b) Aso, Y.; Yoshioka, S.; Zhang, J.; Zografi, G., Effect of Water on the Molecular Mobility of Sucrose and Poly (vinylpyrrolidone) in a Colyophilized Formulation as Measured by 13C-NMR Relaxation Time. *Chemical and pharmaceutical bulletin* **2002,** *50* (6), 822-826; (c) Chan, R.; Pathmanathan, K.; Johari, G., Dielectric relaxations in the liquid and glassy states of glucose and its water mixtures. *The Journal of Physical Chemistry* **1986,** *90* (23), 6358-6362; (d) Heljo, V. P.; Nordberg, A.; Tenho, M.; Virtanen, T.; Jouppila, K.; Salonen, J.; Maunu, S. L.; Juppo, A. M., The effect of water plasticization on the molecular mobility and crystallization tendency of amorphous disaccharides. *Pharmaceutical research* **2012,** *29* (10), 2684-2697.
66. Ermolina, I.; Smith, G., Dielectric spectroscopy of low-losses sugar lyophiles: III: The influence of moisture on the dielectric response of freeze-dried lactose. *Journal of non-crystalline solids* **2011,** *357* (2), 671-676.
67. Kaminski, K.; Adrjanowicz, K.; Kaminska, E.; Grzybowska, K.; Hawelek, L.; Paluch, M.; Tarnacka, M.; Gruszka, I.; Kasprzycka, A., Impact of water on molecular dynamics of amorphous α-, β-, and γ-cyclodextrins studied by dielectric spectroscopy. *Physical Review E* **2012,** *86* (3), 031506.

Chapter 2

1. Aso, Y.; Yoshioka, S.; Kojima, S., Molecular Mobility Based Estimation Of The Crystallization Rates Of Amorphous Nifedipine And Phenobarbital In Poly (vinylpyrrolidone) Solid Dispersions. *J. Pharm. Sci* **2004,** *93* (2), 384-391.
2. Bhattacharya, S.; Suryanarayanan, R., Molecular Motions in Sucrose-PVP and Sucrose-sorbitol dispersions: I. Implications of Global and Local mobility on Stability. *Pharm.Res.* **2011,** *28* (9), 2191-2203.
3. Bhattacharya, S.; Bhardwaj, S. P.; Suryanarayanan, R., Molecular Motions in Sucrose-PVP and Sucrose-Sorbitol Dispersions—II. Implications of Annealing on Secondary Relaxations. *Pharm.Res.* **2014,** *31* (10), 2822-2828.
4. Bhugra, C.; Rambhatla, S.; Bakri, A.; Duddu, S. P.; Miller, D. P.; Pikal, M. J.; Lechuga Ballesteros, D., Prediction Of The Onset Of Crystallization Of Amorphous Sucrose Below The Calorimetric Glass Transition Temperature From Correlations With Mobility. *J. Pharm. Sci* **2007,** *96* (5), 1258-1269.
5. Bhugra, C.; Shmeis, R.; Krill, S. L.; Pikal, M. J., Prediction of Onset of Crystallization From Experimental Relaxation Times. II. Comparison between predicted and experimental onset times. *J.Pharm.Sci.* **2008,** *97* (1), 455-472.
6. Shamblin, S. L.; Hancock, B. C.; Pikal, M. J., Coupling Between Chemical Reactivity and Structural Relaxation in Pharmaceutical Glasses. *Pharm.Res.* **2006,** *23* (10), 2254-2268.
7. Luthra, S. A.; Hodge, I. M.; Utz, M.; Pikal, M. J., Correlation Of Annealing With Chemical Stability In Lyophilized Pharmaceutical Glasses. *J. Pharm. Sci.* **2008,** *97* (12), 5240-5251.
8. Chevalier, J.; Deville, S.; Münch, E.; Jullian, R.; Lair, F., Critical Effect of Cubic Phase on Aging in 3mol% Yttria-stabilized Zirconia Ceramics For Hip Replacement Prosthesis. *Biomaterials* **2004,** *25* (24), 5539-5545.
9. Chung, H.-J.; Lim, S.-T., Physical Aging of Glassy Normal and Waxy Rice Starches: Effect of Aging Temperature On Glass Transition and Enthalpy Relaxation. *Carbohyd. Polym.* **2003,** *53* (2), 205-211.
10. Hodge, I. M., Physical Aging in Polymer Glasses. *SCIENCE-NEW YORK THEN WASHINGTON-* **1995**, 1945-1945.
11. Jonker, G., Nature of Aging in Ferroelectric Ceramics. *J. Am. Ceram. Soc.* **1972,** *55* (1), 57-58.
12. Kim, Y. J.; Hagiwara, T.; Kawai, K.; Suzuki, T.; Takai, R., Kinetic Process of Enthalpy Relaxation of Glassy Starch and Effect of Physical Aging upon its Water Vapor Permeability Property. *Carbohydrate Polymers* **2003,** *53* (3), 289-296.
13. Levine, H.; Slade, L., A Polymer Physico-chemical Approach to the Study of Commercial Starch Hydrolysis Products (SHPs). *Carbohyd. Polym.* **1986,** *6* (3), 213-244.
14. Zhou, Z.; Robards, K.; Helliwell, S.; Blanchard, C., Ageing of Stored Rice: Changes in Chemical and Physical Attributes. *J. Cereal. Sci.* **2002,** *35* (1), 65-78.
15. Angell, C. A.; Ngai, K. L.; McKenna, G. B.; McMillan, P. F.; Martin, S. W., Relaxation In Glassforming Liquids And Amorphous Solids. *J. Appl. Phys.* **2000,** *88* (6), 3113-3157.
16. McKenna, G.; Booth, C.; Price, C., Comprehensive Polymer Science. *Polymer properties* **1989,** *2*, 311.
17. Berens, A. R.; Hodge, I., Effects of Annealing and Prior History on Enthalpy Relaxation in Glassy Polymers. 1. Experimental Study on Poly (vinyl chloride). *Macromolecules* **1982,** *15* (3), 756-761.
18. Hodge, I. M., Strong and Fragile Liquids - A Brief Critique. *J Non-Cryst Solids* **1996,** *202* (1), 164-172.

19. Mao, C.; Chamarthy, S. P.; Pinal, R., Calorimetric Study And Modeling Of Molecular Mobility In Amorphous Organic Pharmaceutical Compounds Using A Modified Adam-Gibbs Approach. *J. Phys. Chem. B.* **2007,** *111* (46), 13243-13252.
20. Mopsik, F., Precision Time-domain Dielectric Spectrometer. *Review of scientific instruments* **1984,** *55* (1), 79-87.
21. Mopsik, F., The Transformation of Time-Domain Relaxation Data into the Frequency domain. *Electrical Insulation, IEEE Transactions on* **1985,** (6), 957-964.
22. Abdul-Fattah, A. M.; Dellerman, K. M.; Bogner, R. H.; Pikal, M. J., The Effect Of Annealing On The Stability Of Amorphous Solids: Chemical Stability Of Freeze-Dried Moxalactam. *J. Pharm. Sci* **2007,** *96* (5), 1237-1250.
23. Luthra, S. A.; Hodge, I. M.; Pikal, M. J., Investigation of the Impact of Annealing on Global Molecular Mobility in Glasses: Optimization for Stabilization of Amorphous Pharmaceuticals. *J. Pharm. Sci.* **2008,** *97* (9), 3865-3882.
24. Struik, L. C. E. Physical Aging in Amorphous Polymers and Other Materials. TU Delft, Delft University of Technology, 1977.
25. Kremer, F., *Broadband Dielectric Spectroscopy*. Springer Science & Business Media: 2003.
26. Alegria, A.; Goitiandia, L.; Telleria, I.; Colmenero, J., α-relaxation in the Glass-transition range of Amorphous Polymers. 2. Influence of Physical Aging on the Dielectric Relaxation. *Macromolecules* **1997,** *30* (13), 3881-3887.
27. Kollengodu-Subramanian, S.; McKenna, G. B., A Dielectric Study Of Poly (Vinyl Acetate) Using A Pulse-Probe Technique. *J. Therm. Anal. Calorim.* **2010,** *102* (2), 477-484.
28. Richert, R.; Wagner, H., The Dielectric Modulus: Relaxation Versus Retardation. *Solid. State. Ionics.* **1998,** *105* (1), 167-173.
29. Vogel, H., The Law Of The Relation Between The Viscosity Of Liquids And The Temperature. *Phys. Z* **1921,** *22*, 645-646.
30. Fulcher, G. S., Analysis Of Recent Measurements Of The Viscosity Of Glasses. *J. Am. Ceram. Soc.* **1925,** *8* (6), 339-355.
31. Tammann, V.; Hesse, W., Anorg. Allgem. Chem.,. *J. Am. Ceram. Soc* **1926,** *8*, 339.
32. Kothari, K.; Ragoonanan, V.; Suryanarayanan, R., Influence Of Molecular Mobility On The Physical Stability of Amorphous Pharmaceuticals in the Supercooled and Glassy States. *Mol. Pharm.* **2014,** *11* (9), 3048-3055.
33. Wang, L.-M.; Tian, Y.; Liu, R.; Richert, R., Calorimetric Versus Kinetic Glass Transitions In Viscous Monohydroxy Alcohols. *J. Chem. Phys.* **2008,** *128* (8), 084503.
34. Shamblin, S. L.; Zografi, G., Enthalpy Relaxation in Binary Amorphous Mixtures Containing Sucrose. *Pharm. Res.* **1998,** *15* (12), 1828-1834.
35. Shamblin, S. L.; Tang, X.; Chang, L.; Hancock, B. C.; Pikal, M. J., Characterization Of The Time Scales Of Molecular Motion In Pharmaceutically Important Glasses. *J. Phys. Chem. B.* **1999,** *103* (20), 4113-4121.
36. Hancock, B. C.; Shamblin, S. L.; Zografi, G., Molecular Mobility Of Amorphous Pharmaceutical Solids Below Their Glass Transition Temperatures. *Pharm. Res.* **1995,** *12* (6), 799-806.
37. Hancock, B. C.; Shamblin, S. L., Molecular Mobility of Amorphous Pharmaceuticals Determined Using Differential Scanning Calorimetry. *Thermochimica acta* **2001,** *380* (2), 95-107.
38. Struik, L. C. E., *Physical aging in amorphous polymers and other materials*. Elsevier Amsterdam: 1978; Vol. 106.
39. O'Connell, P. A.; McKenna, G. B., Large Deformation Response Of Polycarbonate: Time-temperature, Time-aging time and Time-strain Superposition. *Polym. Eng. Sci.* **1997,** *37* (9), 1485-1495.

40. Alegria, A.; Guerrica-Echevarria, E.; Goitiandia, L.; Telleria, I.; Colmenero, J., . alpha.-Relaxation in the Glass Transition Range of Amorphous Polymers. 1. Temperature Behavior across the Glass transition. *Macromolecules* **1995,** *28* (5), 1516-1527.
41. Lunkenheimer, P.; Wehn, R.; Schneider, U.; Loidl, A., Glassy Aging Dynamics. *Phys. Rev. Lett.* **2005,** *95* (5), 055702.
42. Qiao, J.; Pelletier, J., Kinetics of Structural Relaxation in Bulk Metallic Glasses by Mechanical Spectroscopy: Determination of the Stretching Parameter β KWW. *Intermetallics* **2012,** *28*, 40-44.
43. Bhardwaj, S. P.; Suryanarayanan, R., Use Of Dielectric Spectroscopy To Monitor Molecular Mobility In Glassy And Supercooled Trehalose. *J. Phys. Chem. B.* **2012,** *116* (38), 11728-11736.
44. Goitiandia, L.; Alegria, A., Physical Aging of Poly (vinyl acetate). A Thermally Stimulated Depolarization Current Investigation. *J Non-Cryst Solids* **2001,** *287* (1), 237-241.
45. Gunawan, L.; Johari, G.; Shanker, R. M., Structural Relaxation of Acetaminophen Glass. *Pharm. Res.* **2006,** *23* (5), 967-979.
46. Bhardwaj, S. P.; Suryanarayanan, R., Molecular Mobility As An Effective Predictor Of The Physical Stability Of Amorphous Trehalose. *Mol. Pharm.* **2012,** *9* (11), 3209-3217.
47. Bhardwaj, S. P.; Suryanarayanan, R., Molecular Mobility As a Predictor of the Water Sorption by Annealed Amorphous Trehalose. *Pharm. Res.* **2013,** *30* (3), 714-720

Chapter 3

1. Lipp, R., The Innovator Pipeline: Bioavailability Challenges And Advanced Oral Drug Delivery Opportunities. *American Pharmaceutical Review* **2013,** *16* (3).
2. Shah, N.; Iyer, R. M.; Mair, H.-J.; Choi, D. S.; Tian, H.; Diodone, R.; Fähnrich, K.; Pabst Ravot, A.; Tang, K.; Scheubel, E., Improved Human Bioavailability Of Vemurafenib, a practically insoluble drug, Using An Amorphous Polymer Stabilized Solid Dispersion Prepared By A Solvent Controlled Coprecipitation Process. *J. Pharm. Sci* **2013,** *102* (3), 967-981.
3. Bhugra, C.; Rambhatla, S.; Bakri, A.; Duddu, S. P.; Miller, D. P.; Pikal, M. J.; Lechuga Ballesteros, D., Prediction Of The Onset Of Crystallization Of Amorphous Sucrose Below The Calorimetric Glass Transition Temperature From Correlations With Mobility. *J. Pharm. Sci* **2007,** *96* (5), 1258-1269.
4. Bhardwaj, S. P.; Suryanarayanan, R., Molecular Mobility As An Effective Predictor Of The Physical Stability Of Amorphous Trehalose. *Mol. Pharm.* **2012,** *9* (11), 3209-3217.
5. Kothari, K.; Ragoonanan, V.; Suryanarayanan, R., Influence Of Molecular Mobility On The Physical Stability of Amorphous Pharmaceuticals in the Supercooled and Glassy States. *Mol. Pharm.* **2014,** *11* (9), 3048-3055.
6. Grzybowska, K.; Paluch, M.; Grzybowski, A.; Wojnarowska, Z.; Hawelek, L.; Kolodziejczyk, K.; Ngai, K. L., Molecular Dynamics And Physical Stability Of Amorphous Anti-Inflammatory Drug: Celecoxib. *J. Phys. Chem. B.* **2010,** *114* (40), 12792-12801.
7. Aso, Y.; Yoshioka, S.; Kojima, S., Molecular Mobility Based Estimation Of The Crystallization Rates Of Amorphous Nifedipine And Phenobarbital In Poly (vinylpyrrolidone) Solid Dispersions. *J. Pharm. Sci* **2004,** *93* (2), 384-391.

8. Johari, G. P.; Goldstein, M., Viscous Liquids And The Glass Transition. II. Secondary Relaxations In Glasses Of Rigid Molecules. *J. Chem. Phys.* **1970,** *53* (6), 2372-2388.
9. Johari, G. P., Intrinsic Mobility Of Molecular Glasses. *J. Chem. Phys.* **1973,** *58* (4), 1766-1770.
10. Bhardwaj, S. P.; Arora, K. K.; Kwong, E.; Templeton, A.; Clas, S.-D.; Suryanarayanan, R., Correlation Between Molecular Mobility And Physical Stability Of Amorphous Itraconazole. *Mol. Pharm.* **2013,** *10* (2), 694-700.
11. Dantuluri, A. K. R.; Amin, A.; Puri, V.; Bansal, A. K., Role Of α-relaxation On Crystallization Of Amorphous Celecoxib Above T_g Probed By Dielectric Spectroscopy. *Mol. Pharm.* **2011,** *8* (3), 814-822.
12. Swallen, S. F.; Ediger, M. D., Self-diffusion Of The Amorphous Pharmaceutical Indomethacin Near T_g. *Soft. Matter.* **2011,** *7* (21), 10339-10344.
13. Johari, G. P.; Goldstein, M., Molecular Mobility In Simple Glasses. *J. Phys. Chem.* **1970,** *74* (9), 2034-2035.
14. Vyazovkin, S.; Dranca, I., Physical Stability And Relaxation Of Amorphous Indomethacin. *J. Phys. Chem. B.* **2005,** *109* (39), 18637-18644.
15. Hikima, T.; Adachi, Y.; Hanaya, M.; Oguni, M., Determination Of Potentially Homogeneous Nucleation Based Crystallization In o-terphenyl And An Interpretation Of The Nucleation Enhancement Mechanism. *Phys. Rev. B.* **1995,** *52* (6), 3900.
16. Sun, Y.; Xi, H.; Ediger, M. D.; Yu, L., Diffusionless Crystal Growth From Glass Has Precursor In Equilibrium Liquid. *J. Phys. Chem. B.* **2008,** *112* (3), 661-664.
17. Alig, I.; Braun, D.; Langendorf, R.; Voigt, M.; Wendorff, J. H., Simultaneous Ageing And Crystallization Processes Within The Glassy State Of A Low Molecular Weight Substance. *J. Non-Cryst. Solids.* **1997,** *221* (2), 261-264.
18. Aso, Y.; Yoshioka, S.; Kojima, S., Explanation Of The Crystallization Rate Of Amorphous Nifedipine And Phenobarbital From Their Molecular Mobility As Measured By ^{13}C Nuclear Magnetic Resonance Relaxation Time And The Relaxation Time Obtained From The Heating Rate Dependence Of The Glass Transition Temperature. *J. Pharm. Sci* **2001,** *90* (6), 798-806.
19. Zhou, D.; Zhang, G. G. Z.; Law, D.; Grant, D. J. W.; Schmitt, E. A., Thermodynamics, Molecular Mobility And Crystallization Kinetics Of Amorphous Griseofulvin. *Mol. Pharm.* **2008,** *5* (6), 927-936.
20. Shamblin, S. L.; Tang, X.; Chang, L.; Hancock, B. C.; Pikal, M. J., Characterization Of The Time Scales Of Molecular Motion In Pharmaceutically Important Glasses. *J. Phys. Chem. B.* **1999,** *103* (20), 4113-4121.
21. Johari, G. P.; Shanker, R. M., On Determining The Relaxation Time Of Glass And Amorphous Pharmaceuticals Stability From Thermodynamic Data. *Thermochim. Acta.* **2010,** *511* (1), 89-95.
22. Mao, C.; Chamarthy, S. P.; Pinal, R., Calorimetric Study And Modeling Of Molecular Mobility In Amorphous Organic Pharmaceutical Compounds Using A Modified Adam-Gibbs Approach. *J. Phys. Chem. B.* **2007,** *111* (46), 13243-13252.
23. Hancock, B. C.; Shamblin, S. L.; Zografi, G., Molecular Mobility Of Amorphous Pharmaceutical Solids Below Their Glass Transition Temperatures. *Pharm. Res.* **1995,** *12* (6), 799-806.

24. Bhardwaj, S. P.; Suryanarayanan, R., Use Of Dielectric Spectroscopy To Monitor Molecular Mobility In Glassy And Supercooled Trehalose. *J. Phys. Chem. B.* **2012,** *116* (38), 11728-11736.
25. O'Connell, P. A.; McKenna, G. B., Arrhenius-type Temperature Dependence Of The Segmental Relaxation Below T_g. *J. Chem. Phys.* **1999,** *110* (22), 11054-11060.
26. Kremer, F., Dielectric Spectroscopy - Yesterday, Today and Tomorrow. *J. Non-Cryst. Solids.* **2002,** *305* (1), 1-9.
27. Alie, J.; Menegotto, J.; Cardon, P.; Duplaa, H.; Caron, A.; Lacabanne, C.; Bauer, M., Dielectric Study Of The Molecular Mobility And The Isothermal Crystallization Kinetics Of An Amorphous Pharmaceutical Drug Substance. *J. Pharm. Sci* **2004,** *93* (1), 218-233.
28. Correia, N. T.; Ramos, J. J. M.; Descamps, M.; Collins, G., Molecular Mobility And Fragility In Indomethacin: A Thermally Stimulated Depolarization Current Study. *Pharm. Res.* **2001,** *18* (12), 1767-1774.
29. Cicerone, M. T.; Douglas, J. F., β-Relaxation Governs Protein Stability In Sugar-Glass Matrices. *Soft. Matter.* **2012,** *8* (10), 2983-2991.
30. Sibik, J.; Löbmann, K.; Rades, T.; Zeitler, J. A., Predicting Crystallisation of Amorphous Drugs With Terahertz Spectroscopy. *Mol. Pharm.* **2015**.
31. Gupta, P.; Chawla, G.; Bansal, A. K., Physical Stability And Solubility Advantage From Amorphous Celecoxib: The Role Of Thermodynamic Quantities And Molecular Mobility. *Mol. Pharm.* **2004,** *1* (6), 406-413.
32. Yoshioka, M.; Hancock, B. C.; Zografi, G., Crystallization Of Indomethacin From The Amorphous State Below And Above Its Glass Transition Temperature. *J. Pharm. Sci.* **1994,** *83* (12), 1700-1705.
33. Toby, B. H.; Von Dreele, R. B., GSAS-II: The Genesis Of A Modern Open-Source All Purpose Crystallography Software Package. *J. Appl. Crystallogr.* **2013,** *46(2)*, 544-549.
34. Nunes, C.; Mahendrasingam, A.; Suryanarayanan, R., Quantification Of Crystallinity In Substantially Amorphous Materials By Synchrotron X-ray Powder Diffractometry. *Pharm. Res.* **2005,** *22* (11), 1942-1953.
35. Mopsik, F. I., Precision Time-Domain Dielectric Spectrometer. *Rev. Sci. Instrum.* **1984,** *55* (1), 79-87.
36. Struik, L. C. E., Physical Aging in Amorphous Glassy Polymers. *Ann. Ny. Acad. Sci.* **1976,** *279* (1), 78-85.
37. Cole, K. S.; Cole, R. H., Dispersion And Absorption In Dielectrics I. Alternating Current Characteristics. *J. Chem. Phys.* **1941,** *9* (4), 341-351.
38. Kremer, F., *Broadband Dielectric Spectroscopy*. Springer Science & Business Media: 2003.
39. Kohlrausch; Pogg, R., *Ann. Phys.* **1954,** *XCL, 179*.
40. Williams, G.; Watts, D. C., Non-Symmetrical Dielectric Relaxation Behaviour Arising From A Simple Empirical Decay Function. *T. Faraday. Soc.* **1970,** *66*, 80-85.
41. Kollengodu-Subramanian, S.; McKenna, G. B., A Dielectric Study Of Poly (Vinyl Acetate) Using A Pulse-Probe Technique. *J. Therm. Anal. Calorim.* **2010,** *102* (2), 477-484.
42. Hiemenz, P. C.; Lodge, T. P., *Polymer Chemistry*. CRC press: 2007.

43. Shi, X.; Mandanici, A.; McKenna, G. B., Shear Stress Relaxation and Physical Aging Study On Simple Glass-forming Materials. *J. Chem. Phys.* **2005,** *123* (17), 174507.
44. O'Connell, P. A.; McKenna, G. B., Large Deformation Response Of Polycarbonate: Time-temperature, Time-aging time and Time-strain Superposition. *Polym. Eng. Sci.* **1997,** *37* (9), 1485-1495.
45. Bhugra, C.; Shmeis, R.; Krill, S. L.; Pikal, M. J., Predictions Of Onset Of Crystallization From Experimental Relaxation Times I - Correlation Of Molecular Mobility From Temperatures Above The Glass Transition To Temperatures Below The Glass Transition. *Pharm. Res.* **2006,** *23* (10), 2277-2290.
46. Kaushal, A. M.; Bansal, A. K., Thermodynamic Behavior Of Glassy State Of Structurally Related Compounds. *Eur. J. Pharm. Biopharm.* **2008,** *69* (3), 1067-1076.
47. Vogel, H., The Law Of The Relation Between The Viscosity Of Liquids And The Temperature. *Phys. Z* **1921,** *22*, 645-646.
48. Fulcher, G. S., Analysis Of Recent Measurements Of The Viscosity Of Glasses. *J. Am. Ceram. Soc.* **1925,** *8* (6), 339-355.
49. Tammann, V.; Hesse, W., Anorg. Allgem. Chem.,. *J. Am. Ceram. Soc* **1926,** *8*, 339.
50. Angell, C. A.; Ngai, K. L.; McKenna, G. B.; McMillan, P. F.; Martin, S. W., Relaxation In Glassforming Liquids And Amorphous Solids. *J. Appl. Phys.* **2000,** *88* (6), 3113-3157.
51. Böhmer, R.; Angell, C. A., Correlations Of The Nonexponentiality And State Dependence Of Mechanical Relaxations With Bond Connectivity In Ge-As-Se Supercooled Liquids. *Phys. Rev. B* **1992,** *45* (17), 10091.
52. Plazek, D. J.; Ngai, K. L., Correlation Of Polymer Segmental Chain Dynamics With Temperature-dependent Time-scale Shifts. *Macromolecules* **1991,** *24* (5), 1222-1224.
53. Schneider, U.; Brand, R.; Lunkenheimer, P.; Loidl, A., Excess Wing In The Dielectric Loss of Glass Formers: A Johari-Goldstein β Relaxation? *Phys. Rev. Lett.* **2000,** *84* (24), 5560.
54. Ngai, K. L., Relation Between Some Secondary Relaxations And The α-relaxations In Glass-Forming Materials According To The Coupling Model. *J. Chem. Phys.* **1998,** *109* (16), 6982-6994.
55. Ngai, K. L., An Extended Coupling Model Description Of The Evolution Of Dynamics With Time In Supercooled Liquids And Ionic Conductors. *J. Phys-Condens. Mat.* **2003,** *15* (11), S1107.
56. Ngai, K. L.; Paluch, M., Classification Of Secondary Relaxation In Glass-formers Based On Dynamic Properties. *J. Chem. Phys.* **2004,** *120* (2), 857-873.
57. Paluch, M.; Roland, C. M.; Pawlus, S.; Zioło, J.; Ngai, K. L., Does The Arrhenius Temperature Dependence Of The Johari-Goldstein Relaxation Persist Above T_g? *Phys. Rev. Lett.* **2003,** *91* (11), 115701.
58. Hensel-Bielowka, S.; Paluch, M.; Ziolo, J.; Roland, C. M., Dynamics Of Sorbitol At Elevated Pressure. *J. Phys. Chem. B.* **2002,** *106* (48), 12459-12463.
59. Wojnarowska, Z.; Adrjanowicz, K.; Wlodarczyk, P.; Kaminska, E.; Kaminski, K.; Grzybowska, K.; Wrzalik, R.; Paluch, M.; Ngai, K. L., Broadband Dielectric Relaxation

Study At Ambient And Elevated Pressure Of Molecular Dynamics Of Pharmaceutical: Indomethacin. *J. Phys. Chem. B.* **2009,** *113* (37), 12536-12545.
60. Lu, G. W.; Hawley, M.; Smith, M.; Geiger, B. M.; Pfund, W., Characterization Of A Novel Polymorphic Form Of Celecoxib. *J. Pharm. Sci.* **2006,** *95* (2), 305-317.
61. Johnson, W. A.; Mehl, R. F., Reaction Kinetics In Processes Of Nucleation And Growth. *Trans. Aime* **1939,** *135* (8), 396-415.
62. Avrami, M., Kinetics of Phase Change. I General Theory. *J. Chem. Phys.* **1939,** *7* (12), 1103-1112.
63. Avrami, M., Kinetics of Phase Change. II Transformation-Time Relations For Random Distribution Of Nuclei. *J. Chem. Phys.* **1940,** *8* (2), 212-224.
64. Sun, Y.; Xi, H.; Chen, S.; Ediger, M. D.; Yu, L., Crystallization Near Glass Transition: Transition From Diffusion-Controlled To Diffusionless Crystal Growth Studied With Seven Polymorphs. *J. Phys. Chem. B.* **2008,** *112* (18), 5594-5601.
65. Sun, Y.; Zhu, L.; Kearns, K. L.; Ediger, M. D.; Yu, L., Glasses Crystallize Rapidly At Free Surfaces By Growing Crystals Upward. *P. Natl. Acad. Sci.* **2011,** *108* (15), 5990-5995.
66. Okamoto, N.; Oguni, M., Discovery Of Crystal Nucleation Proceeding Much Below The Glass Transition Temperature In a Supercooled Liquid. *Solid State Commun* **1996,** *99* (1), 53-56.
67. Ediger, M. D.; Harrowell, P.; Yu, L., Crystal Growth Kinetics Exhibit A Fragility Dependent Decoupling From Viscosity. *J. Chem. Phys.* **2008,** *128* (3), 034709.
68. Ngai, K. L.; Magill, J. H.; Plazek, D. J., Flow, Diffusion And Crystallization Of Supercooled Liquids: Revisited. *J. Chem. Phys.* **2000,** *112* (4), 1887-1892.
69. Ediger, M. D., Spatially Heterogeneous Dynamics In Supercooled Liquids. *Ann. Rev. Phys. Chem.* **2000,** *51* (1), 99-128.
70. Wu, T.; Yu, L., Origin Of Enhanced Crystal Growth Kinetics Near T_g Probed With Indomethacin Polymorphs. *J. Phys. Chem. B.* **2006,** *110* (32), 15694-15699.
71. Cicerone, M. T.; Ediger, M. D., Enhanced Translation Of Probe Molecules In Supercooled o-terphenyl: Signature Of Spatially Heterogeneous Dynamics. *J. Chem. Phys.* **1996,** *104* (18), 7210-7218.
72. Grzybowska, K.; Paluch, M.; Wlodarczyk, P.; Grzybowski, A.; Kaminski, K.; Hawelek, L.; Zakowiecki, D.; Kasprzycka, A.; Jankowska-Sumara, I., Enhancement Of Amorphous Celecoxib Stability By Mixing It With Octaacetylmaltose: The Molecular Dynamics Study. *Mol. Pharm.* **2012,** *9* (4), 894-904.
73. Hikima, T.; Hanaya, M.; Oguni, M., Microscopic Observation Of A Peculiar Crystallization In The Glass Transition Region And β-process As Potentially Controlling The Growth Rate In Triphenylethylene. *J. Mol. Struct.* **1999,** *479* (2), 245-250.

Chapter 4

1. Van Eerdenbrugh, B.; Taylor, L. S., An Ab Initio Polymer Selection Methodology To Prevent Crystallization In Amorphous Solid Dispersions By Application Of Crystal Engineering Principles. *CrystEngComm. 13*, 6171-6178 (2011).
2. Zecevic, D. E.; Wagner, K. G., Rational Development Of Solid Dispersions Via Hot-Melt Extrusion Using Screening, Material Characterization, And Numeric Simulation Tools. *J. Pharm. Sci. 102*, 2297-2310 (2013).

3. Baird, J. A.; Taylor, L. S., Evaluation Of Amorphous Solid Dispersion Properties Using Thermal Analysis Techniques. *Adv. Drug. Deliver. Rev. 64*, 396-421 (2012).
4. Konno, H.; Taylor, L. S., Influence Of Different Polymers On The Crystallization Tendency Of Molecularly Dispersed Amorphous Felodipine. *J. Pharm. Sci. 95*, 2692-2705 (2006).
5. Tao, J.; Sun, Y.; Zhang, G. G. Z.; Yu, L., Solubility Of Small-Molecule Crystals In Polymers: D-mannitol in PVP, Indomethacin in PVP/VA, and Nifedipine in PVP/VA. *Pharm. Res. 26*, 855-864 (2009).
6. Sun, Y. E.; Tao, J.; Zhang, G. G. Z.; Yu, L., Solubilities Of Crystalline Drugs In Polymers: An Improved Analytical Method And Comparison Of Solubilities Of Indomethacin And Nifedipine in PVP, PVP/VA, and PVAc. *J. Pharm. Sci. 99*, 4023-4031 (2010).
7. Marsac, P. J.; Shamblin, S. L.; Taylor, L. S., Theoretical And Practical Approaches For Prediction Of Drug – Polymer Miscibility And Solubility. *Pharm. Res. 23*, 2417-2426 (2006).
8. Kothari, K.; Ragoonanan, V.; Suryanarayanan, R., The Role of Drug – Polymer Hydrogen Bonding Interactions on the Molecular Mobility and Physical Stability of Nifedipine Solid Dispersions. *Mol. Pharm. 12*, 162–170 (2014).
9. Bhardwaj, S. P.; Suryanarayanan, R., Molecular Mobility As An Effective Predictor Of The Physical Stability Of Amorphous Trehalose. *Mol. Pharm. 9*, 3209-3217 (2012).
10. Bhardwaj, S. P.; Arora, K. K.; Kwong, E.; Templeton, A.; Clas, S.-D.; Suryanarayanan, R., Mechanism Of Amorphous Itraconazole Stabilization In Polymer Solid Dispersions: Role Of Molecular Mobility. *Mol. Pharm. 11*, 4228-4237 (2014).
11. Kothari, K.; Ragoonanan, V.; Suryanarayanan, R., Influence Of Molecular Mobility On The Physical Stability of Amorphous Pharmaceuticals in the Supercooled and Glassy States. *Mol. Pharm. 11*, 3048-3055 (2014).
12. Kestur, U. S.; Taylor, L. S., Role Of Polymer Chemistry In Influencing Crystal Growth Rates From Amorphous Felodipine. *CrystEngComm. 12*, 2390-2397 (2010).
13. Wegiel, L. A.; Mauer, L. J.; Edgar, K. J.; Taylor, L. S., Mid-Infrared Spectroscopy As A Polymer Selection Tool For Formulating Amorphous Solid Dispersions. *J. Pharm. Pharmacol. 66*, 244-255 (2014).
14. Mistry, P.; Mohapatra, S.; Gopinath, T.; Vogt, F. G.; Suryanarayanan, R., Role of the Strength of Drug – Polymer Interactions on the Molecular Mobility and Crystallization Inhibition in Ketoconazole Solid Dispersions. *Mol. Pharm. 12*, 3339-3350 (2015).
15. Kothari, K.; Ragoonanan, V.; Suryanarayanan, R., The Role of Polymer Concentration on the Molecular Mobility and Physical Stability of Nifedipine Solid Dispersions. *Mol. Pharm. 12*, 1477–1484 (2015).
16. Mehta, M.; Ragoonanan, V.; McKenna, G. B.; Suryanarayanan, R., Correlation Between Molecular Mobility And Physical Stability In Supercooled And Glassy Pharmaceuticals. *Manuscript under review.* (2015).
17. Mehta, M.; Zhao, J.; Ragoonanan, V.; McKenna, G. B.; Suryanarayanan, R., Dielectric Spectroscopy: A Technique To Measure Structural Relaxation In Glassy Pharmaceuticals. *Published abstract, AAPS meeting.* (2014).
18. Grzybowska, K.; Paluch, M.; Grzybowski, A.; Wojnarowska, Z.; Hawelek, L.; Kolodziejczyk, K.; Ngai, K. L., Molecular Dynamics And Physical Stability Of Amorphous Anti-Inflammatory Drug: Celecoxib. *J. Phys. Chem. B. 114*, 12792-12801 (2010).
19. Adrjanowicz, K.; Wojnarowska, Z.; Wlodarczyk, P.; Kaminski, K.; Paluch, M.; Mazgalski, J., Molecular Mobility In Liquid And Glassy States Of Telmisartan (TEL) Studied By Broadband Dielectric Spectroscopy. *Eur. J. Pharm. Sci. 38*, 395-404 (2009).
20. Zorn, R.; Mopsik, F. I.; McKenna, G. B.; Willner, L.; Richter, D., Dynamics Of Polybutadienes With Different Microstructures. 2. Dielectric Response And Comparisons With Rheological Behavior. *J. Chem. Phys. 107*, 3645-3655 (1997).

21. O'Connell, P. A.; McKenna, G. B., Large Deformation Response Of Polycarbonate: Time-temperature, Time-aging time and Time-strain Superposition. *Polym. Eng. Sci. 37*, 1485-1495 (1997).
22. Read, B. E.; Dean, G. D.; Tomlins, P. E., Effects Of Physical Ageing On Creep In Polypropylene. *Polymer. 29*, 2159-2169 (1988).
23. Read, B. E.; Dean, G. D.; Tomlins, P. E.; Lesniarek-Hamid, J. L., Physical Ageing And Creep In PVC. *Polymer. 33*, 2689-2698 (1992).
24. Read, B. E.; Dean, G. D., Physical Ageing And Short-Term Creep In Amorphous And Semicrystalline Polymers. *Polymer. 31*, 1204-1215 (1990).
25. Cerrada, M. L.; McKenna, G. B., Creep Behavior In Amorphous And Semicrystalline PEN. *ASTM special technical publication. 1357*, 47-69 (2000).
26. McKenna, G. B.; Kovacs, A. J., Physical Aging Of Poly (methyl methacrylate) In The Nonlinear Range: Torque And Normal force measurements. *Polym. Eng. Sci. 24*, 1138-1141 (1984).
27. Mopsik, F. I., Precision Time-Domain Dielectric Spectrometer. *Rev. Sci. Instrum. . 55*, 79-87 (1984).
28. Kollengodu-Subramanian, S.; McKenna, G. B., A Dielectric Study Of Poly (Vinyl Acetate) Using A Pulse-Probe Technique. *J. Therm. Anal. Calorim. 102*, 477-484 (2010).
29. Cerrada, M. L.; McKenna, G. B., Physical Aging Of Amorphous PEN: Isothermal, Isochronal and Isostructural Results. *Macromolecules. 33*, 3065-3076 (2000).
30. Struik, L. C. E. Physical aging in amorphous polymers and other materials. TU Delft, Delft University of Technology, 1977.
31. Kohlrausch; Pogg, R., *Ann. Phys. XCL, 179*, (1954).
32. Williams, G.; Watts, D. C., Non-Symmetrical Dielectric Relaxation Behaviour Arising From A Simple Empirical Decay Function. *T. Faraday. Soc. . 66*, 80-85 (1970).
33. Struik, L. C. E., Physical Aging in Amorphous Glassy Polymers. *Ann. Ny. Acad. Sci. 279*, 78-85 (1976).
34. Ferry, J. D., *Viscoelastic Properties Of Polymers*. John Wiley & Sons: 1980.
35. Gordon, M.; Taylor, J. S., Ideal Copolymers And The Second-Order Transitions Of Synthetic Rubbers. i. Non-Crystalline Copolymers. *J. Appl. Chem. 2*, 493-500 (1952).
36. Forster, A.; Hempenstall, J.; Tucker, I.; Rades, T., The Potential Of Small-Scale Fusion Experiments And The Gordon-Taylor Equation To Predict The Suitability Of Drug/Polymer Blends For Melt Extrusion. *Drug. Dev. Ind. Pharm. 27*, 549-560 (2001).
37. Khougaz, K.; Clas, S. D., Crystallization Inhibition In Solid Dispersions Of MK-0591 And Poly (vinylpyrrolidone) Polymers. *J. Pharm. Sci. 89*, 1325-1334 (2000).
38. Hancock, B. C.; Zografi, G., The Relationship Between The Glass Transition Temperature And The Water Content Of Amorphous Pharmaceutical Solids. *Pharm. Res. 11*, 471-477 (1994).
39. Shamblin, S. L.; Taylor, L. S.; Zografi, G., Mixing Behavior Of Colyophilized Binary Systems. *J. Pharm. Sci. 87*, 694-701 (1998).
40. Richert, R.; Wagner, H., The Dielectric Modulus: Relaxation Versus Retardation. *Solid. State. Ionics. . 105*, 167-173 (1998).
41. Kremer, F., *Broadband Dielectric Spectroscopy*. Springer Science & Business Media: 2003.
42. Zhang, S.; Painter, P. C.; Runt, J., Dynamics Of Polymer Blends With Intermolecular Hydrogen Bonding: Broad-band Dielectric Study Of Blends Of Poly (4-vinyl phenol) With Poly (vinyl acetate) and EVA70. *Macromolecules. 35*, 8478-8487 (2002).
43. Vogel, H., The Law Of The Relation Between The Viscosity Of Liquids And The Temperature. *Phys. Z. 22*, 645-646 (1921).
44. Fulcher, G. S., Analysis Of Recent Measurements Of The Viscosity Of Glasses. *J. Am. Ceram. Soc. 8*, 339-355 (1925).

45. Tammann, V.; Hesse, W., Anorg. Allgem. Chem.,. *J. Am. Ceram. Soc. 8*, 339 (1926).
46. Angell, C. A.; Ngai, K. L.; McKenna, G. B.; McMillan, P. F.; Martin, S. W., Relaxation In Glassforming Liquids And Amorphous Solids. *J. Appl. Phys. 88*, 3113-3157 (2000).
47. Böhmer, R.; Angell, C. A., Correlations Of The Nonexponentiality And State Dependence Of Mechanical Relaxations With Bond Connectivity In Ge-As-Se Supercooled Liquids. *Phys. Rev. B. 45*, 10091 (1992).
48. Plazek, D. J.; Ngai, K. L., Correlation Of Polymer Segmental Chain Dynamics With Temperature-dependent Time-scale Shifts. *Macromolecules. 24*, 1222-1224 (1991).
49. Qin, Q.; McKenna, G. B., Correlation Between Dynamic Fragility And Glass Transition Temperature For Different Classes Of Glass Forming Liquids. *J. Non-Cryst. Solids. 352*, 2977-2985 (2006).
50. Wang, L.-M.; Tian, Y.; Liu, R.; Richert, R., Calorimetric Versus Kinetic Glass Transitions In Viscous Monohydroxy Alcohols. *J. Chem. Phys. 128*, 084503 (2008).
51. (a) Rumondor, A. C. F.; Ivanisevic, I.; Bates, S.; Alonzo, D. E.; Taylor, L. S., Evaluation Of Drug-Polymer Miscibility In Amorphous Solid Dispersion Systems. *Pharm. Res. 26*, 2523-2534 (2009); (b) Abdul-Fattah, A. M.; Dellerman, K. M.; Bogner, R. H.; Pikal, M. J., The Effect Of Annealing On The Stability Of Amorphous Solids: Chemical Stability Of Freeze-Dried Moxalactam. *J. Pharm. Sci. 96*, 1237-1250 (2007).
52. Kalogeras, I. M., A Novel Approach For Analyzing Glass-Transition Temperature vs. Composition Patterns: Application To Pharmaceutical Compound + Polymer Systems. *Eur. J. Pharm. Sci. 42*, 470-483 (2011).
53. Liu, C.-T.; Lee, W.-H., Fabrication Of An Organic Thin-Film Transistor By Inkjet Printing. *ECS J. Solid State Sci. Technol. 1*, N97-N102 (2012).
54. Zheng, W.; McKenna, G. B.; Simon, S. L., The Viscoelastic Behavior Of Polymer/Oligomer Blends. *Polymer. 51*, 4899-4906 (2010).
55. Heo, Y.; Larson, R. G., Universal Scaling Of Linear And Nonlinear Rheological Properties Of Semidilute And Concentrated Polymer Solutions. *Macromolecules. 41*, 8903-8915 (2008).
56. Plazek, D. J.; Riande, E.; Markovitz, H.; Raghupathi, N., Concentration Dependence Of The Viscoelastic Properties Of Polystyrene-tricresyl Phosphate Solutions. *J. Polyn. Sci. Pol. Phys. 17*, 2189-2213 (1979).
57. Kumar, S. K.; Colby, R. H.; Anastasiadis, S. H.; Fytas, G., Concentration Fluctuation Induced Dynamic Heterogeneities In Polymer Blends. *J. Chem. Phys. 105*, 3777-3788 (1996).
58. Vyazovkin, S.; Dranca, I., Physical Stability And Relaxation Of Amorphous Indomethacin. *J. Phys. Chem. B. . 109*, 18637-18644 (2005).
59. Vyazovkin, S.; Dranca, I., Effect of physical aging on nucleation of amorphous indomethacin. *The Journal of Physical Chemistry B. 111*, 7283-7287 (2007).
60. Brian, C. W.; Yu, L., Surface Self-Diffusion Of Organic Glasses. *J. Phys. Chem. A. . 117*, 13303-13309 (2013).

Chapter 5

1. Kilburn, D.; Townrow, S.; Meunier, V.; Richardson, R.; Alam, A.; Ubbink, J., Organization And Mobility Of Water In Amorphous And Crystalline Trehalose. *Nat. Mater.* **2006,** *5* (8), 632-635.
2. Ohtake, S.; Shalaev, E., Effect of water on the chemical stability of amorphous pharmaceuticals: I. Small molecules. *J. Pharm. Sci* **2013,** *102* (4), 1139-1154.
3. Heljo, V. P.; Nordberg, A.; Tenho, M.; Virtanen, T.; Jouppila, K.; Salonen, J.; Maunu, S. L.; Juppo, A. M., The effect of water plasticization on the molecular mobility

and crystallization tendency of amorphous disaccharides. *Pharm. Res.* **2012,** *29* (10), 2684-2697.
4. Greco, S.; Authelin, J.-R.; Leveder, C.; Segalini, A., A practical method to predict physical stability of amorphous solid dispersions. *Pharm. Res.* **2012,** *29* (10), 2792-2805.
5. Makower, B.; Dye, W. B., Sugar Crystallization, Equilibrium Moisture Content And Crystallization Of Amorphous Sucrose And Glucose. *J. Agr. Food. Chem.* **1956,** *4* (1), 72-77.
6. Kedward, C. J.; MacNaughtan, W.; Mitchell, J. R., Crystallization Kinetics Of Amorphous Lactose As A Function Of Moisture Content Using Isothermal Differential Scanning Calorimetry. *J. Food. Sci.* **2000,** *65* (2), 324-328.
7. Konno, H.; Taylor, L. S., Ability of different polymers to inhibit the crystallization of amorphous felodipine in the presence of moisture. *Pharm. Res.* **2008,** *25* (4), 969-978.
8. Andronis, V.; Zografi, G., The Molecular Mobility Of Supercooled Amorphous Indomethacin As A Function Of Temperature And Relative Humidity. *Pharm. Res.* **1998,** *15* (6), 835-842.
9. Aso, Y.; Yoshioka, S.; Zhang, J.; Zografi, G., Effect of Water on the Molecular Mobility of Sucrose and Poly (vinylpyrrolidone) in a Colyophilized Formulation as Measured by 13C-NMR Relaxation Time. *Chemical and pharmaceutical bulletin* **2002,** *50* (6), 822-826.
10. Miller, D. P.; Lechuga-Ballesteros, D., Rapid assessment of the structural relaxation behavior of amorphous pharmaceutical solids: effect of residual water on molecular mobility. *Pharm. Res.* **2006,** *23* (10), 2291-2305.
11. Aso, Y.; Yoshioka, S.; Kojima, S., Relationship Between Water Mobility, Measured As Nuclear Magnetic Relaxation Time, And The Crystallization Rate Of Amorphous Nifedipine In The Presence Of Some Pharmaceutical Excipients. *Chem. Pharm. Bull.* **1996,** *44* (5), 1065-1067.
12. Chan, R. K.; Pathmanathan, K.; Johari, G. P., Dielectric Relaxations In The Liquid And Glassy States Of Glucose And Its Water Mixtures. *J. Phys. Chem.* **1986,** *90* (23), 6358-6362.
13. Nyqvist, H., Saturated salt solutions for maintaining specified relative humidities. *Int. J. Pharm. Tech. Prod. Mfr* **1983,** *4* (2), 47-48.
14. Hammersley, A. P., FIT2D: An Introduction And Overview. *European Synchrotron Radiation Facility Internal Report ESRF97HA02T* **1997**.
15. Hammersley, A. P.; Svensson, S. O.; Hanfland, M.; Fitch, A. N.; Hausermann, D., Two-Dimensional Detector Software: From Real Detector To Idealised Image Or Two-Theta Scan. *International Journal of High Pressure Research* **1996,** *14* (4-6), 235-248.
16. Nunes, C.; Mahendrasingam, A.; Suryanarayanan, R., Quantification Of Crystallinity In Substantially Amorphous Materials By Synchrotron X-ray Powder Diffractometry. *Pharm. Res.* **2005,** *22* (11), 1942-1953.
17. Kremer, F., *Broadband Dielectric Spectroscopy*. Springer Science & Business Media: 2003.
18. Laredo, E.; Hernandez, M. C., Moisture effect on the low and high temperature dielectric relaxations in nylon-6. *J. Polym. Sci. Pol. Phys.* **1997,** *35* (17), 2879-2888.
19. Vogel, H., The Law Of The Relation Between The Viscosity Of Liquids And The Temperature. *Phys. Z* **1921,** *22*, 645-646.

20. Fulcher, G. S., Analysis Of Recent Measurements Of The Viscosity Of Glasses. *J. Am. Ceram. Soc.* **1925,** *8* (6), 339-355.
21. Tammann, V. G.; Hesse, W., Anorg. Allgem. Chem.,. *J. Am. Ceram. Soc* **1926,** *8*, 339.
22. Angell, C. A.; Ngai, K. L.; McKenna, G. B.; McMillan, P. F.; Martin, S. W., Relaxation In Glassforming Liquids And Amorphous Solids. *J. Appl. Phys.* **2000,** *88* (6), 3113-3157.
23. Shalaev, E. Y.; Zografi, G., How does residual water affect the solid-state degradation of drugs in the amorphous state? *J. Pharm. Sci* **1996,** *85* (11), 1137-1141.
24. Green, J. L.; Fan, J.; Angell, C. A., The Protein-Glass Analogy: New Insight From Homopeptide Comparisons. *J. Phys. Chem.* **1994,** *98* (51), 13780-13790.
25. Girlich, D.; Lüdemann, H. D.; Buttersack, C.; Buchholz, K., c, T-dependence of the self diffusion in concentrated aqueous sucrose solutions. *Zeitschrift für Naturforschung C* **1994,** *49* (3-4), 258-264.
26. Angell, C. A.; Bressel, R. D.; Green, J. L.; Kanno, H.; Oguni, M.; Sare, E. J., Liquid Fragility And The Glass Transition In Water And Aqueous Solutions. *J. Food. Eng.* **1994,** *22* (1), 115-142.
27. Schmitt, E.; Davis, C. W.; Long, S. T., Moisture-Dependent Crystallization Of Amorphous Lamotrigine Mesylate. *J. Pharm. Sci* **1996,** *85* (11), 1215-1219.
28. Flory, P. J., Principles of polymer chemistry. **1953**.
29. Frushour, B. G., Water as a melting point depressant for acrylic polymers. *Polym. Bull.* **1982,** *7* (1), 1-8.
30. Meaurio, E.; Zuza, E.; Sarasua, J.-R., Miscibility and specific interactions in blends of poly (L-lactide) with poly (vinylphenol). *Macromolecules* **2005,** *38* (4), 1207-1215.
31. Marsac, P. J.; Shamblin, S. L.; Taylor, L. S., Theoretical And Practical Approaches For Prediction Of Drug – Polymer Miscibility And Solubility. *Pharm. Res.* **2006,** *23* (10), 2417-2426.
32. Zhou, D.; Zhang, G. G. Z.; Law, D.; Grant, D. J. W.; Schmitt, E. A., Physical Stability Of Amorphous Pharmaceuticals: Importance Of Configurational Thermodynamic Quantities And Molecular Mobility. *J. Pharm. Sci.* **2002,** *91* (8), 1863-1872.
33. Böhmer, R.; Angell, C. A., Correlations Of The Nonexponentiality And State Dependence Of Mechanical Relaxations With Bond Connectivity In Ge-As-Se Supercooled Liquids. *Phys. Rev. B* **1992,** *45* (17), 10091.
34. Hodge, I. M., Physical aging in polymer glasses. *Science.* **1995**, 1945-1945.
35. Zhou, D.; Grant, D. J. W.; Zhang, G. G. Z.; Law, D.; Schmitt, E. A., A Calorimetric Investigation Of Thermodynamic And Molecular Mobility Contributions To The Physical Stability Of Two Pharmaceutical Glasses. *J. Pharm. Sci* **2007,** *96* (1), 71-83.
36. Aso, Y.; Yoshioka, S.; Kojima, S., Molecular Mobility Based Estimation Of The Crystallization Rates Of Amorphous Nifedipine And Phenobarbital In Poly (vinylpyrrolidone) Solid Dispersions. *J. Pharm. Sci* **2004,** *93* (2), 384-391.
37. Bhardwaj, S. P.; Arora, K. K.; Kwong, E.; Templeton, A.; Clas, S.-D.; Suryanarayanan, R., Correlation Between Molecular Mobility And Physical Stability Of Amorphous Itraconazole. *Mol. Pharm.* **2013,** *10* (2), 694-700.

38. Kothari, K.; Ragoonanan, V.; Suryanarayanan, R., Influence Of Molecular Mobility On The Physical Stability of Amorphous Pharmaceuticals in the Supercooled and Glassy States. *Mol. Pharm.* **2014,** *11* (9), 3048-3055.
39. Mehta, M.; Ragoonanan, V.; McKenna, G. B.; Suryanarayanan, R., Correlation Between Molecular Mobility And Physical Stability In Supercooled And Glassy Pharmaceuticals. *Manuscript under review* **2015**

Chapter 6

R., Correlation Between Molecular Mobility And Physical Stability Of Amorphous Itraconazole. *Mol. Pharm.* **2013,** *10* (2), 694-700.
2. Kothari, K.; Ragoonanan, V.; Suryanarayanan, R., Influence Of Molecular Mobility On The Physical Stability of Amorphous Pharmaceuticals in the Supercooled and Glassy States. *Mol. Pharm.* **2014,** *11* (9), 3048-3055.
3. Bhardwaj, S. P.; Suryanarayanan, R., Molecular Mobility As An Effective Predictor Of The Physical Stability Of Amorphous Trehalose. *Mol. Pharm.* **2012,** *9* (11), 3209-3217.
4. Bhardwaj, S. P.; Arora, K. K.; Kwong, E.; Templeton, A.; Clas, S.-D.; Suryanarayanan, R., Mechanism of amorphous itraconazole stabilization in polymer solid dispersions: role of molecular mobility. *Mol. Pharm.* **2014,** *11* (11), 4228-4237.
5. Kothari, K.; Ragoonanan, V.; Suryanarayanan, R., The Role of Polymer Concentration on the Molecular Mobility and Physical Stability of Nifedipine Solid Dispersions. *Mol. Pharm.* **2015**.
6. Kilburn, D.; Townrow, S.; Meunier, V.; Richardson, R.; Alam, A.; Ubbink, J., Organization and mobility of water in amorphous and crystalline trehalose. *Nat. Mat.* **2006,** *5* (8), 632-635.
7. Miyazaki, T.; Yoshioka, S.; Aso, Y.; Kawanishi, T., Crystallization rate of amorphous nifedipine analogues unrelated to the glass transition temperature. *Int. J. Pharm.* **2007,** *336* (1), 191-195.
8. Schmitt, E.; Davis, C.; Long, S., Moisture-dependent crystallization of amorphous lamotrigine mesylate. *J. Pharm. Sci* **1996,** *85* (11), 1215-1219.
9. Greco, S.; Authelin, J.-R.; Leveder, C.; Segalini, A., A practical method to predict physical stability of amorphous solid dispersions. *Pharm. Res.* **2012,** *29* (10), 2792-2805.
10. Nyqvist, H., Saturated salt solutions for maintaining specified relative humidities. *Int. J. Pharm. Tech. Prod. Mfr* **1983,** *4* (2), 47-48.
11. Toby, B. H.; Von Dreele, R. B., GSAS-II: The Genesis Of A Modern Open-Source All Purpose Crystallography Software Package. *J. Appl. Crystallogr.* **2013,** *46(2)*, 544-549.
12. Nunes, C.; Mahendrasingam, A.; Suryanarayanan, R., Quantification Of Crystallinity In Substantially Amorphous Materials By Synchrotron X-ray Powder Diffractometry. *Pharm. Res.* **2005,** *22* (11), 1942-1953.
13. Vogel, H., The Law Of The Relation Between The Viscosity Of Liquids And The Temperature. *Phys. Z* **1921,** *22*, 645-646.
14. Fulcher, G. S., Analysis Of Recent Measurements Of The Viscosity Of Glasses. *J. Am. Ceram. Soc.* **1925,** *8* (6), 339-355.

15. Tammann, V.; Hesse, W., Anorg. Allgem. Chem., 156,246 (1926). *J. Am. Ceram. Soc* **1926,** *8*, 339.
16. Angell, C. A.; Ngai, K. L.; McKenna, G. B.; McMillan, P. F.; Martin, S. W., Relaxation In Glassforming Liquids And Amorphous Solids. *J. Appl. Phys.* **2000,** *88* (6), 3113-3157.
17. Angell, C.; Bressel, R.; Green, J.; Kanno, H.; Oguni, M.; Sare, E., Liquid fragility and the glass transition in water and aqueous solutions. *J. Food. Eng.* **1994,** *22* (1), 115-142.
18. Magill, J.; Li, H.-M., Physical properties of aromatic hydrocarbons: V. The solidification behavior of 1: 2 diphenylbenzene. *J. Cryst. Growth.* **1973,** *20* (2), 135-144.
19. Plazek, D. J.; Magill, J. H., Physical Properties of Aromatic Hydrocarbons. I. Viscous and Viscoelastic Behavior of 1: 3: 5-Tri-α-Naphthyl Benzene. *J. Chem. Phys.* **1966,** *45* (8), 3038-3050.
20. Ediger, M. D., Spatially Heterogeneous Dynamics In Supercooled Liquids. *Ann. Rev. Phys. Chem.* **2000,** *51* (1), 99-128.